THE LIFE SAFETY OBJECTIVE IN STRUCTURAL FIRE SAFETY DESIGN

Doktorsavhandling i ämnet Stålbyggnad

Joakim Sandström

2019-06-13

THE LIFE SAFETY OBJECTIVE IN STRUCTURAL FIRE SAFETY DESIGN

Joakim Sandström

Steel Structures

LULEÅ
UNIVERSITY
OF TECHNOLOGY

THE LIFE SAFETY OBJECTIVE IN STRUCTURAL FIRE SAFETY DESIGN

Joakim Sandström

Luleå, May 2019

Acknowledgement

You can only die once. The saying, in its literal sense, captures the essence of the approach in the thesis which is based on the concept that it is impossible to die twice. However, the original version of the quote is a figurative saying to encourage someone in a dangerous or difficult enterprise, a version more suitable for the endeavor of doctoral studies.

I would like to thank all of my encouraging colleagues, with special mention to some for participating in the crafting of this thesis. Prof. Milan Veljkovic who encouraged me to become a PhD student, prof. Ove Lagerqvist who encouraged me to pursue the concept that ended up in this thesis, and prof. Sven Thelandersson who encouraged me to follow the black swans and probabilistic design.

My colleagues at Brandskyddslaget's office in Karlstad have also encouraged me over the years with the kind of camaraderie that makes heavy clouds go away any day. A special mention goes to Jörgen Thor who tirelessly have encouraged and mentored me in the fine arts of structural fire safety design.

Encouragement is important also in monetary form. The funding agencies; Brandforsk, SBUF, and ÅForsk have encouraged me by believing in my ideas funding the work leading to this thesis.

However, my sincerest gratitude goes to my principal supervisor prof. Ulf Wickström who has guided me through my studies for over a decade. I have always been encouraged by his ability to transform theory into useful concepts.

With all this encouragement, it would seem impossible to fail. Still, there is a need for support from family and friends with everything from babysitting to 'innebandy' and singing. For this, I'm very grateful and can never thank everybody enough. Without all of you, and your support, this would not have been possible.

Finally, to my wife Erika and my children Elsa, Signe and August, I am truly curious to see what life has to bring with you by my side. This one is for you.

Abstract

Performance-based fire design of structures is most commonly aiming at ensuring structural stability during the entire event of a fire. This is a rational and sound approach for buildings where structural fire damage can affect occupants that are unaware of the fire. However, for other cases such as single-story, single-compartment buildings, this approach tends to overshoot society's ambition with regards to life safety.

This thesis presents a unified structural fire safety design approach focused specifically on life safety. The new approach is based on the assumption that if, for an area, survival is precluded due to hot fire gases, structural damage will not increase the risk for loss of life. For such cases, structural fire protection may be unnecessary and the structural fire resistance requirements relaxed.

The new approach is demonstrated on a single-story steel frame building where a case study shows that there is a high probability of structural fire damage for steel trusses without structural fire protection. However, the case study also shows that there is a low probability for loss of life from structural fire damage as the structural fire damage would occur after lethal fire conditions have developed. Thus, safety with regards to life is achieved even though the steel trusses are left without structural fire protection.

For buildings where structural fire damage should be limited to prevent loss of life, the safety assumptions in the EN 1991-1-2 semi-probabilistic method was evaluated. The evaluation indicates that the semi-probabilistic approach in EN 1991-1-2 is conservative and lacks precision when accounting for changes in e.g. the opening factor. The impact of several parameters was investigated showing that alteration of the parameters does not only change the required amount of applied fire protection but also influences the overall uncertainty of the calculations.

Abstract in Swedish

Funktionsbaserad dimensionering av brandutsatta bärande konstruktioner har ofta som mål att säkerställa en byggnads stabilitet under ett helt brandförlopp. Detta angreppssätt är rationellt och begripligt för byggnader där en skada på konstruktionen kan skada personer som inte kan förväntas vara medvetna om branden. För enplansbyggnader utan innerväggar där personer istället kan antas vara medvetna om en brand i byggnaden kan angreppssättet därför bidra till krav på mer brandskydd än nödvändigt.

Avhandlingen redovisar en ny metod för att utvärdera personskaderisk i förhållande till brott i brandutsatta bärande konstruktioner. Den nya metoden bygger på antagandet att personrisken inte ökar vid brott i en konstruktion i de fall temperaturerna till följd av branden gör det omöjligt att vara vid liv i skadeområdet vid tiden för brottet. För dessa fall kan brandkrav på de bärande konstruktionerna i många fall sänkas utan att äventyra personsäkerheten i byggnaden.

Den nya metoden kan användas för att bestämma brandmotståndstid för en byggnad utifrån personrisk samtidigt som den ger verktyg att förstå varför krav på brandmotstånd kan vara onödigt i många byggnader. I en fallstudie utvärderas personrisken i en enplans stålhall med hjälp av den nya metoden. Personrisken i stålhallen är liten vid brott i de brandutsatta fackverken trots att de har stor

sannolikhet att gå till brott vid brand. God personsäkerhet kan därför anses vara uppnådd även om stålfackverken i byggnaden utförs utan brandskydd.

Som komplement utvärderades säkerhetsnivåerna i EN 1991-1-2 för en byggnad där brott till följd av brand bör förhindras. Undersökningen visade att den semi-probabilistiska metod för brandutsatta konstruktioner som anges i EN 1991-1-2 är konservativ och missar hänsyn till viktiga parametrar. Ändringar i dessa parametrar, t.ex. öppningsfaktorn, ändrar inte bara kravet på mängden brandskydd som krävs för att uppnå en viss säkerhetsnivå, det påverkar också osäkerheten i beräkningarna som helhet.

Contents

1 INTRODUCTION

The load-bearing capacity of the construction can be assumed for a specific period of time.

(Construction Product Regulation, annex 1, article 2 (b))

With the introduction of performance-based codes, the need for understanding the objectives in structural fire safety design has increased. A study by Strömgren et al. (2014) showed a great diversity among practitioners in interpreting the desired performance-based design objective for a single-story steel frame buildings even within the same performance-based code framework. Many of the difficulties in understanding the performance-based design objectives comes from a lack of guidance in the codes (Almgren and Hansson, 2010).

This thesis is about a new structural fire safety design approach (first presented in paper A) and it elaborates on its application. The approach states that structural fire damage shall be prevented in locations where survival from thermal exposure is possible, but it also states that structural fire damage is acceptable if survival from thermal exposure is precluded. The approach works as a base-line requirement for all buildings within a performance-based design setting, even when no other structural fire safety requirements apply.

1.1   Background

Many national building codes have gone from prescriptive to performance-based in order to meet a growing desire to enable more innovative fire safety designs and cost-efficient buildings (Buchanan and Abu, 2016). Many countries have adopted a hierarchical structure for the performance-based framework with objectives, functional statements, performance requirements and building solutions as suggested by the Building Code of Australia (ABCB, 2015), see figure 1.
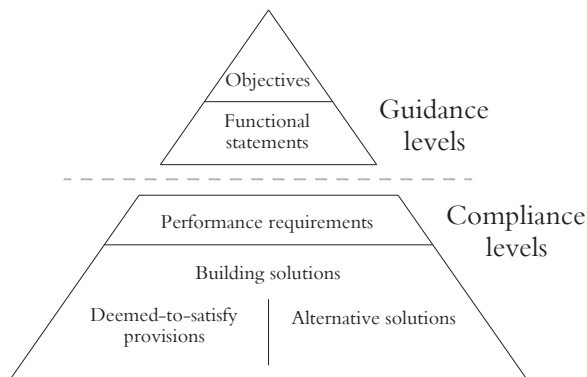
Figure 1 Hierarchy of the performance-based design code in the Australian Building Code (adaptation from (ABCB, 2015)).

Many of the difficulties with the life safety objective in performance-based design of fire exposed structures stem from a lack of coherence in the guidance levels (see figure 1). This lack of coherence can be illustrated with Strömgren et al. (2014) who studied how Swedish practitioners interpreted the objective of life safety in single-story steel frame buildings. The Swedish building code states that structural fire safety requirements should be decided based on risk for personal injury indicating that life safety is the only objective (Boverket, 2015). Simultaneously, the Swedish building code accepts an exception of fire protection requirements for roof structures within given span lengths. The code allows design without fire protection for longer spans but provides no clear guidance on how to achieve this.

The study by Strömgren et al. showed that practitioners and authorities interpret the life safety objective differently. Designs being approved or not depend on the involved parties rather than on the quality of the engineering solution. The focus of this thesis is therefore on elaborating on the guidance levels.

1.1.1 Objectives in performance-based design

The objectives in performance-based codes can be described as 'overall objectives' (Hadjisophocleous and Bénichou, 2000) or 'hidden intentions' (Almgren and Hansson, 2010). Haviland first suggested two main objectives, saving life or saving property (Haviland, 1978). Hadjisophocleous and Bénichou (2000) expanded the second of Haviland's objectives to include minimizing loss of building content and protection of adjacent buildings while Buchanan and Abu adds consideration to the environment as a third objective (Buchanan and Abu, 2016). These objectives are also concluded in the European Union Constructions Product Regulation, CPR, which states that construction works should not endanger the safety of lives or property, nor damage the environment (CPR, 2011). In this thesis, focus is on the life safety objective and how this can be interpreted in a performance-based setting ignoring the other objectives.

1.1.2 Functional statements in performance-based design

CPR (2011) concretize its structural fire safety objectives by functional statements for fire exposed structures with technical specifications for safety in case of fire. All the functional statements in CPR can be derived from the life safety objective but most of them refer to smoke management and limitation of fire spread rather than load-bearing structures. The only statement with a distinct connection to load-bearing structures is

> *The load-bearing capacity of the construction can be assumed for a specific period of time.* (CPR, Annex 1 – article 2(b))

Meacham uses the same functional statement but refers to a 'reasonable' period of time (Meacham, 1996) while Wang et al. refers to an 'appropriate' period of time (Wang et al., 2012). None of the terms bring clarity to the concept of time itself and the term 'specific' in CPR is subsequently criticized by Wegrzynski and Sulik (2016) who points out that the statement does not give any guidance on what to achieve with the 'specific period of time'.

National Fire Protection Association include more specific reasons in their functional statement for fire exposed load-bearing elements indicating that the 'specific period of time' is needed to 'evacuate, relocate, or defend in place occupants who are not intimate with the initial fire development' (NFPA, 2006). Buchanan and Abu further broadens the concept by formulating the *functional statements* as structural fire resistance time to be the time to achieve one or several of the following (Buchanan and Abu, 2016).

1. The time required for occupants to escape from the building.
2. The time for firefighters to carry out rescue activities.
3. The time for firefighters to surround and contain the fire.
4. The duration of a burnout of the fire compartment with no intervention.

Based on the works in paper A, B and C it is possible to add a fifth functional statement in addition to those of Buchanan and Abu as

5. The time required to presume that survival is precluded in a given area.

This latter statement focusses only on the life safety objective.

1.2   Aim, scope and limitations

The aim of this doctoral thesis is to discuss the new approach mentioned above for addressing the life safety objective in structural fire safety as stated in the fifth *functional statement*. Thus, the research questions can be stated as

1. How can structural fire safety design based on the fifth functional statement be performed?

2. Which parameters are significant for inducing unsafe conditions in structural fire safety design and why?

The thesis presents the basic concept of the approach in a design case study of a single-story steel frame building using deterministic and probabilistic design methods (paper A, B and C). The study of the approach is supported by the experimental investigation in paper D and E. The thesis also evaluates the partial coefficient method in EN 1991-1-2 for multi-story buildings where structural fire damage presents a high risk for loss of life (paper F).

The principles of 'consistent level of crudeness' apply stating that no model is better than its crudest component (Elms, 1992). In this thesis, all models are chosen to obtain a sufficient refinement for the application aiming for a necessary level of crudeness knowing that no model is perfect.

For all examples given in this thesis, it is assumed that there are no economic, social or environmental consequences to consider.

1.3   Appended papers

The new design approach was handed down from a Swedish context of practitioners for single-story buildings but refined to work in a more complex design setting by Sandström in paper A. Sandström have also contributed with the majority of the work in each of the papers such as leading the experiments (paper D), developing the analytical and numerical models to use in the work (paper E) as well as writing the code for executing all calculations (papers B, C and F).

A more extensive summary of the papers is presented in section 2.

Paper A

Sandström, J., Wickström, U., Thelandersson, S. and Lagerqvist, O. (2017), "The life safety objective in performance-based design for structural fire safety", *Proceedings of the 2nd International Conference on Structural Safety Under Fire and Blast Loading, CONFAB 2017*, Brunel University London, pp. 411–417.

Paper B

Sandström, J. (Accepted 2019), "Life safety in single-story steel frame buildings, Part I - deterministic design", *Journal of Fire Protection Engineering*.

Paper C

Sandström, J. (Submitted 2019), "Life safety in single-story steel frame buildings, Part II - probabilistic design", *Journal of Fire Protection Engineering*.

Paper D

Sandström, J., Wickström, U., Sjöström, J., Veljkovic, M., Iqbal, N. and Sundelin, J. (2015), "Steel Truss Exposed to Localized Fires", LTU, Luleå, Sweden

Paper E

Sandström, J., Sjöström, J. and Wickström, U. (2019), "Thermal exposure from localized fires to horizontal surfaces below the hot gas layer", LTU, Luleå, Sweden.

Paper F

Sandström, J. and Thelandersson, S. (Accepted 2018), "Comparing performance-based fire safety design using stochastic modelling to Eurocode partial coefficient method", *Book of Abstract (Peer-Reviewed)*, Nordic Fire & Safety Days 2018, Trondheim, Norway.

2 THE LIFE SAFETY OBJECTIVE

You can only die once.

(English proverb, mid–15th century)

Instead of saying that evacuation has to be completed before critical conditions, paper A states that evacuation is impossible after the critical conditions has occurred. The statement implies that people can die in a fire, but that they only can die once. If structural damage occurs after the death of all occupants and/or firefighters in a given area, the structural fire damage will not be a decisive cause of injury or harm. This statement enables new design possibilities, but also enjoin great responsibilities to the designer. In the appended papers, where the structural fire safety design is optimized according to the fifth functional statement in section 1.1.2, the criteria are therefore chosen conservatively with firefighter safety in mind as they are inherently better protected than occupants.

This section will present the thread between the papers in this thesis and briefly describe the key findings in each of them.

2.1 Paper A – The Life Safety Objective in Performance-Based Design for Structural fire Safety

Paper A, *The Life Safety Objective in Performance-Based Design for Structural Fire Safety*, by Sandström et al. presents a general approach to structural fire safety design from

the viewpoint of life safety. The approach to target life safety as a stand–alone objective has evolved from discussions in previous literature (Guowei et al., 2016; Sandman, 1989) and is founded on the understanding of two main design components; the structural fire damage area, and the lethal fire conditions area. These two areas are each connected to a time of occurrence which also plays a vital part in understanding the approach. These concepts can be defined as:

Structural fire damage area, A_{str}

The structural fire damage area, A_{str} is the area, where danger of harm or injury to occupants or firefighters can be expected, due to loss of structural integrity initiated by fire.

Lethal fire conditions area, A_{crit}

The lethal fire conditions area, A_{crit}, is the area where survival is precluded for occupants or firefighters due to exposure to the harmful conditions for very short times.

Time to structural fire damage, t_{str}

t_{str} is defined as the time when damage occurs in any part of the fire exposed load-bearing structure.

Time to lethal fire conditions, $t_{crit} + t_{margin}$

The time to lethal fire conditions is the time when survival is precluded given critical conditions and is composed of two parts; t_{crit}, and t_{margin}. t_{crit} is the time to harmful conditions, i.e. sustained exposure of this magnitude can yield harm or death.

t_{margin} is the time required for the harmful exposure to preclude survival. To determine both times, the critical condition needs to be defined in terms of what the exposure consists of as well as what level is reasonable.

Evaluating structural fire safety by combining these design components enables a more nuanced approach to the life safety objective in structural fire safety design than has previously been done. A structural fire safety design with these design components can be evaluated in the time domain or in the area domain.

Structural fire safety design in the time domain is performed by ensuring that the time of structural fire damage, t_{str}, occurs after the time to lethal conditions, i.e. $t_{crit} + t_{margin}$. This design approach is valid for defined areas where the structural fire damage area is equal in size or smaller than the lethal fire conditions area. One example of this is where uniform fire conditions can be assumed in an entire building simultaneously. The design criterion in the time domain is written as

$$t_{str} \geq \left(t_{crit} + t_{margin} \right) \qquad (1)$$

Note that structural damage should be prevented in the cooling phase after the time when the conditions are no longer harmful, see figure 2.
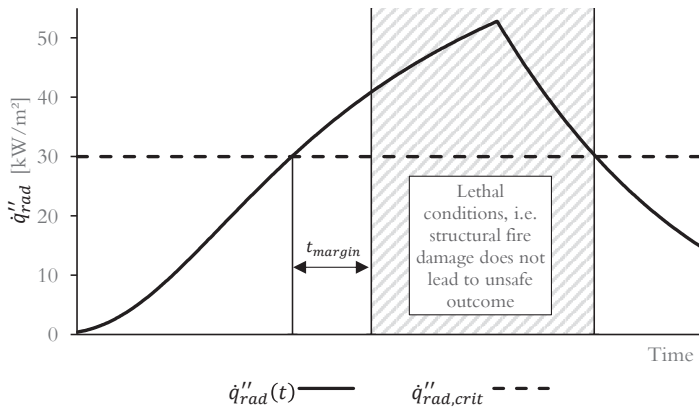

Figure 2 t_{crit}, t_{margin} and time interval where structural fire damage does not lead to unsafe outcome, (paper B)

Structural fire safety design in the area domain is performed by ensuring that A_{str} is smaller than, and within the bounds of A_{crit} at the time t_{str}, or $t_{str} - t_{margin}$ for

the lethal fire conditions area to include for the margin time. The design criterion in the area domain is written as

$$A_{crit}\left(t_{str} - t_{margin}\right) \geq A_{str}(t_{str}) \qquad (2)$$

Examples of how the approach is implemented is illustrated in section 3.

2.2 Paper B - E – Life safety in a single-compartment building

Paper B and C evaluate the life safety in the time domain for a building where the structural fire damage area can be assumed equal to the lethal fire conditions area, i.e. $A_{str} = A_{crit}$. Paper B, *Life safety in single-story steel frame buildings, Part I - deterministic design*, examines the design approach using deterministic design values as suggested by standards. Paper C, *Life safety in single-story steel frame buildings, Part II - probabilistic design*, acts as a complement by examining the probability of unsafe outcome in the building and evaluate what parameters are the most important for inducing an unsafe outcome using crude Monte Carlo simulation. In both studies, an unsafe outcome was deemed to occur if the design criterion as stated in equation (1) was fulfilled.

$$t_{str} \geq t_{crit} + t_{margin} \qquad (1)$$

With lethal conditions in the entire building at the time of structural damage, progressive collapse would not increase the risk of harm to occupants and/or firefighters within the building. For the case study in paper B and C, the lethal condition was determined to stem from thermal radiation at a level of $\dot{q}''_{rad,crit} = 30 \text{ kW/m}^2$ for more than 150 s, i.e. the margin time, t_{margin}.

For each simulation, structural fire damage was assumed not to lead to an unsafe outcome if the thermal radiation from the hot gas layer in the compartment was

higher than $\dot{q}''_{rad,crit} = 30$ kW/m² and had been so for at least $t_{margin} = 150$ s, see figure 2 in section 2.1.

For the deterministic design case, paper B, it was shown that the structural fire damage occurred well within the bounds of not creating an unsafe outcome, see figure 3. The initial steel temperature in figure 3 is higher than the hot gas layer temperature due to direct exposure from the localized fire plume.
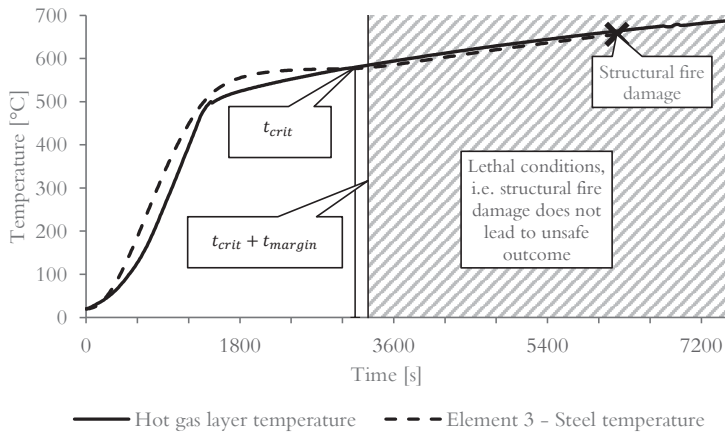
Figure 3 Global hot gas layer temperature and local steel temperature
for the most critical truss element (adaptation from paper B)

Thus, the building could be considered safe for occupants and firefighters even without further fire protection. This reduced the cost of the truss compared to generic design with a factor 1,7 without increasing the risk of harm or death to occupants and firefighters.

For the probabilistic design case, paper C, the same numerical model assumptions were made for calculation of the outcome in each simulation. However, spatial consideration was included for the localized fire in relation to each truss element. To enable this consideration in the simulations, a new model for thermal action to the lower truss chord was required.

Based on data from a large-scale experiment conducted in Trondheim, paper D, *Steel truss exposed to localized fires*, three different model assumptions of thermal action to the lower chord truss elements were validated in paper E, *Thermal exposure from localized fires to horizontal surfaces below the hot gas layer*. The models evaluated in paper E were the radiating disc assumption as suggested by Zhang and Usmani (2015), the point source assumption as suggested by Beyler (2002), and a new model by the authors of the report.

In the comparison of the different models for the thermal action to the lower chord, it was found that the models by Zhang and Usmani, and Beyler showed reasonable correlation to measured data outside the plume with a slight tendency to under-predict the temperatures. However, inside the plume, the existing models either under-predicted the temperatures (Zhang and Usmani), or were inconsistent with regards to over-, or under-prediction of the temperature (Beyler).

Figure 4 shows the three methods where method A is the new method presented in paper E, method B is the radiating disc assumption by Zhang and Usmani, and method C is the point source assumption as presented by Beyler.
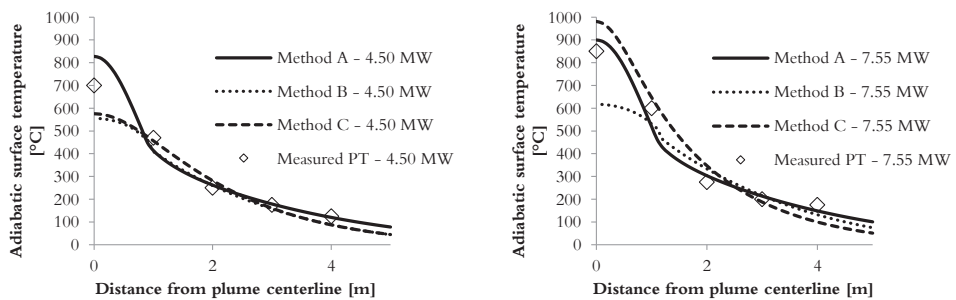

Figure 4 Thermal action/exposure at the lower chord expressed as adiabatic surface temperatures, measured by plate thermometers, compared to analytical solutions (paper E).

The model chosen in paper C was the new model based on Heskestad's plume correlation in combination with radiation from the cylindrical plume perimeter to

horizontal surfaces at given distances. The choice of Heskestad's plume correlation enabled a situation where all calculations, both the localized fire exposure and zone model were based on the same plume correlation. Thus, a more 'consistent level of crudeness' of the combined calculations were achieved (Elms, 1992; Frank et al., 2011).

The probabilistic case study in paper C confirmed the achieved level of safety in comparison to the deterministic study (paper B), but it also isolated several key factors important for understanding what drives a higher probability of unsafe outcomes. The European standard EN 1990 stipulates for public buildings with 'medium consequences for loss of human life' (RC2), a target probability for structural instability in case of extreme events of $7{,}23 \cdot 10^{-5}$ over a reference time of 50 years. As this target was not achieved with regards to structural stability (it was calculated as being $2{,}47 \cdot 10^{-3}$), the structure is considered unsafe according to the European standard. However, by using the new approach, it was shown that the risk for unsafe outcomes was lower than that target probability ($1{,}90 \cdot 10^{-5}$). Thus, the risk for loss of life could be deemed sufficiently low and the life safety objective met. This indicates that there is a gap in the understanding of life safety in structural fire safety design in existing codes and research literature.

Among the parameters that can induce a high probability of unsafe outcome with a risk for loss of life are

- High maximum heat release rate,
- High heat release rate per unit area,
- Low critical steel temperature, and
- Short distance from the plume centerline to the most sensitive elements in the lower chord.

However, none of these parameters can be isolated in an analysis but in combination with any of the others they increase the risk.

2.3 Paper F – Life safety in a multiple-story building

For many buildings there is a risk for injury or death of occupants or firefighters due to structural fire damage outside of the lethal fire conditions area. An example of this is provided in section 3.3 in this thesis. For these buildings, the design should aim at providing sufficient protection of the load-bearing structure to prevent structural fire damage. Sandström and Thelandersson investigated in paper F, *Comparing performance-based fire safety design using stochastic modelling to Eurocode partial coefficient method,* the importance of different parameters in the Eurocode semi–probabilistic model for fire safety design of structures to resist a full duration of a fire.

Paper F shows that the Eurocode focus on fuel load density is insufficient. There is an impact from variations in ventilation as well as load ratio which affects the safety levels beyond what Eurocode stipulates. Even though it was proven difficult to assess relevant data for all parts of the simulation, the observed tendency was that Eurocode is somewhat conservative.

3 DESIGN EXAMPLES

Yes, it works in practice, but does it work in theory?

(Mathieu Richard)

Paper A outlines the most important aspects of the life safety design approach. This section will give examples of how the approach can be implemented in practical design. The examples are intended to provide guidance on the implementation of the approach.

For all examples given in this thesis, only the new approach to achieve the life safety objective is demonstrated. Thus, it is assumed that there are no other objectives or consequences to consider.

3.1   General approach

Paper A presented the design process in the form of a flowchart which is reproduced here in figure 5.
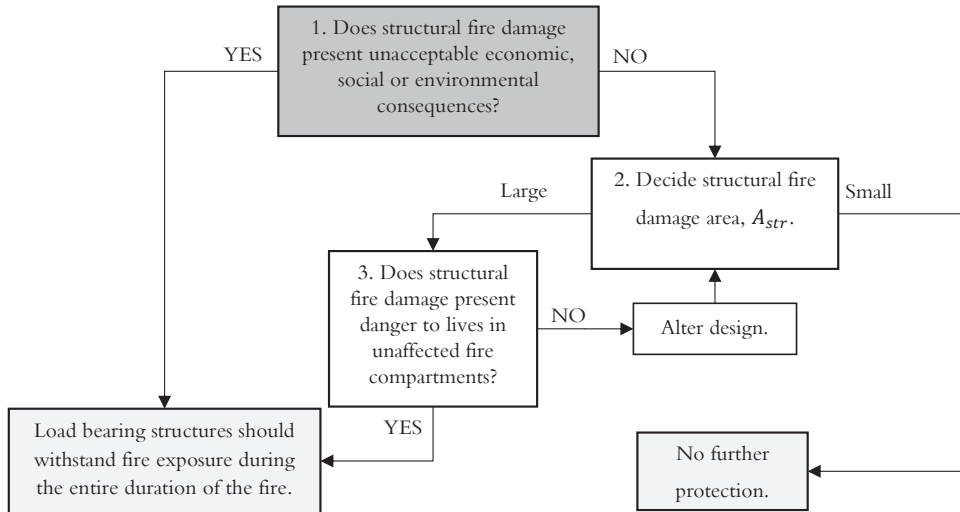
Figure 5 Flow-chart for design approach.

The concept of area for question 2 in figure 5 relates to the size of structural fire damage in relation to the lethal fire conditions area. This question can be answered in the time, or area domain where the time domain is a simplification of the area domain concept. Figure 6 shows the process for deciding whether the structural fire damage area is small or large according to design in the area domain. If the concept of no structural fire damage is adopted, $A_{str} = 0$, thus always smaller than A_{crit}.

When defining the structural fire damage area in relation to question 3 in figure 5 for multi-compartment buildings, active systems such as sprinklers and fire alarms should be ignored. The approach calls for a conservative onset with regards to active systems as structural fire protection in this context is considered a final safety
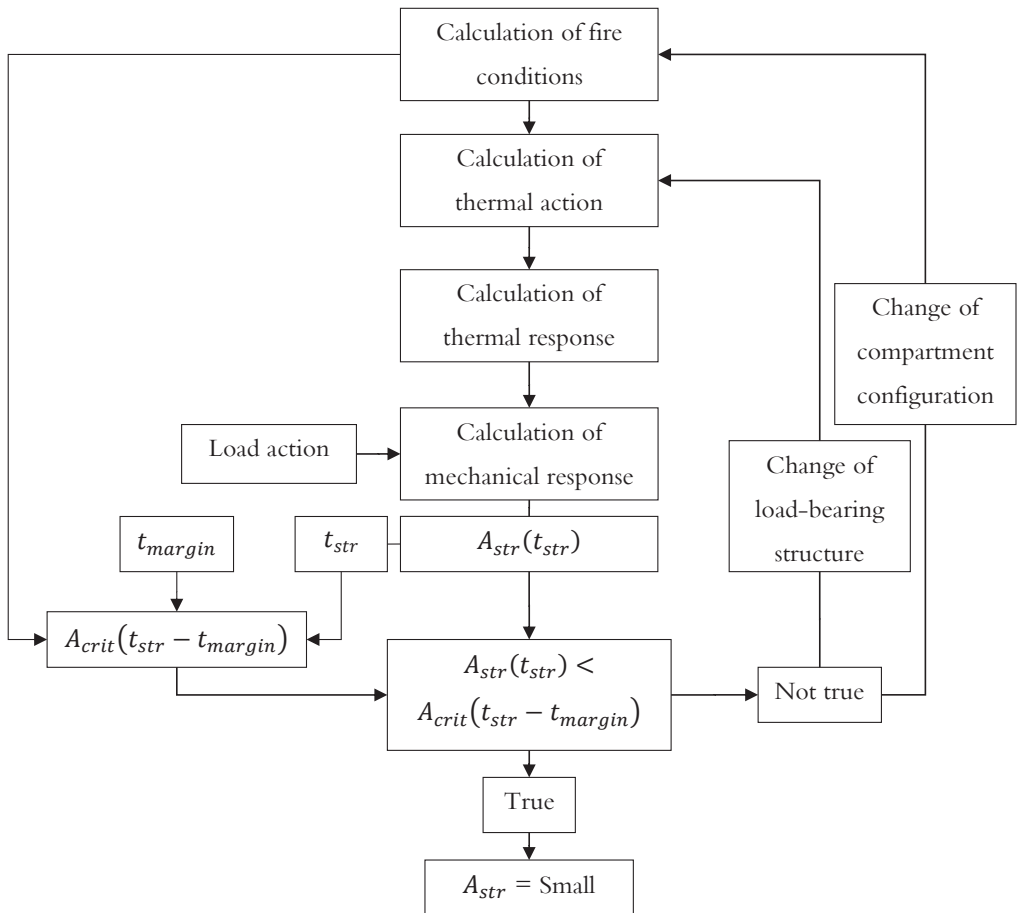
*Figure 6 Flow-chart in the area domain for deciding if the
structural fire damage area in figure 5 is small.*

barrier. However, when estimating actual safety levels with regards to structural
fire damage, active systems can play a vital part in the overall assessment.

For multiple-compartment buildings, question 3 in figure 5 discusses whether
unaware occupants outside the lethal fire conditions area can be affected by the
structural fire damage. In these cases, the structural fire damage area can be assumed
to go beyond the compartment affected by the lethal fire conditions, i.e. $A_{str} >$
A_{crit}. Thus, for a multiple-compartment building, progressive collapse must be

addressed in an adequate way to prevent the structural fire damage outside the lethal fire conditions area. The same concept applies to scenarios where a fire will affect only parts of a building.

In buildings consisting of only one compartment where the conditions can be assumed homogenous in case of fire and structural fire damage does not affect occupants or firefighters outside the compartment, the flow chart in figure 6 can be simplified to allow for design in the time domain, see figure 7.
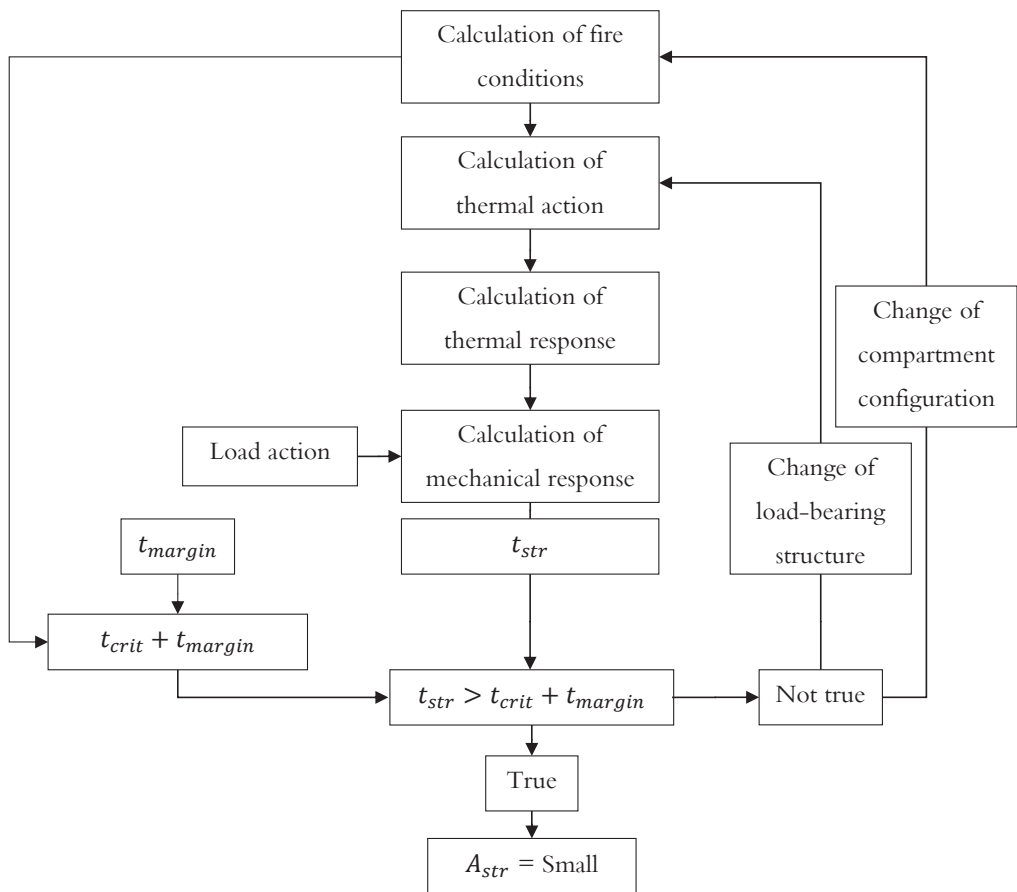

Figure 7 Flow-chart in the time domain for deciding if the structural fire damage area in figure 5 is small.

3.2 Single-compartment buildings

A single-compartment building with no interior walls present a situation where occupants and/or firefighters subject to a possible structural fire damage is notified by the fire beforehand. The notification, or warning, can be from a fire alarm, sprinkler or any other active system. However, even if all active systems fail, the fire itself will present sufficient warning before any structural fire damage.

Fires in single-compartment buildings can be divided into two different scenarios, with or without homogenous fire conditions in the compartment. The single-compartment building with homogenous fire conditions is a good first example of how the approach can be applied in real design cases. This is also shown in papers B and C with a design case study in the time domain.

3.2.1 Homogenous conditions

For single-compartment buildings, where the structural fire damage can be assumed to occur from heating by the homogenous hot gas layer temperature, the lethal fire conditions area and building area can be considered equal, i.e. $A_{str} = A_{crit} = A_{building}$. If outwards collapse is prevented, the size of the structural fire damage area is only limited by the building area, see figure 8.
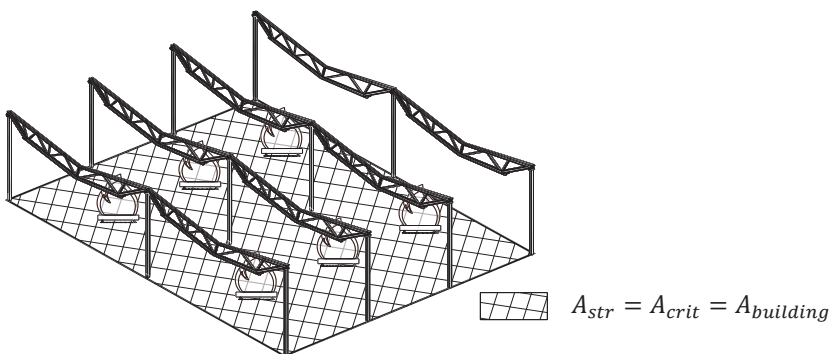

$$A_{str} = A_{crit} = A_{building}$$

Figure 8 Single-compartment building with homogeneous conditions.

Design is preferably carried out in the time domain and should aim at delaying structural fire damage, t_{str}, until after the time to lethal fire conditions, $t_{crit} + t_{margin}$, have occurred in the compartment. Thus, the design criterion is stated as in equation (1).

$$t_{str} \geq \left(t_{crit} + t_{margin} \right) \qquad (1)$$

For situations where firefighting tactics include working on the roof, or where occupants can be on the roof while heating progresses underneath, it should be considered if structural fire damage is acceptable.

3.2.2 Non–homogenous conditions

It is rare in large compartments that the hot gas layer has a homogenous temperature with simultaneous flashover in the entire compartment. Thus, structural fire damage due to local conditions can occur before untenable fire conditions prevent firefighting in all parts of the compartment. For this case, it is important to divide the compartment in a lethal fire conditions area, A_{crit}, and a structural fire damage area, A_{str}, see figure 9.
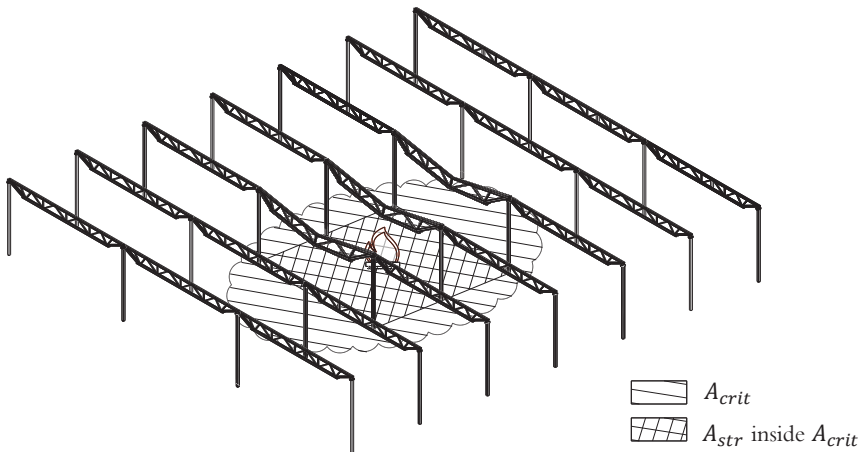

A_{crit}
A_{str} inside A_{crit}

Figure 9 A_{crit} and A_{str} for a compartment with non-homogenous fire conditions.

Design is preferably carried out in the area domain and should aim at limiting the size of the structural fire damage. At the time of structural fire damage, t_{str}, A_{str} should be smaller and within the bounds of A_{crit}. The design criterion is then be stated as in equation (2).

$$A_{crit}\left(t_{str} - t_{margin}\right) \geq A_{str}(t_{str}) \qquad \textit{(2)}$$

3.3   Multiple-compartment buildings

Multiple-compartment buildings have many similarities to single-compartment buildings with non–homogenous conditions. The main difference is that, while for the single-compartment case where the conditions are limited by the fire size, for the multiple-compartment building the conditions can be limited in size by the compartment size as well. For this reason, as will be explained below, the life safety objective in structural fire safety design can for some cases of multiple-compartments buildings only be achieved by prevention of structural fire damage.

3.3.1 Single–story buildings

The first step is to adopt a single-compartment approach (section 3.2) for each compartment to ensure the probability of unsafe outcome is limited in each of the compartments. The second step is to evaluate the probability for progression of a structural fire damage to an adjacent, non-exposed compartment. Adjacent compartments should be treated as outside the lethal fire conditions area; thus, it is important to limit progressive collapse outside the initial compartment.
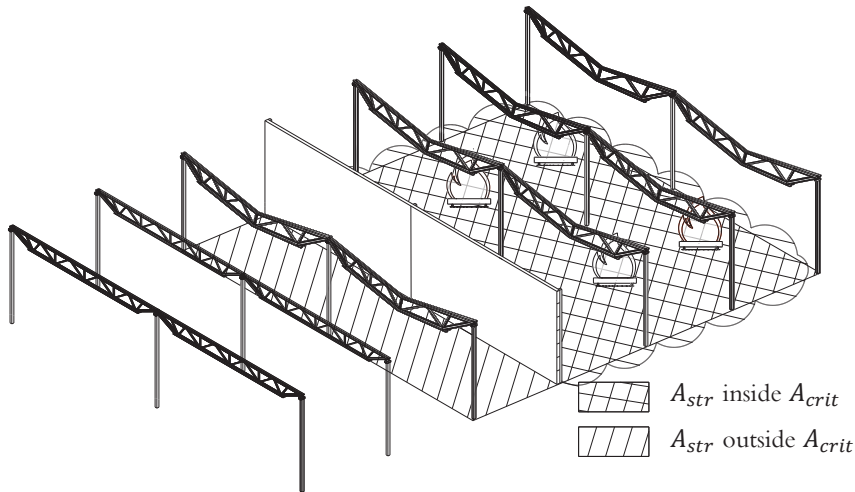
Figure 10 A_{crit} and A_{str} for a single-story, multi-compartment building with homogenous fire conditions in one of the compartments.

A tragic example of a case where this did not work as intended is a fire in Malmköping, Sweden, 1980. Two firefighters were protected from fire exposure behind a concrete wall but got crushed from a concrete beam falling down on top of them due to structural fire damage on the exposed side (Lilieh, 1980; Ödeen, 1980).

3.3.2 Multiple-story buildings

This scenario is based on the same principles as single-story, multiple-compartment buildings in the previous section but with vertical compartmentation rather than horizontal ditto. When progression of structural fire damage to floors above and below the fire exposed compartment is possible, the structure should withstand the entire duration of a fire. However, a light-weight top floor can locally be considered as a single-story building if the roof does not contribute to the overall stability of the building and no downward progression of a structural fire damage can be assumed, see figure 11.

This principle of locally considering the top floor to act as a single-story building in a multiple-story ditto can be found in the British building codes which stipulates an exception of fire resistance for structures only supporting the roof (HM Government, 2007). In the context of the new approach in this thesis, the British exception of structural fire resistance for the top floor should require that structural fire damage to the roof structure does not induce progressive collapse downwards.
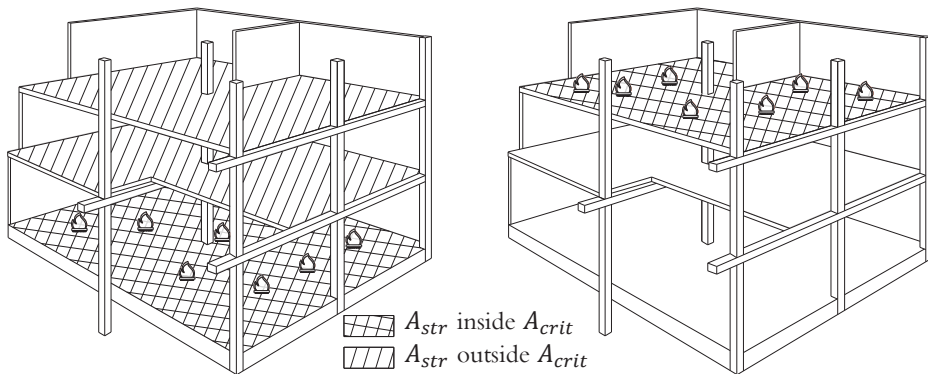

A_{str} inside A_{crit}
A_{str} outside A_{crit}

Figure 11 A_{crit} and A_{str} for a multi-story, multi-compartment building. The top floor can for special cases be considered a single-story building.

The fire in WTC twin towers is a tragic illustration of structural fire damage area in relation to fire conditions area in a multiple-story building (Shyam-Sunder, 2005). After the airplanes crashed in to each of the towers, an intense fire broke out at a mid-level story of the building. Occupants in stories above the fire at the time of impact was eventually prevented from exiting the building. For this case, occupants residing both below and above the fire conditions area were not killed by the fire itself but by the structural fire damage. The only feasible way to address life safety in this building would be to adopt a structural fire safety design strategy of preventing structural fire damage during the entire event of a fire. Unfortunately, in the WTC case, the building was unable to withstand the entire duration of the fire leading to the great tragedy.

4 DISCUSSIONS AND CONCLUSIONS

The electric light did not come from the continuous improvement of candles.

(Oren Harari)

4.1 Performance-based design

Performance-based design of fire exposed structures suffers from lack of coherency with regards to the life safety objective. There is a need for a common understanding and vocabulary to enable a more informed discussion regarding the basis of each statement in the performance-based design hierarchy.

This thesis provides and expands the interpretation of the life safety objective by adding a functional statement that always apply in structural fire safety design. The functional statement also explains why loss of life due to structural fire damage is rare in e.g. single-story steel frame buildings without applied structural fire protection. For most cases in these buildings, it is impossible to be alive due to the fire conditions at the time of structural fire damage.

4.2 Design aiming for the life safety objective

To address the life safety objective, a new design approach was described in paper A. Paper B and C demonstrate how to apply the conceptual content of paper A into practical design by implementing the design approach in a simple building.

The approach covers multiple engineering topics, some of which are in themselves extensive and impossible to cover in full detail in a thesis like this. However, by adopting the principle of achieving a 'necessary level of crudeness' with regards to the accuracy of the models, paper B is assumed to present a reliable enough design procedure with regards to the life safety objective.

When further combining the design procedure in paper B with Monte Carlo simulation, most of the causes for unsafe outcome was exposed. Thus, the calculated safety levels in paper C is deemed to represent the safety in the building.

The new approach is based on a straight-forward assumption; if survival is precluded for an area, structural damage limited to that area will not increase the risk for human injury. Even though the rationale is simple to understand, the application of the approach has not previously been formulated in a design setting. The formulation of the design process for the new approach enables scrutinization of each design step with the transparency required for good engineering practice.

4.3   Which parameters are important?

In paper C, the probabilistic study of life safety in a single-story steel frame building, no single parameter could be pin-pointed as the most important. For most cases, unsafe outcome occurs due to heating of the steel truss from direct localized fire exposure rather than from heating from the hot gas layer. This requires two or more extreme values of the identified parameters to coincide (extreme end in parentheses).

1. Maximum heat release rate (high),
2. Heat release rate per unit area (high)
3. Critical steel temperature (low), and
4. Distance from the plume centerline to the most sensitive elements of the lower chord of the steel truss (short).

In real fires, it is improbable that two or more of these parameters simultaneously have values within the threshold of posing a risk. This was shown in paper C as a low probability of unsafe outcome.

In paper F, parameters were assumed beforehand and the importance of them evaluated in the calculations. It was noted that changes to any of the parameters affected the achieved safety level in relation to the safety level calculated using the partial coefficient method as stipulated in EN 1991-1-2. This indicates a need for including more parameters in the semi-probabilistic approach in EN 1991-1-2 and that the EN-approach is conservative.

4.4   Concluding remarks

The new approach presented in this thesis addresses life safety in structural fire safety design even though structural fire damage is permitted. Thus, the safety levels can be evaluated even for buildings where structural fire damage is most likely. Consideration to other interests, such as economic, societal, and environmental values introduces another dimension where resisting the full duration of the fire might be a preferred option.

By making a clear distinction between the life safety and the saving property objectives, it is possible to make more informed and nuanced decisions and to address each of the objectives adequately.

Finally, it is crucial to note that the approach presented in this paper evaluates structural fire safety. First and foremost, fire safety principles regarding safe evacuation are required. However, if all systems fail, the approach aids in evaluating what level of structural fire resistance suffice to minimize the risk for loss of life.

4.5   Future research

Research on structural fire damage needs to consider the relevance of structural integrity in relation to the fire conditions in the building. Work on structural fire damage is usually based on standard fire test exposure with a one-sided focus on time. This focus needs to include localized fire exposures and a view of the fire resistance time as a consequence of fire conditions and the risk for loss of life.

To enable relevant considerations to fire conditions, harm from thermal radiation to firefighters requires further investigation. Research in this area is currently mainly focused on thermal burns to the level of pain while little is performed on mortality. The assumptions in regarding mortality in paper B and C are therefore chosen to be conservative. These assumptions can be refined, and design values adjusted to relevant levels.

Parallel to investigations on harm from thermal radiation, research is required on what mode of structural fire damage causes the least risk for harm to occupants and/or firefighters. Work on modes of structural damage in single-story steel frame buildings exposed to localized fires have been performed by Iqbal (2016) showing a high level of resilience in steel frames. However, his study only demonstrated one of several possible damage modes and further studies are needed. Such studies should include fire induced progressive collapse in single-story buildings as this creates large structural fire damage areas posing a risk for occupants and/or firefighters outside the lethal fire conditions area.

Stochastic modelling of structural fire damage from natural fires, requires work in the area of input parameters such as probability of ignition in connection to number of occupants, cooking facilities etc. Another parameter of importance is heat release per unit area where only scarce and deviating guidance can be found.

Advancing the knowledge on the issues mentioned in this section would promote the full potential of the new approach presented in this thesis. However, not all questions are for the engineers alone to solve. Legislators needs to act on questions such as lethality criteria which include difficult ethical considerations. However, it is the authors hope that this contribution can inspire to a change in the fire engineering community and a new way of looking at structural fire safety design.

REFERENCES

ABCB. (2015), *NCC, National Construction Code 2015 Building Code of Australia - Volume Two*.

Almgren, E. and Hansson, P. (2010), "'Finding the performance in Performance Based Codes' - Lessons learned from the pre-study for the renewal of the Swedish Fire Safety Code due to 2010", *Proceedings of the 8th International Conference on Performance-Based Codes and Safety Design Methods*, Society of Fire Protection Engineers, Lund, pp. 125–134.

Beyler, C.L. (2002), "Fire Hazard Calculations for Large open Hydrocarbon Fires", in DiNenno, P.J. (Ed.), *SFPE Handbook of Fire Protection Engineering, 3nd Edition*, National Fire Protection Association, pp. 2–45 – 2–87.

Boverket. (2015), *EKS 10, Boverket Mandatory Provisions Amending the Board's Mandatory Provisions and General Recommendations (2011:10) on the Application of European Design Standards (Eurocodes), EKS*, Vol. BFS 2015:6.

Buchanan, A.H. and Abu, A.K. (2016), *Structural Design for Fire Safety, Second Edition*, John Wiley & Sons, Ltd., https://doi.org/ 10.1002/9781118700402.

CPR. (2011), *Construction Product Regulation, Regulation (EU) No 305/2011of the European Parliament and of the Council Laying down Harmonised Conditions for the Marketing of Construction Products and Repealing Council Directive 89/106/EEC*.

Elms, D.G. (1992), "Consistent Crudeness in System Construction", in Topping, B.H.V. (Ed.), *Optimization and Artificial Intelligence in Civil and Structural Engineering: Volume I: Optimization in Civil and Structural Engineering*, Springer Netherlands, Dordrecht, pp. 71–85.

Frank, K., Spearpoint, M., Fleischmann, C.M. and Wade, C.A. (2011), "A Comparison of Sources of Uncertainty for Calculating Sprinkler Activation", *Fire Safety Science*, Vol. 10, pp. 1101–1114.

Guowei, Z., Guoqing, Z., Guanglin, Y. and Yong, W. (2016), "Quantitative risk assessment methods of evacuation safety for collapse of large steel structure gymnasium caused by localized fire", *Safety Science*, Vol. 87, pp. 234–242.

Hadjisophocleous, G.V. and Bénichou, N. (2000), "Development of performance-based codes, performance criteria and fire safety engineering methods", *International Journal on Engineering Performance-Based Fire Codes*, Vol. 2 No. 4, pp. 127–142.

Haviland, D.S. (1978), *Toward a Performance Approach to Life Safety from Fire in Building Code and Regulations, NBS-GCR-78-118*, Center for Fire Research, National Bureau of Standards, US Department of Commerce.

HM Government. (2007), *Volume 2 - Buildings Other than Dwellinghouses, Approved Document B (Fire Safety), The Building Regulations 2010.*

Iqbal, N. (2016), *Analysis of Catenary Effect in Steel Beams and Trusses Exposed to Fire*, PhD Thesis, Luleå University of Technology, Luleå, Sweden.

Lilieh, H. (1980), "★ redan 1.32 efter larmet", *Brandförsvar*, No. 4.

Meacham, B.J. (1996), *The Evolution of Performance-Based Codes & Fire Safety Design Methods*, Society of Fire Protection Engineers.

NFPA. (2006), *NFPA 101, Life Safety Code®.*

Ödeen, K. (1980), "Brandsäker! Men vad händer vid en brand", *Brandförsvar 4.*

Sandman, T. (1989), *Brand i Hallbyggnader, SBI Publikation 113*, Stålbyggnadsinstitutet.

Shyam-Sunder, S. (2005), *Federal Building and Fire Safety Investigation of the World Trade Center Disaster: Final Report of the National Construction Safety Team on the Collapses of the World Trade Center Towers (NIST NCSTAR 1)*, National Institute of Standards and Technology, Gaithersburg, MD.

Strömgren, M., Nilsson, M., Sandström, J., Jönsson, R. and Järphag, T. (2014), *Bärförmåga Vid Brand i Hallbyggnader Med Samlingslokal (Br2), SP Report 2014:49*, SP – Swedish Technical Research Institute.

Wang, Y., Burgess, I., Wald, F. and Gillie, M. (2012), *Performance-Based Fire Engineering of Structures*, CRC Press.

Węgrzyński, W. and Sulik, P. (2016), "The philosophy of fire safety engineering in the shaping of civil engineering development", *Bulletin of the Polish Academy of Sciences Technical Sciences*, Vol. 64 No. 4, pp. 719–730.

Zhang, C. and Usmani, A. (2015), "Heat transfer principles in thermal calculation of structures in fire", *Fire Safety Journal*.

PAPER A

The Life Safety Objective in Performance-Based Structural Fire Safety

Sandström, J., Wickström, U., Thelandersson, S. and Lagerqvist, O.

THE LIFE SAFETY OBJECTIVE IN PERFORMANCE-BASED DESIGN FOR STRUCTURAL FIRE SAFETY

J. Sandström, *Luleå University of Technology, Sweden*
U. Wickström, *Luleå University of Technology, Sweden*
S. Thelandersson, *Lund University, Sweden*
O. Lagerqvist, *Luleå University of Technology, Sweden*

ABSTRACT

Structural stability is not necessarily required for buildings where life safety is the sole structural fire safety objective. However, a structural collapse is only acceptable in an area where lethal fire conditions have developed. Therefore, structural failures due to fire resulting in risks of progressing outside of the area of lethal fire conditions need to be addressed. Thus, a new type of design principles for the life safety objectives is presented here which enables an evaluation of more precise risk assessments and more cost-efficient solutions without compromising human safety.

1 INTRODUCTION

1.1 FIRE SAFETY OBJECTIVES

The first step in a performance-based fire safety design process according to Hadjisophocleous et al. is to identify and list all code objectives [1]. Haviland [2] condensed this to two objectives:

1. Save lives, and
2. Save property.

In the Eurocodes, the first objective is the same, but the second objective is differently phrased: "property" has been changed to "economic, societal and environmental costs" [3].

In the late 90's, Buchanan found that the focus tended to shift from an emphasis on property protection to life safety [4]. Life safety as an objective is, however, difficult to handle separately in structural fire safety engineering. It is therefore usually correlated to structural stability during the entire event of a fire [5–11]. Another approach is to compare the time of structural stability to the time to evacuate and the time necessary for the fire rescue service to begin fire suppression activities [12, 13].

Buchanan argues that codes should clearly state its objectives and performance requirements [14]. However, the approach of maintaining structural stability to allow for fire rescue service intervention is difficult to combine with buildings with no formal requirement of fire protection. This leads to an unclear understanding of the background to the time requirements specified as a "specific" period of time [15], a "reasonable" period of time [16] or an "appropriate" period of time [17] in the codes. Without any clear understanding of these time concepts, time itself becomes the structural fire safety objective rather than the objective to save lives often leading to more expensive solutions.

To understand the life safety objective and the time requirement, a new approach is required. One such approach was introduced by Guowei in 2016 when evaluating life-safety in correlation to structural fire safety design for a steel frame building [18]. Guoweis evaluated whether tenable conditions occurred in a fire compartment before structural failure. With a strict interpretation of Guoweis's views, the life safety objective is met when

structural failure no longer presents any additional risk to the occupants due to lethal fire conditions in a building. The functional requirement can therefore be formulated based on the relation between lethal fire conditions and structural failure.

Adopting this approach enables the two objectives presented earlier to be handled separately on a more detailed level, and it opens opportunities for a higher precision in structural fire safety design.

1.2 OBJECTIVES AND LIMITATIONS

The main objective of this paper is to present an alternative basis for structural fire safety design with focus on life safety as a specific objective.

However, it does not:

- address or evaluate the concepts of economic, social or environmental costs,
- evaluate the benefits of active fire protection measures, or
- present any explicit design criteria,

2 DEFINITIONS

2.1 LETHAL FIRE CONDITIONS AREA, A_{crit}

Lethal fire conditions area, $A_{crit}(t)$, is defined as the area where it is not possible to survive even for very short times for ordinary humans as well as trained fire rescue personnel at the time t.

2.2 STRUCTURAL FIRE DAMAGE AREA, A_{str}

Structural fire damage area, $A_{str}(t)$ is defined as the area, where danger of harm

or injury to humans can be expected, due to loss of structural integrity initiated by fire. This includes secondary system effects such as progressive failure affecting areas outside the region directly exposed to fire. The area A_{str} is zero until failure due to fire exposure first occurs in a structural element, t_{str}.

2.3 FIRE RESISTANCE TIME FOR STRUCTURAL ELEMENTS

When the design objectives are limited to saving lives, structural integrity in the structural fire damage area, A_{str}, is no longer an issue after the time, t_{crit}, when lethal fire conditions occurs in the same area. The following failure criteria for the structure can be formulated

$$t_{str} > t_{crit} + t_{margin}$$
$$\left(\text{within area } A_{str}(t_{str})\right) \qquad (1)$$

or

$$A_{str}(t_{str}) < A_{crit}\left(t_{str} - t_{margin}\right) \qquad (2)$$

where

t_{margin} = time margin accounting for prediction uncertainties.

Equation (1) states that the time to loss of structural integrity, t_{str}, must exceed the time, $t_{crit} + t_{margin}$, when lethal fire conditions has developed in the entire area $A_{str}(t_{str})$. The time margin, t_{margin}, is a safety margin introduced to limit the probability of violation of the proposed failure criterion.

Equation (2) states that the lethal fire conditions area, A_{crit}, must exceed the structural fire damage area, A_{str}, before the time of structural failure, t_{str}[1].

---

[1] Note that the concept of time introduced here should not be interpreted as fire resistance time related to standardized fire resistance time.

If it can be verified that equation (1) or (2) is fulfilled, no further action is needed. If this is not the case, the fire safety design of the structural system has to be altered. This can involve

- Changing the structural system to reduce the structural fire damage area, $A_{str}(t_{str})$,
- Increasing the fire resistance of the structure, t_{str}.

In cases where loss of structural integrity due to fire leads to unacceptable, economic or environmental consequences, the structure should be designed to withstand the thermal action during the entire event of the fire.

2.4 FIRE COMPARTMENTATION

A building is usually divided into fire compartments with separating barriers to limit fire and smoke spread and to facilitate evacuation.

3 CONSEQUENCE ANALYSIS

The practical application of the consequence analysis consists of three steps as in boxes 3.1 - 3.3 in the flow chart of Figure 1.

3.1 ESTABLISH STRUCTURAL SAFETY OBJECTIVE

It is necessary to establish whether the only structural fire safety objective is to save lives <u>or</u> to save economic, societal or environmental values as well. This decision can be based on input such as the buildings societal importance or the startup cost after the event of a fire. A hospital requires for example a short startup period after a fire.

3.2 STRUCTURAL FIRE DAMAGE AREA

The structural fire damage area is considered *small* when the lethal fire conditions area has the size of the entire building at the time of structural instability, i.e. $A_{crit}(t_{str}) = A_{building}$, , see Figure 2. For these cases, equation (1) is most relevant. When $A_{crit}(t_{str}) = A_{building}$ it is important that the building is prone to inward collapse to prevent structural fire damage outside the lethal fire conditions area, e.g. the building area.
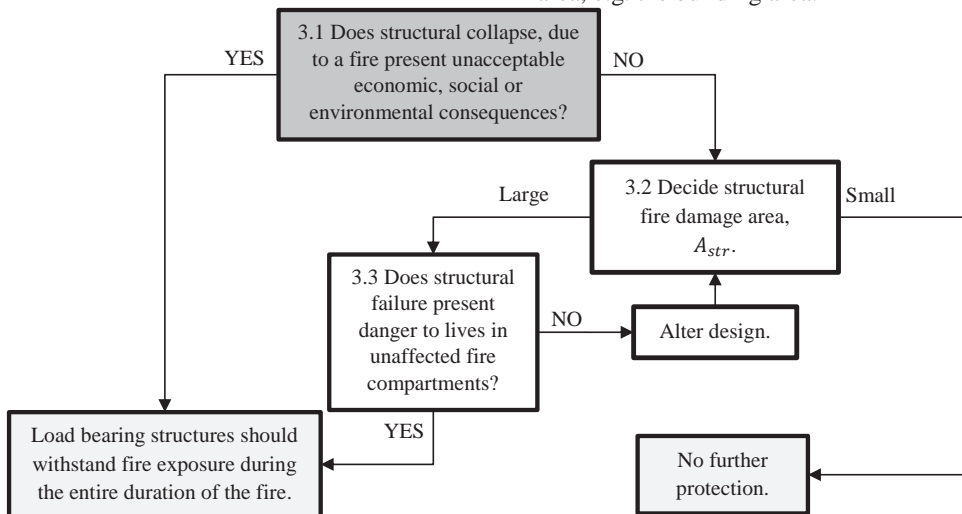
Figure 1 Flow chart for design approach.

Figure 2 Lethal fire conditions in the entire building simultaneously.

The structural fire damage area, A_{str}, is considered *small* when it is smaller than the lethal fire conditions area, A_{crit}, according to equation (2). This may be the case for large open fire compartments with non-homogenous fire conditions. Then it is important to address progressive collapse as such phenomena drastically increase the structural fire damage area.

In Figure 3, the fire damage area, A_{str}, is assumed limited to span B and C. For case 1, $A_{crit}(t_{str} - t_{margin})$ (hatched) is smaller than $A_{str}(t_{str})$. Thus, the building is not considered structurally safe as lives are endangered due to structural failure outside the lethal fire conditions area. In this scenario, the structural fire damage area is *large*. For case 2 in Figure 3, $A_{crit}(t_{str} - t_{margin})$ (hatched) exceeds $A_{str}(t_{str})$. In this scenario, the structural fire damage area is *small*. For this scenario, with $A_{crit}(t_{str} - t_{margin}) > A_{str}(t_{str})$, prevention of progressive failure to span A and/or span D is necessary in order to limit the structural fire damage to an area inside of the lethal fire conditions area.

3.3 OCCUPANTS IN ADJACENT FIRE COMPARTMENTS

Adjacent fire compartments are per definition outside the lethal fire conditions area. Therefore, compartmented buildings require extra consideration as structural fire failure outside a compartment on fire presents a risk to the life of humans.
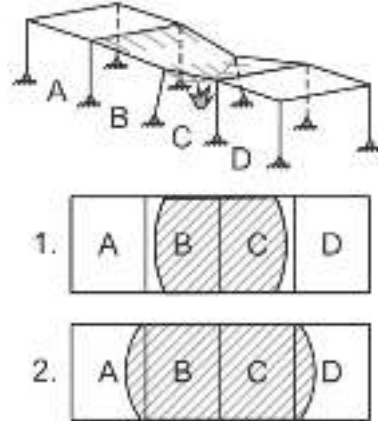
Figure 3 Lethal fire conditions area, $A_{crit}(t_{str} - t_{margin})$, (hatched) in relation to the structural fire damage area, $A_{str}(t_{str})$.

There are three distinct phases in assessing the risk of human life in a fire compartment other than the initial, A, see Figure 4. The first phase is when the integrity of the fire compartmentation is intact as shown in Figure 4. The entire fire compartment A can be a lethal fire exposure area, A_{crit}, but as long as the structural stability in compartment B is unaffected, there is no risk of human injury in this compartment (B). The second phase occurs when the separating structure fails, see Figure 4. From this point in time, phase three occurs, see Figure 4.3. If evacuation is possible from compartment B, the two fire compartments should be considered as one larger compartment and the assessment of risk for human injury or death, should be repeated for the new compartment (A + B) according to 3.2.

Evacuation can be prevented by the fire at the time of awareness presenting danger to lives, as illustrated to the left in Figure 5. For this scenario, compartment D and E will have no safe route from the building as the occupants are unable to pass compartment C due to lethal fire exposure.

Figure 4 The three phases in assessing the safety of humans in fire compartments other than the initial. When compartmentation is intact, (1), when the separating structure fails, (2), and when the fire has spread to the adjacent compartment (3).

If the occupants, however, are able to evacuate the building from compartment D and E, see Figure 5 to the right, but can be considered unaware of the structural instability, i.e. they are in compartment E, the fire compartmentation and the structural stability needs to be considered during the entire event of the fire. This should also be considered if structural failure in compartment C, see Figure 5 to the right, occurs simultaneously or even before the integrity of the compartmentation is compromised.
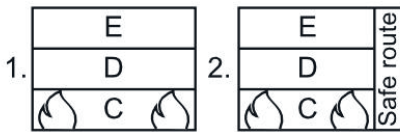
Figure 5 Structural instability in compartment C should not increase the risk of human injury in compartment D and E.

4   DISCUSSION

4.1   GENERAL COMMENT

The approach presented here attempts to be general with respect to load-bearing structures. No specific criteria are therefore established other than the concept of a sequential design, i.e. structural fire damage must not occur before lethal fire conditions have developed in a given area. The approach should be applicable to single

member analysis as well as sub-system or global analysis.

4.2   COMPARISON TO NATIONAL CONSTRUCTION CODES

National construction codes have different approaches. The approach presented in this paper for evaluating the risk of life safety, can, however, be found indirectly in many construction codes. Countries with no fire protection requirements for a particular type of construction use some kind of risk evaluation with regards to structural stability in case of fire.

In an international study 2014 [19], building codes from different countries were investigated. Many of these codes had similar features as can be explained by the approach presented in this paper.

The Danish [20] and Swedish construction codes [21] do not require fire protection for single story buildings given the fulfillment of certain design requirements with respect to *structural fire damage area.*

Structures only supporting the roof in the British [22] and Norwegian [23] building code do not need fire protection if they meet certain design requirements with respect to material and the overall stability. This can be explained by assuming that a fire on the top floor will not prevent evacuation. The Danish code [20], in a similar way, allows for less structural fire resistance on the entire top floor of a high-rise building.

5   CONCLUSION

The consequence analysis approach presented in this paper introduces a set of structural design principles and design criteria. It enables policy-makers to calibrate and evaluate construction codes to make optimal and well underpinned

decisions on structural fire safety requirements.

Although there is still work to be done, based on this approach it should be possible to design a common construction code for fire exposed load-bearing structures based a common or differentiated set of safety levels for each country.

6 ACKNOWLEDGMENTS

7 REFERENCES

1. Hadjisophocleous, G. V., Benichou, N., & Tamim, A. S. (1998). Literature Review of Performance-Based Fire Codes and Design Environment. *Journal of Fire Protection Engineering*, *9*(1), 12–40.

2. Haviland, D. S. (1978). *Toward a Performance Approach to Life Safety from Fire in Building Code and Regulations, NBS-GCR-78-118*. Center for Fire Research, National Bureau of Standards, US Department of Commerce.

3. *EN 1991-1-7. Action on structures - Part 1-7: General actions - Accidental actions*. (2006). Brussels: European Committee for Standardization, CEN.

4. Buchanan, A. H. (1999). Implementation of performance-based fire codes. *Fire Safety Journal*, *32*, 377–383.

5. Iqbal, S., & Harichandran, R. S. (2010). Reliability-Based Capacity Reduction and Fire Load Factors for Design of Steel Members Exposed to Fire. In *Structures in Fire: Proceedings of the Sixth International Conference* (pp. 75–82).

6. Au, S. K., Wang, Z.-H., & Lo, S.-M. (2007). Compartment fire risk analysis by advanced Monte Carlo simulation. *Engineering Structures*, *29*(9), 2381–2390. doi:10.1016/j.engstruct.2006.11.024

7. De Sanctis, G., Fischer, K., Kohler, J., Faber, M. H., & M., F. (2014). Combining engineering and data-driven approaches: Development of a generic fire risk model facilitating calibration. *Fire Safety Journal*, *70*, 23–33.

8. He, Y. (2013). Probabilistic fire-risk-assessment function and its application in fire resistance design. *Procedia Engineering*, *62*, 130–139. doi:10.1016/j.proeng.2013.08.050

9. Magnusson, S.-E. (1974). *Probabilistic analysis of fire exposed steel structures* (No. Bulletin 27). Lund Institute of Technology, Division of structural mechanics and concrete construction.

10. Schleich, J.-B. (2009). Performance Based Design for the Fire situation, Theory and Practice. In *Proceedings of Nordic Steel Construction Conference 2009* (pp. 146–155).

11. Schleich, J.-B. (2005). Calibration of Reliability Parameters. In *Implementation of Eurocodes, Handbook 5 - Design of Buildings for the Fire Situation*.

12. Buchanan, A. H., & Abu, A. K. (2016). *Structural Design for Fire Safety, Second Edition*. John Wiley & Sons, Ltd. doi:10.1002/9781118700402

13. Kruppa, J., Buchanan, A. H., Fontana, M., Jackman, P. E., Kokkala, M., Landro, H., … Walsh, C. J. (2001). *Rational fire safety engineering approach to fire resistance of buildings, Publication 269*. CIB W014.

14. Buchanan, A. H. (1994). Fire Engineering for a Performance Based Code. *Fire Safety Journal*, *23*, 1–16.

15. Regulation (EU) No 305/2011 of the European Parliament and of the Council. (2011, March 9). Council Directive 89/106/EEC.

16. Meacham, B. J. (1996). *The Evolution of Performance-Based Codes & Fire Safety Design methods*. Society of Fire Protection Engineers.

17. Wang, Y., Burgess, I., Wald, F., & Gillie, M. (2012). *Performance-Based Fire Engineering of Structures*. CRC Press.

18. Guowei, Z., Guoqing, Z., Guanglin, Y., & Yong, W. (2016). Quantitative risk assessment methods of evacuation safety for collapse of large steel structure gymnasium caused by localized fire. *Safety Science*.

19. Strömgren, M., Nilsson, M., Sandström, J., Jönsson, R., & Järphag, T. (2014). *Bärförmåga vid brand i hallbyggnader med samlingslokal (Br2), SP report 2014:49*. SP - Swedish Technical Research Institute.

20. Eksempelsamling om brandsikring af byggeri 2012, 2. reviderede udgave 2016 (2016). Trafik- og Byggestyrelsen.

21. *Boverkets föreskrifter och allmänna råd om tillämpning av europeiska konstruktionsstandarder (eurocoder), BFS 2015:6*. (2016). Karlskrona: Boverket.

22. The Building Regulations 2010 - Approved document B (Fire safety) (2010). HM Government.

23. Byggteknisk forskrift (TEK10) (2016). Direktoratet for byggkvalitet.

PAPER B

Life Safety in single story steel frame building,
Part I – Deterministic design

Sandström, J.

Life safety in single story steel frame buildings, Part I - deterministic design

Joakim Sandström, Luleå University of Technology

1 Abstract

This paper discusses fire safety design of single story-, single compartment buildings and evaluates whether time to structural damage is a relevant criterion when lethal fire conditions develop long before any structural fire damage can occur. Current performance-based design practice aims at achieving the life safety objective by preventing structural failure for the entire duration of a natural fire or for a fixed time of standard fire exposure. Prevention of structural fire damage is always relevant for multistory buildings, or buildings with complex geometries as structural fire damage may then threaten occupants and/or firefighters outside the area directly affected by the fire. However, for single-story-, single-compartment buildings, prevention of structural fire damage is less relevant in relation to the life safety objective.

The advantage of the new design philosophy presented in this paper is the possibility to define how the level of structural fire resistance in single-story-, single-compartment buildings can be determined in a consistent way. This level of fire resistance requirement in these buildings differ amongst countries but could be harmonized by accepting of the design philosophy suggested in this paper.

The proposed approach is demonstrated in a design case study of a steel truss in a typical Swedish single-story steel frame building. While not complying with deemed to satisfy fire resistance ratings, it is argued that the proposed design still can fulfill the life safety objective.

Keywords: Structural fire safety design, Performance based design, fire engineering, life safety

2 Introduction

2.1 Background

National building authorities require different levels of structural fire protection to achieve the life safety objective in buildings (Strömgren et al., 2014). The most common way to address the life safety objective is to associate life safety to a fire resistance time requirement, e.g. R 30/60, or, as in performance-based design as *no failure during an entire fire*.

Sandström et al (2017) introduced the concept of dividing the requirements into *no failure during an entire fire* and *no failure during a limited duration of a fire* as a tool for understanding the fire resistance requirements. As the requirement *no failure during an entire fire* is clear and well defined, it is not elaborated on further in this paper. However, the connection between times of fire resistance and the life safety objective for the requirement *no failure during a limited duration of a fire* is not clear creating a situation where structural fire resistance requirements are based on magical numbers (Law and Beever, 1995).

This paper presents a structural fire safety design study of a single-story steel frame building adopting the approach by Sandström et al. (2017). The approach is based on the principle that structural fire damage shall be prevented in locations where survival from thermal exposure is possible. As firefighters are better protected against harmful environments, the focus in this paper is on preventing structural fire damage in relation to the capabilities of firefighters. Thus, when the assessment at a structure fire permits firefighting in a given area, the probability of structural fire damage should be prevented. On the other hand, if the fire conditions due to high thermal exposures in a given area make firefighting impossible, then additional structural fire protection does not decrease the risk of injury or harm to firefighters.

Using thermal exposure for estimation of lethality simplifies the comparison to structural fire damage as both the lethality and structural fire damage then stems from high fire temperatures. The approach and design methodology are elaborated on in more detail in the following sections.

2.2 Limitations

The limitations in the study are that:

1. Societal-, economic- and environmental values are not considered,
2. The structural response model only accounts for failure according to element analysis of the truss members, not accounting for any global behavior,
3. Active fire protection measures such as sprinklers and smoke ventilation are not considered,
4. Toxicity is not considered as firefighters are protected against toxicity to a much larger extent than against thermal burns,
5. The conditions for lethality due to burn injuries are determined based on calculations and information found in the literature, see section 2.4.

2.3 The life safety objective

The approach to structural fire safety design used in this paper considers life safety as the sole design objective as presented by Sandström et al. (2017). Sandström et al. states that the structural fire damage affecting an area, A_{str}, at the time of structural fire damage, t_{str}, can be accepted if lethal fire conditions have already developed in the same area.

A critical level of thermal radiation, $\dot{q}''_{rad,crit}$, does not imply immediate lethality to firefighters but by prolonging the exposure over a time, t_{margin}, survival is precluded even if a firefighter enters the building at $t(\dot{q}''_{rad,crit})$ without prior heating. $t(\dot{q}''_{rad,crit})$ is referred to as t_{crit} in the remainder of this paper. Even though pre-heating of the human body is relevant when analyzing firefighter safety (Lawson, 1996), it is ignored in this paper. Thus, lethal conditions is present in an area when the thermal radiation is higher than $\dot{q}''_{rad,crit}$ and has been so for at least t_{margin}, see Figure 1.
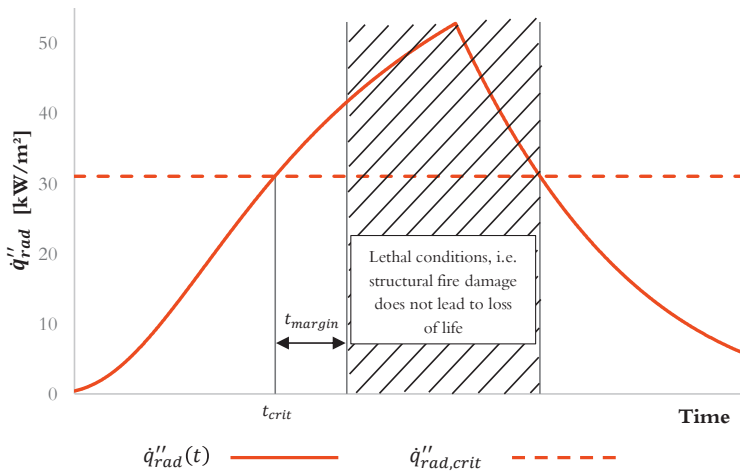
Figure 1 Relation between t_{crit}, t_{margin} and t_{str}. The time range when structural collapse yields acceptable consequences is indicated.

This is formulated as the failure criterion for the area A_{str}

$$t_{str} < t_{crit} + t_{margin} \qquad (1)$$

2.4 Lethal fire conditions

Lethal fire conditions are defined as a condition where it is impossible to survive even for very short times (Sandström et al., 2017). The lethal conditions as applied in this paper is determined as a combination of thermal radiation, $\dot{q}''_{rad,crit}$, and time, t_{margin}, as shown in Figure 1. $\dot{q}''_{rad,crit}$ is estimated based on a literature review. t_{margin} is determined from complementing calculations as shown below.

To estimate the time to burn injuries from surface heat flux, thermal burn is calculated using Henriques burn integral, HBI (Barker et al., 2006). The time to lethality is then defined as the time to reach third degree burns over the entire body, or HBI > 1.0. This agrees with suggestions by Hymes et al. (1993). For this paper, thermal exposure is assumed to act simultaneously on the entire body.

The time to HBI > 1.0 for different values of $\dot{q}''_{rad,crit}$ is calculated using the one-dimensional numerical approach (finite element) for skin temperatures as presented by Torvi and Dale (1994). Calculated values are shown in Table 1 where clothing and skin properties are as suggested by Jiang et al. (2010).

Torvi et al. suggests a two-step evaluation of the lethality from thermal burns for personnel with personal protection equipment, PPE (Torvi et al., 2000). The first step is to determine the time to ignition or deterioration of the PPE, and the second step is to determine the subsequent time to reach HBI > 1.0, see Table 1. The deterioration temperature of the PPE is assumed to be 520 °C which corresponds to Nomex™ in three layers (Kuchta et al., 1969).

As a complement, the time to HBI > 1.0 is also estimated without assumed deterioration of PPE. Calculated times are shown in Table 1.

Table 1 Time to Henriques burn integral HBI > 1.0 for calculations with or without clothing deterioration.

	Time to HBI > 1.0 for		
	$\dot{q}''_{rad,crit} = 20$ kW/m²	$\dot{q}''_{rad,crit} = 30$ kW/m²	$\dot{q}''_{rad,crit} = 40$ kW/m²
Two-step method (deterioration of PPE + time to burn)	(no deterioration occurs)	54 s (12 + 42)	21 s (11 + 10)
No deterioration of PPE	123 s	100 s	87 s

t_{margin} should at least be equal to the corresponding higher value for $\dot{q}''_{rad,crit}$ in table 1. For the calculations in this paper, $\dot{q}''_{rad,crit} = 30$ kW/m² is chosen to occur in the upper range of flashover which usually happens when the incident thermal radiation is in the range of $15 - 30$ kW/m² (Peacock et al., 1999). To warrant a design on the safe side $t_{margin} = 150$ s is therefore chosen for this paper.

2.5 Fire-fighting tactics

Standard tactics used in firefighting starts with an assessment of the situation by the commander in chief to evaluate risk versus benefit for entering the fire compartment. If the assessment concludes that no occupants can be alive at the time of arrival, the incentives for firefighters to enter a building with life-threatening conditions are non-existing (Mattsson and Eriksson, 2010). One such strong indicator of a

life-threatening condition is flashover; thus, it is here assumed that fire-fighters do not enter a building after flashover and retreat at first indication of flashover if inside the building. However, if saving lives is considered possible, entering a building can be deemed a viable option regardless of conditions.

Figure 2 shows the possible outcomes of different firefighting decisions at a structure fire. For this paper, there are four outcomes where structural fire failure is relevant to compare to lethal fire conditions. These outcomes are referred to as 1 - 3 in their flowchart boxes respectively.

Outcome 1 does not present unacceptable consequences regardless of structural fire failure or not.

Outcome 2 does not present unacceptable consequences if structural fire failure occurs after the time to lethal conditions.

Outcome 3 does not present unacceptable consequences if structural fire failure due to local fire is prevented.

Outcome 4 does present unacceptable consequences. However, by preventing structural fire damage for outcomes $1 - 3$, the unacceptable consequences are not due to structural fire failure but due to the lethality of the fire conditions in the compartment.
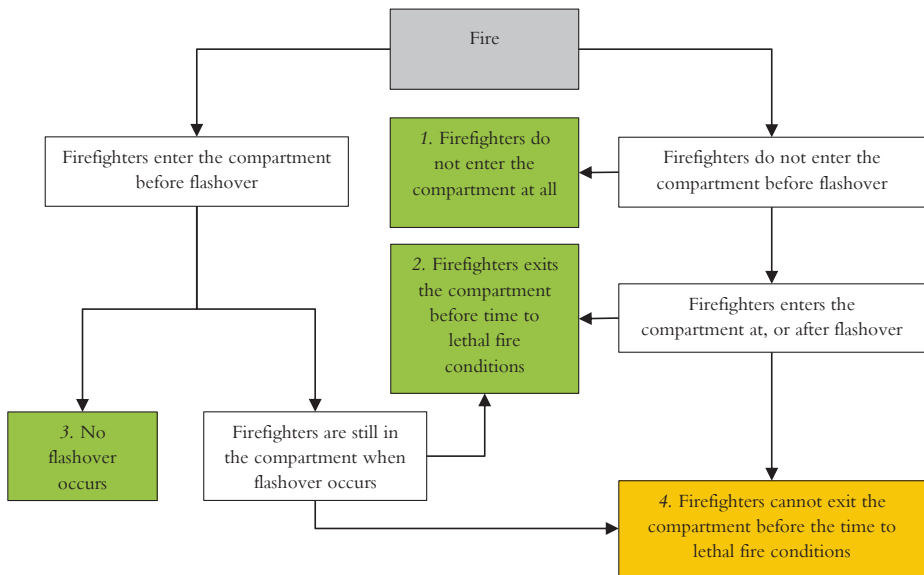
Figure 2 Different outcomes for firefighters at the structure fire used in this paper.

3 Case study

A single-story steel frame building with the dimensions 42 m by 87 m for selling utensils is analyzed. The maximum and minimum building heights are 8.5 m and 6.0 m, respectively. The structural design is based on columns and trusses with a stabilizing steel sheet roof. The lower chord is at a height of 4.6 m at its lowest point, see Figure 3.
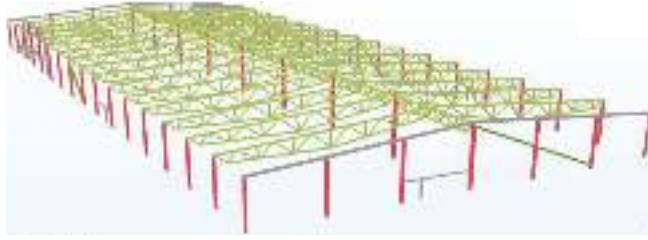
Figure 3 Overview of the load-bearing structure. Drawings from the entrepreneur.

The main entrance consists of sliding doors of 3 m by 3 m with an adjacent glass sections of an additional 3 m by 3 m. The entrance is open from the beginning and the glass section breaks after 855 s due to thermal tensions according to the B-Risk glass breakage model as described by Parry et al. (2003).

There is an opening of dimensions 3 m by 3 m for loading goods and six doors of dimensions 1.2 m by 2 m for egress, all assumed fully open.

3.1 Steel truss

The element numbers of the truss are presented in Figure 4 and their properties in Table 1.
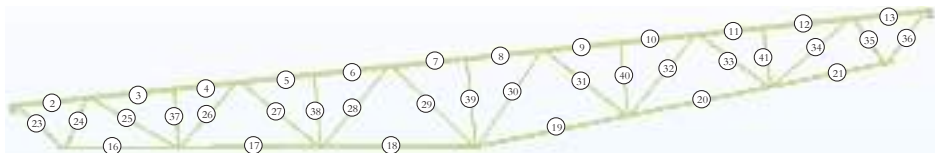
Figure 4 Truss layout with element numbers.

Table 1 Steel properties for the three different simulations.

	Steel Quality	Dimensions	$\mu_{0,fi,max}$	A_m/V	k_{sh} [ii]
Upper chord	S420J	L 100x10	0,34	203 m^{-1}	0.63
Lower chord	S355J	L 100x10	0,23	203 m^{-1}	0.87
Diagonals	S355J	UNP 100	0,31	320 m^{-1}	0.78

[i] further reference on calculation of shadow effects are presented in section 3.4

The fire resistance for the steel truss in prescriptive design is determined to 13 min if exposed to standard fire.

3.2 Calculation procedure

The calculation procedure using B-Risk (Wade et al., 2016) and the connection to Eurocode calculations is briefly described in Figure 5. Blue boxes represent design input values while black boxes represent deterministic calculations based on these values. If the condition in the last box, $t_{str} < t_{crit} + t_{margin}$, is true, then the failure of the structural element can lead to unacceptable consequences, i.e. firefighter fatality due to structural fire damage.
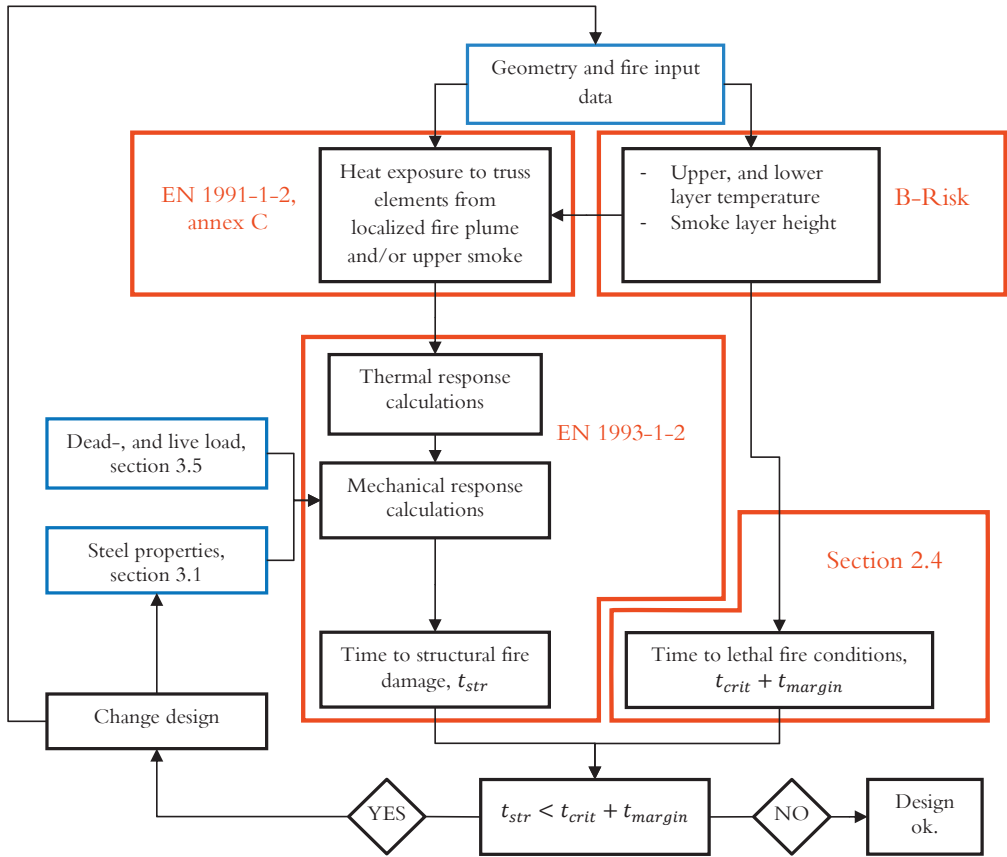
Figure 5 Flow chart describing the calculation process. Blue boxes represent design values, while black boxes are calculations using deterministic methods.

3.3 Design fire calculations

The fire compartment conditions are calculated using B-Risk, a two zone model developed by BRANZ in New Zealand (Wade et al., 2016). B-Risk is equipped with the ability to perform Monte Carlo simulations making it suitable primarily for the calculations in part II (Sandström, 2019) of this paper. The design values for the fire calculations are presented in Table 2.

Table 2 Fire design values used in B-Risk.

Parameter	Design value	Unit	Reference
Heat release per unit area	500	kW/m²	A, B
Fuel load density	600	MJ/m²	B
Fire growth rate, α	0.047	kW/s²	B
Height of fire above floor	1.3	m	Est.
Horizontal distance from plume centerline to each element in truss	0	m	–
Thermal inertia of sandwich walls $\sqrt{k\rho c}$	2400	J/m²Ks^{½}	C

[A] (*PD 7974-1*, 2003)
[B] (*Guide for Smoke and Heat Venting, NFPA 204M*, 1985)
[C] Approximated for reference according to the method used in (*EN 1991-1-2*, 2002) annex A.

In the pre-flashover stage of the fire, HRR is calculated according to αt^2, while HRR in post-flashover stage is calculated by B-Risk from the available oxygen from openings in the façade, see Figure 6. Only the initial part of the fire development is included to illustrate the fast fire growth, and the fully developed phase of the fire. Flashover occurs in the model after 1 460 s and all fuel is consumed at 28 900 s.
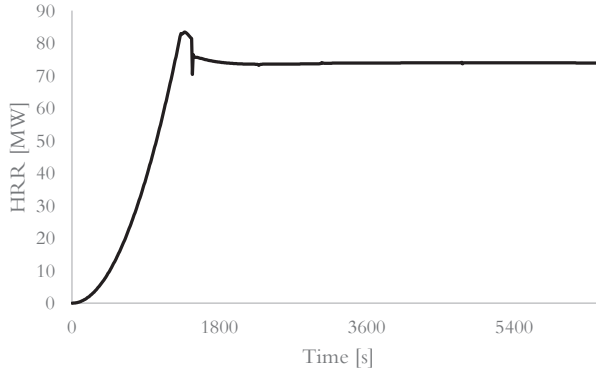
Figure 6 HRR in the fire compartment from calculations in B-Risk.

Thermal action on the steel truss elements is calculated from the gas temperature, T_g, assumed as the current maximum value of the hot gas layer, and the plume center line temperature at the corresponding height as suggested by Franssen et al (2001). In this paper, the localized fire temperature in the plume was calculated using the Heskestad approach as adopted in the Eurocodes (*EN 1991-1-2*, 2002).

3.4 Steel temperature calculations

The steel temperature in each element was calculated according to Eurocode 1993-1-2 as shown in the recursion formula:

$$T_s^{i+1} = T_s^i + k_{sh} \frac{A_m/V}{c_s \rho_s} \cdot \dot{q}_{tot}'' \cdot \Delta t \tag{2}$$

where T_s^i is the steel temperature at time step i, k_{sh} the correction factor for the section factor, A_m/V, to account for shadow effects. c_s is the specific heat of the steel, ρ_s is the density, and Δt is the size of the time step. $\dot{q}_{tot}''$ is calculated according to equation (3).

$$\dot{q}_{tot}'' = \varepsilon \sigma \left(T_g^4 - T_s^4\right) + h_c \left(T_g - T_s\right) \tag{3}$$

where $\varepsilon = 0.7$ for steel and $h_c = 35$ W/m²K for natural fires. All material properties used are the temperature dependent steel properties presented in EN 1993-1-2.

For open cross sections, not all surfaces are exposed to an equal amount of radiation. To account for this shadow effect, the perimeter of the cross section is reduced using a correction factor, k_{sh}. k_{sh} for the upper and lower chord is calculated to account only for the real amount of radiation heating the cross section (*EN 1993-1-2*, 2005; Franssen and Vila Real, 2010; Wickström, 2016).

For both the upper and lower chord, the combined cross section perimeter of the angled elements is considered as shown in Figure 7.
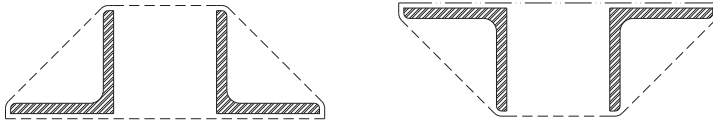
Figure 7 Assumptions of the combined cross section perimeter for calculation of the section factor including shadow effects for the lower (left) and upper (right) chord.

For the upper chord (to the right in Figure 7), the upper faces of the elements are partly shielded by the corrugated steel sheet as illustrated in Figure 8.
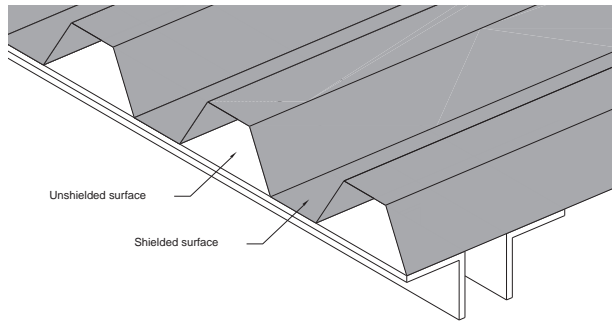
Figure 8. The upper face of the upper chord is partially exposed due to the corrugated steel sheet.

Table 1 shows the section factors and shadow effect correction factor, k_{sh}, for the different upper and lower chord, and the diagonals.

3.5   Load calculations

The characteristic snow load for the city of Skövde in Sweden is $s_k = 2.5$ kN/m², the shape factor for the roof, $\mu_i = 0.8$, and the partial coefficient for accidental loads in Sweden is the frequent value factor, $\psi_1 = 0.4$ (Boverket, 2016). The evenly distributed accidental design load was calculated as

$$E_{d,fi} = G_k + \psi_1\mu_i s_k = 0.77 + 0.4 \cdot 0.8 \cdot 2.5 = 1.57 \; kN/m^2 \qquad (4)$$

Data on the characteristic dead load, $G_k = 0.77$ kN/m², was presented by steel truss manufacturer.

4   Results

4.1   Time to lethal conditions

At the time of structural fire failure, t_{str}, flashover has occurred, and the compartment can be considered well mixed with uniform temperature in the entire compartment. Thus, thermal radiation to occupants is estimated only from the hot gas layer temperature, T_g, ignoring the direct thermal radiation from the plume. The time to lethal fire conditions, $t_{crit} + t_{margin}$, is calculated to 3140 + 150 s after ignition, e.g. t_{crit} is an output from the fire model as the time when the thermal radiation from the hot gas layer reaches 30 kW/m² and t_{margin} is decided according to section 2.4, see Figure 9. Figure 9 also shows the

steel temperature and time to structural fire failure, t_{str}, for the most critical element in the steel truss, element 3 (green cross).
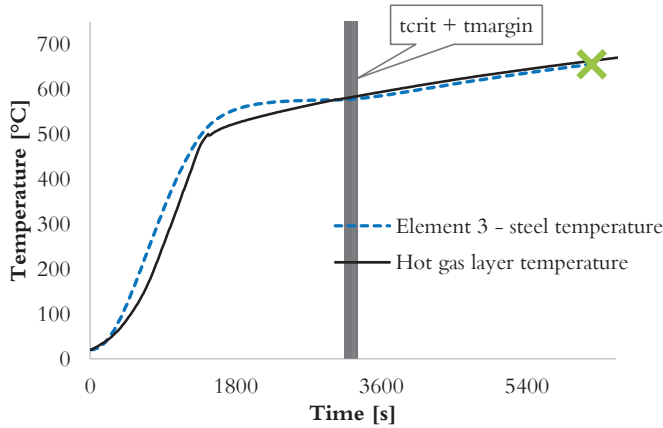
Figure 9 Global hot gas layer temperature and local steel temperature
for the most critical truss element, element 3.

Initially, the steel is heated by the localized fire, thus the steel element temperature, T_s, is higher than the global hot gas layer temperature, T_g.

4.2   Cost estimation

Deemed to satisfy solutions, or code compliance for steel trusses in national building codes are usually based on classification equivalent to R 30 or R 60 (Strömgren et al., 2014), and the most common way to achieve this for steel trusses is to apply fire intumescent paint. The cost is estimated by asking an entrepreneur for the cost of applying fire intumescent paint equivalent to R 30 (175 SEK/m²) and R 60 (275 SEK/m²) in comparison to regular corrosion protection paint (50 SEK/m²). The cost for the steel is based on the list price given by the steel truss manufacturer. Figure 10 shows the relative cost for the different deemed to satisfy solutions compared to the studied design case in this paper.
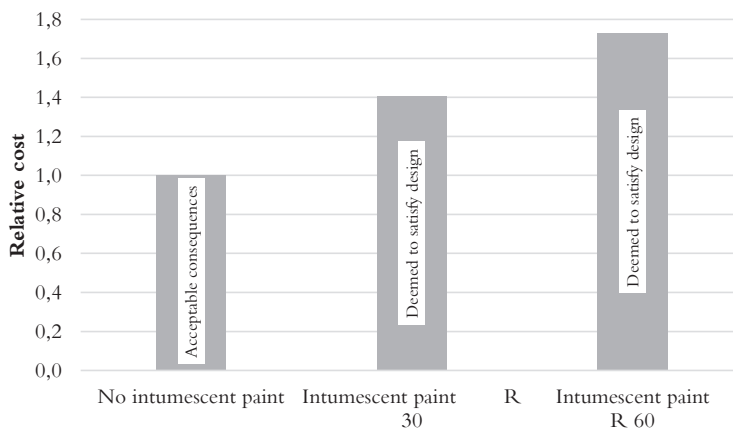
Figure 10 Relative cost for deemed to satisfy solutions compared to the studied design case.

5   Discussion

By shifting focus from time as a sole criterion to a more holistic view of the design, it is shown that life safety can be achieved even though the deemed to satisfy solution, i.e. R30/60, and *no failure during an entire fire* objective are disregarded. This change in perspective on structural fire resistance requirements shows a feasible path forward for achieving the life safety objective in a more nuanced way than previously possible.

Even though the approach creates room for a more nuanced design and, in this case unprotected structural elements, classification will always be needed for rational design solutions. The approach in this paper should rather be considered a complement to classification, and a way to interpret building code objectives.

In the studied fire case, the lower chord was designed to withstand the direct thermal impact from the localized plume fire prolonging the time for structural fire failure until after flashover and past the time to lethal fire conditions. Thus, instead of fulfilling the deemed to satisfy solution presented as time of fire resistance, the design strategy in this paper can be condensed to:

1.   Prevention of structural damage due to localized plume fire, and
2.   Prevention of structural fire damage prior to the time to lethal fire conditions due to incident thermal radiation from the hot gas layer.

Fire fighter safety is difficult to estimate as personal protective equipment, PPE, enables firefighters to work in very hot environments without sensing the heat. This is beneficial as the PPE prevents injury if the firefighters retreat in time, but the protection given by the PPE can also prevent firefighters from correct interpretation of the thermal danger.

There is much in this field to explore and thoroughly evaluate in order to find practical adaptations for different structural configurations as well as a reasonable balance between structural integrity and life safety both with regards to design numbers as well as firefighting tactics. However, it is the authors strong conviction that finding these common principles are possible and that this paper presents a way for doing that.

6   Conclusion

This paper has shown that the steel trusses in the studied building can be safe without additional fire protection. This reduces building cost without increasing the probability of unacceptable conditions due to structural damage.

It has also been shown that the life safety objective can be achieved even for structures that does not comply to deemed to satisfy fire resistance time requirements. Thus, fire resistance time itself should not be regarded as the sole criterion to meet in structural fire safety design, rather one among others such as *no failure during an entire fire* or structural stability in fire until after the time to lethal fire conditions.

7   Acknowledgements

8 References

Barker, R.L., Guerth-Schacher, C., Grimes, R.V. and Hamouda, H. (2006), "Effects of Moisture on the Thermal Protective Performance of Firefighter Protective Clothing in Low-level Radiant Heat Exposures", *Textile Research Journal*, Vol. 76 No. 1, pp. 27–31.

Boverket. (2016), *Boverkets föreskrifter och allmänna råd om tillämpning av europeiska konstruktionsstandarder (eurocoder), BFS 2015:6*, Boverket, Karlskrona.

EN 1991-1-2. (2002), *Action on Structures - Part 1-2: General Actions - Actions on Structures Exposed to Fire.*

EN 1993-1-2. (2005), *Design of Steel Structures - Part 1-2: General Rules - Structural Fire Design.*

Franssen, J.-M., Cadorin, J.-F. and Pintea, D. (2001), *The Design Fire Tool OZone V2.0 - Theoretical Description and Validation On Experimental Fire Tests*, University of Liege, Liege.

Franssen, J.-M. and Vila Real, P. (2010), *Fire Design of Steel Structures*, Wilhelm Ernst & Son, Berlin.

Guide for Smoke and Heat Venting, NFPA 204M. (1985), , National Fire Protection Association, Quincy, MA.

Hymes, I., Brearley, S., Prescott, B. and Zahid, M. (1993), *The Prognosis of Burn Injury Victims*, SRD/HSE Report R600, Safety and Reliability Directorate, Culcheth, Chesire, UK.

Jiang, Y.Y., Yanai, E., Nishimura, K., Zhang, H., Abe, N., Shinohara, M. and Wakatsuki, K. (2010), "An integrated numerical simulator for thermal performance assessments of firefighters' protective clothing", *Fire Safety Journal*, Vol. 45, pp. 314–326.

Kuchta, J.M., Furno, A.L. and Martindill, G.H. (1969), "Part I Ignition temperatures and flame spread rates", *Fire Technology*, Vol. 5 No. 3, pp. 203–216.

Law, M. and Beever, P. (1995), "Magic numbers and golden rules", *Fire Technology*, Vol. 31 No. 1, pp. 77–83.

Lawson, J.R. (1996), *Fire Fighter's Protective Clothing and Thermal Environments of Structural Fire Fighting*, No. NISTIR 5804, Buildingand Fire Research Laboratory, NIST, Gaitherburg, MD, p. 28.

Mattsson, M. and Eriksson, L. (2010), *Taktikboken : En Handbok i Hur Man På Ett Scenariobaserat Sätt Genomför Effektiva Insatser Vid Brand i Byggnad*, Informationsbolaget, Malmö.

Parry, R., Wade, C.A. and Spearpoint, M. (2003), "Implementing a Glass Fracture Module in the BRANZFIRE Zone Model", *Journal of Fire Protection Engineering*, Vol. 13 No. 3, pp. 157–183.

PD 7974-1. (2003), *Application of Fire Safety Engineering Principles to the Design of Buildings - Part 1: Initiation and Development of Fire within the Enclosure of Origin (Sub-System 1)*, p. 76.

Peacock, R.D., Reneke, P.A., Bukowski, R.W. and Babrauskas, V. (1999), "Defining flashover for fire hazard calculations", *Fire Safety Journal*, Vol. 32 No. 4, pp. 331–345.

Sandström, J. (2019), "Life safety in single-story steel frame buildings, Part II - probabilistic design", *Journal of Fire Protection Engineering (to Be Submitted)*.

Sandström, J., Wickström, U., Thelandersson, S. and Lagerqvist, O. (2017), "The life safety objective in performance-based design for structural fire safety", *Proceedings of the 2nd International Conference*

on Structural Safety Under Fire and Blast Loading, CONFAB 2017, Brunel University London, pp. 411–417.

Strömgren, M., Nilsson, M., Sandström, J., Jönsson, R. and Järphag, T. (2014), *Bärförmåga Vid Brand i Hallbyggnader Med Samlingslokal (Br2), SP Report 2014:49*, SP – Swedish Technical Research Institute.

Torvi, D.A. and Dale, J.D. (1994), "A Finite Element Model of Skin Subjected to a Flash Fire", *Journal of Biomechanical Engineering*, Vol. 116 No. 3, pp. 250–255.

Torvi, D.A., Hadjisophocleous, G.V. and Hum, J. (2000), "A new method for estimating the effects of thermal radiation from fires on building occupants", *Proceedings of the ASME Heat Transfer Division*, Vol. 5, pp. 65–72.

Wade, C., Baker, G., Frank, K., Harrison, R. and Spearpoint, M. (2016), *B-RISK 2016 User Guide and Technical Manual*, BRANZ Ltd., Judgeford, New Zealand.

Wickström, U. (2016), *Temperature Calculation in Fire Safety Engineering*, Springer-Verlag.

PAPER C

Life Safety in single story steel frame building,
Part II – probabilistic design

Sandström, J.

Life safety in single-story steel frame buildings, Part II – probabilistic design

Joakim Sandström, Luleå University of Technology/Brandskyddslaget AB

1 Abstract

Including consideration to the fire conditions in structural fire safety design enables a nuanced evaluation of the life safety objective in single-story-, single-compartment buildings. This paper investigates the probability of unacceptable consequences from structural fire damage in a typical Scandinavian single-story steel frame building and discusses it in relation to life safety. The investigated building does not meet the safety levels as stipulated by EN 1990 for structural fire damage. However, by including consideration to the fire conditions in the compartment, it is shown that the life safety objective is not compromised by the structural fire damage, i.e. the structure remains intact as long as any individuals/firefighters can survive within the fire area compartment.

This paper is a complement to the paper Life safety in single-story steel frame buildings, Part I – deterministic design by Sandström (2019) considering the same design philosophy but with a deterministic design approach.

Keywords: Structural fire safety design, Performance-based design, Fire engineering, Life safety, Monte Carlo simulation

2 Introduction

2.1 Background

The probability of structural fire damage using probabilistic methods have been evaluated in several studies. Most of them focus on multi-story buildings where the life safety objective is addressed by ascertaining a sufficiently low probability of structural fire damage (Shi et al., 2013; Van Coile et al., 2013). Sandström et al. (2017) shifted the focus for structural fire safety design of single-story, single-compartment buildings from structural fire damage alone to include consideration to the fire conditions in the fire compartment. In previous work, Sandman (1989) addressed the combination of structural fire safety of steel frame buildings and fire conditions by suggesting that interior firefighting attack was impossible if flashover had occurred in the fire compartment. Sandman promoted early suppression as the only feasible means of saving the building content. In more recent work, Guowei et al. compared the time to structural fire damage with the time of egress from a sports arena as one of several critical conditions (Guowei et al., 2016).

The approach to evaluate the life safety in relation to structural fire damage in single-story, single-compartment buildings as suggested in this paper, was first presented in a paper by Sandström (2019). Sandström showed that a steel truss in the investigated building could meet the life safety criterion even

though the structural stability was compromised in case of fire and without achieving code compliance. In this paper, the probability of unacceptable consequences to firefighters due to structural fire damage is investigated for the same building configuration but by using the Monte Carlo method (Metropolis and Ulam, 1949).

2.2 Lethal fire conditions

It is assumed that after a certain time of a fire, survival of occupants and firefighters are not possible in a zone adjacent to the fire. Sandström (2019) introduced the concept of a critical time, t_{crit}, as the time when the level of thermal radiation to occupants or firefighters, $\dot{q}''_{rad}$, exceeds a critical threshold value, $\dot{q}''_{rad,crit}$. However, the thermal radiation at the threshold level is only lethal in combination with a sufficiently long time of exposure, here denoted t_{margin}. Sandström (2019) suggested the combination of $\dot{q}''_{rad,crit} = 30$ kW/m during the time of exposure, $t_{margin} = 150$ s as a conservative estimate of conditions that preclude survival of occupants egressing, and/or firefighters performing interior attack. Thus, a structural design where the time to structural fire damage, t_{str}, is longer than $t_{crit} + t_{margin}$ implies acceptable fire resistance with respect to life safety, see Figure 1.
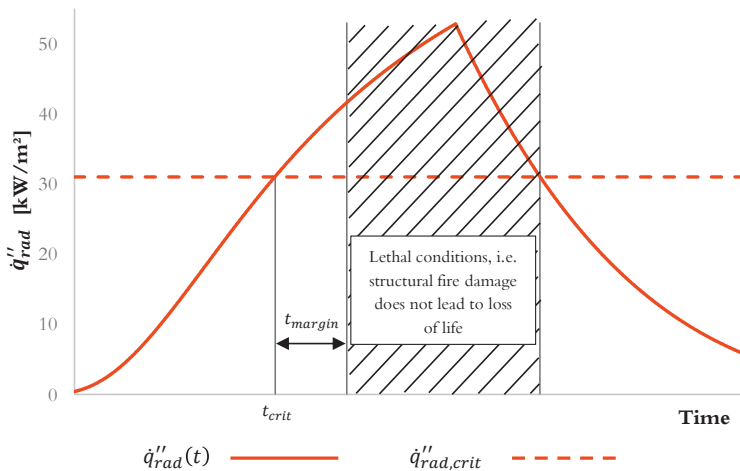
Figure 1 t_{crit}, t_{margin} and time interval where structural fire damage does not lead to unacceptable consequences, (Sandström, 2019)

Structural fire damage in the cooling phase is assumed to present negligible consequences. Thus, the failure criterion for the area affected by structural fire damage, in this case study the entire building, can be formulated as

$$t_{str} < t_{crit} + t_{margin} \tag{1}$$

That is; failure, or unsafe outcome, occurs if structural fire damage take place prior to lethal conditions being present in the building.

2.3 Case study building

The geometry of the building is identical to that of the building evaluated in the case study by Sandström (2019). Thus, information on some of the deterministic models and design assumption used can be found there.

The studied commercial single-story steel frame building for selling utensils has a load-bearing structure as shown in Figure 2. More details regarding the dimensions are presented in Table 1.
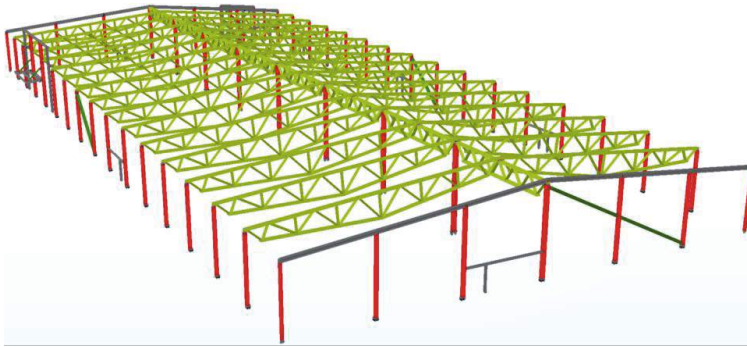
Figure 2 Overview of the load-bearing structure in the case study, from Sandström (2019).

3   Stochastic case study

To demonstrate the capabilities of the approach, methods and situations in this paper are chosen with the concept of 'consistent level of crudeness' and especially the epistemic uncertainty in mind, i.e. the uncertainty in the modelling process and uncertainty regarding discrepancy between the model and reality (Elms and Brown, 2006). However, combining the models and using a conservative approach is assumed to present an efficient model with reasonable results on the safe side (Frank et al., 2011).

Important parameters were assumed randomly distributed. Others were assumed to be deterministic, since they were assessed to have negligible impact on the overall results.

3.1   Building and fire parameters

The fire was modelled with the computer code B-Risk (Wade et al., 2016). With this code it is possible to use crude Monte Carlo simulation with randomized variables. Each simulation is initiated by realization of the stochastic parameters. For assumptions regarding openings and other building parameters, see Table 1.

At the back of the building, there is a rolling door for loading goods with a low probability of being open. However, to create a variation of the heat release rate, HRR in the post–flashover stage the opening height of the rolling door was assigned a stochastic distribution in the model. This variation was induced to evaluate the importance of HRR in relation to the risk for loss of life.

Table 1 Assumptions regarding stochastic parameters used in the fire modelling.

	Distribution	Mean	CoV	Comment
Building envelope				
Length	Deterministic	87 m	–	
Width	Deterministic	42 m	–	
Height	Deterministic	$6 - 8.5$ m	–	Eaves to ridge
Thermal inertia of sandwich walls $\sqrt{k\rho c}$	Deterministic	2400 J/m²Ks$^{\frac{1}{2}}$	–	Steel − rockwool − steel sandwich panel
Openings				
Width of main entrance	Deterministic	3 m	–	Open at all times
Height of main entrance	Deterministic	3 m	–	
Width of glass section	Deterministic	3 m	–	Breaks according to model in B–Risk[a]
Height of glass section	Deterministic	3 m	–	
Width of port for loading	Deterministic	3 m	–	
Height of rolling door for loading	Normal	3 m	1	Bounded by dimensions
Width of doors for egress	Deterministic	1.2 m	–	Probability of open during fire is 0.1 for each of 6 doors
Height of doors for egress	Deterministic	2 m	–	
Fire				
Heat release rate per unit area, $\dot{q}''_{fi}$	Normal	460 kW/m²	0.15	Est.[b,d]
Fuel load density	Normal	600 MJ/m²	0.15	Est.[c,d]
Fire growth rate	Normal	0.04 kW/s²	0.5	Fast growth rate[d] (bounded by 0.01 and 0.2)
Height of fire	Deterministic	1.3 m	–	Est. [d]

a (Parry et al., 2003)

b (*PD 7974-1*, 2003)

c (*EN 1991-1-2*, 2002)

d (Sandström, 2019)

3.2 Thermal action on steel elements

The heat flux from the fire to the steel elements is calculated as the maximum of heat flux from the hot upper gas layer temperature, $\dot{q}''_{UL}$, and the heat flux from localized exposure, $\dot{q}''_{plume}$.

$$\dot{q}''_{tot} = max \begin{cases} \dot{q}''_{UL} \\ \dot{q}''_{plume} \end{cases} \qquad (2)$$

The heat flux from hot gas layer to the steel structure, $\dot{q}''_{UL}$, is calculated according to equation (3) based on the hot gas layer temperature, $T_{g,UL}$, calculated by B-Risk.

$$\dot{q}''_{UL} = h_c(T_{g,UL} - T_s) + \varepsilon_{UL}\varepsilon_s\sigma(T_{g,UL}{}^4 - T_s{}^4) \qquad (3)$$

T_s is the steel temperature, h_c is the convective heat transfer coefficient, ε_{UL} the emissivity of the upper gas layer for the purpose of this paper assumed equal to unity, ε_s the emissivity of the steel surfaces and $\sigma = 5.67\cdot10^{-8}$ Wm^{-2}K^{-4} is Stefan–Boltzmann's constant. $h_c = 35$ W/m²K and $\varepsilon_s = 0.7$ for all subsequent calculations in the following sections as suggested for natural fires and steel surfaces by EN 1991-1-2 and EN 1993-1-2 respectively.

The calculation of $\dot{q}''_{plume}$ for different relations between the structural elements and the localized fire is described in the following sections.

3.2.1 Fire origin area

The spatial relation between each structural element and the fire plume was renewed for each simulation. Thus, the origin of the plume central axis defined by the x and y values was randomized with a uniform distribution within the bounds of the fire origin. From the assumption of symmetry, the area was located only on one side of the truss with a width of 3 m from the truss center line, see Figure 3.

Investigated steel truss
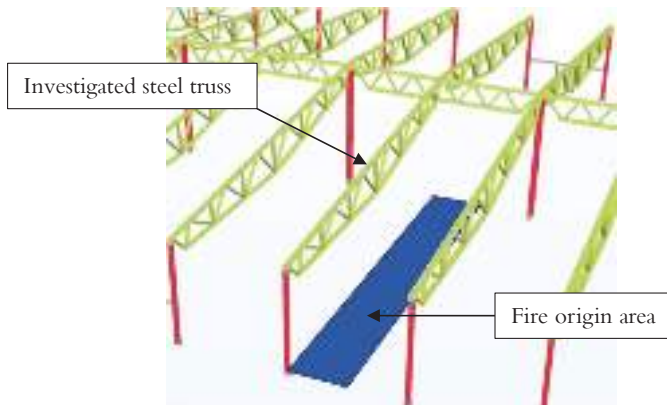
Fire origin area

Figure 3 A symmetric part of the fire origin area in relation to the investigated steel truss.

3.2.2 Heat transfer to the lower chord

The heat flux from the localized fire to each element in the lower chord is calculated as

$$\dot{q}''_{plume} = \varepsilon_s \sigma \left(T_{pl}(z,r)^4 - T_s^{\,4}\right) + h_c\left(T_{pl}(z,r) - T_s\right) \tag{4}$$

$T_{pl}(z,r)$ is the plume temperature at height z (m), and the distance r (m) from the plume central axis. Figure 4 illustrates the different key concepts regarding the calculation of $T_{pl}(z,r)$ along the distance from the plume central axis and outwards.
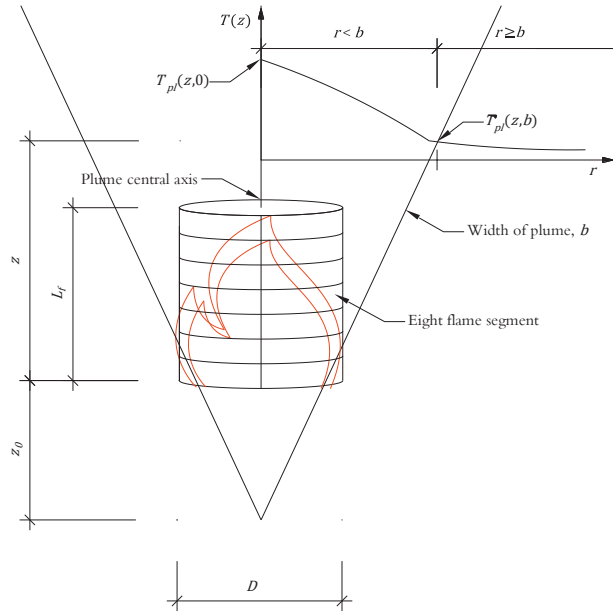
Figure 4 Key concepts regarding the calculation of $T_{pl}(z,r)$ at the lower chord.

The first step in each simulation is to find the plume radius, b (m), as defined by Heskestad (2008), see equation (5).

$$b = 0.12\left(\frac{T_{pl}(z,0)}{T_{g,LL}}\right)^{1/2} (z - z_0) \tag{5}$$

$T_{g,LL}$ is the lower layer temperature, and $T_{pl}(z,0)$ is the plume central axis temperature at height z (m), calculated according to Eurocode (*EN 1991-1-2*, 2002), see equation (6).

$$T_{pl}(z,0) = 20 + 0.25\left(\chi_c \dot{q}_{fi}\right)^{2/3}(z - z_0)^{-5/3} \le 900 \tag{6}$$

$\dot{q}_{fi}$ is the total heat release rate in W from the localized fire, $\chi_c = 0.8$ is the convective heat fraction of $\dot{q}_{fi}$, z is the vertical distance in m from the plume base to the element, and z_0 (m) is the height of the

virtual plume origin, i.e. a translation from point to area source of the plume to account for differences in heat release rate per unit area, $\dot{q}''_{fi}$, calculated as.

$$z_0 = -1.02D + 0.00524\dot{q}_{fi}^{2/5} \tag{7}$$

The second step is to calculate the thermal exposure to each element located at $r \geq b$ at its corresponding element height z, i.e. $T_{pl}(z,r)$. This is done by assuming $T_{pl}(z,r)$ equal to the adiabatic surface temperature (Wickström et al., 2018) calculated from the combination of the thermal radiation from the flame to the element, $\dot{q}''_{inc}(z,r)$, and the gas temperature at element height, $T_g(z)$, see equation (8). This numerical translation is performed to obtain a consistent quantity of the thermal exposure, i.e. temperature, along r.

$$\varepsilon_s\big(\dot{q}''_{inc}(z,r) - \sigma T_{pl}(z,r)^4\big) + h_c\left(T_g(z) - T_{pl}(z,r)\right) = 0 \tag{8}$$

The gas temperature near the element, $T_g(z)$, is calculated in B-Risk as either $T_{g,UL}$, or $T_{g,LL}$ depending on the vertical location of the element in relation to the height of the gas layer interface. The incident thermal radiation from the flame to element at distance r, from the plume central axis, $\dot{q}''_{inc}(z,r)$, is estimated by simplifying the flame as a cylinder with the same diameter as the fire base, D (m). To consider the differentiated temperature along the flame height, the flame is divided into segments, each of them radiating to the horizontal element based on the segment mean plume central axis temperature. The view factor, Φ_i, from each flame segment perimeter, $A_{1,i}$, to the annual ring segment, A_2, is calculated as proposed by Brockmann (1994) with adjustments by Antwerpen and Greyvenstein (2008), see Figure 5.
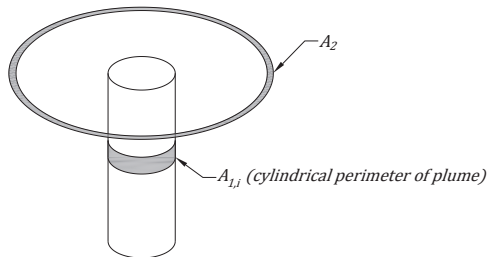
Figure 5 The view factor is calculated from the surface of each flame segment, $A_{1,i}$, and the annual ring at the distance of the receiving element, A_2.

The incident radiation from the plume to the annual ring A_2 at the distance r from the plume central axis, $\dot{q}''_{inc}(z,r)$, is integrated in eight discrete steps over the height of the fire plume and is adjusted to the receiving surface as

$$\dot{q}''_{inc}(r) = \frac{1}{A_2}\sum_{i=1} \sigma A_{1,i}\Phi_i\varepsilon_{fl}T_{fl,i}^4 \tag{9}$$

The flame emissivity, ε_{fl} is calculated with equation (10) (Mudan and Croce, 1988; Tien et al., 2008) and is assumed equal over the entire flame height.

$$\varepsilon_{fl} = 1 - e^{-\kappa L_b} \tag{10}$$

κ is assumed to 0.8 m⁻¹. The κ-value is an approximation from Hägglund & Persson (1976), and Beyreis et al. (1971). L_b is the mean beam length of the fire cylinder calculated according to Tien et al. (2008) as

$$L_b = 3.6 \frac{V}{A} \tag{11}$$

The heat transfer from the fire plume to the element, $\dot{q}''_{plume}$, is then calculated depending on the element height, z, and gas layer interface height, LH, as

$$\dot{q}''_{plume} = \varepsilon_s \left(\dot{q}''_{inc}(r) - \sigma T_s^4 \right) + h_c \left(T_g(z) - T_s \right) \tag{12}$$

The third step is to estimate the plume temperature, $T_{pl}(z, r)$, at $0 < r \leq b$. The temperature is assumed to follow a Gaussian distribution as suggested by Heskestad (2008) from the plume central axis temperature, $T_{pl}(z, 0)$, to the temperature at the plume radius, $T_{pl}(z, b)$, see Figure 4.

3.2.3 Heat transfer to the upper chord

For elements at ceiling height, $z = H$, the choice of equation for calculating the heat transfer from the fire plume to the elements, $\dot{q}''_{plume}$, is governed by the flame height, L_f, in m as

$$\dot{q}''_{plume} = \begin{cases} \varepsilon_s \sigma \left(T_{pl}(z,0)^4 - T_s^4 \right) + h_c \left(T_{pl}(z,0) - T_s \right) & for \ L_f < H \\ \dot{q}''_{in} - \varepsilon_s \sigma \left((T_s + 273)^4 - 293^4 \right) - h_c(T_s - 20) & for \ L_f \geq H \end{cases} \tag{13}$$

$T_{pl}(z, 0)$ is calculated as the plume central axis temperature at distance $z = H + r$ in m from the plume base, see equation (6), where r is the horizontal distance from the plume central axis to the element, see Figure 6. L_f is calculated in m as suggested by Heskestad (2008) from the fire diameter, D (m), and heat release rate, $\dot{q}_{fi}$ (W), see Figure 6 and equation (14).

$$L_f = -1.02D + 0.0148 \dot{q}_{fi}^{2/5} \tag{14}$$

$\dot{q}''_{in}$ in equation (13) is the sum of the incoming heat flux to a surface at a temperature of 20 °C with the same heat transfer properties, ε_s, and h_c as is assumed for the target body surface. According to EN 1991-1-2, Annex C (*EN 1991-1-2*, 2002) $\dot{q}''_{in}$ is specified in W/m² as

$$\dot{q}''_{in} = \begin{cases} 100\,000 & for \ y \leq 0.3 \\ 136\,300 - 121\,000y & for \ 0.3 < y \leq 1.0 \\ 15\,000 y^{-3.7} & for \ 1 < y \end{cases} \tag{15}$$

y is a dimensionless parameter that depends on the rate of heat release, $\dot{q}_{fi}$, the diameter of the fire base, D, the distance from the fire base, H, and the horizontal distance from the plume central axis to the element, r, see Figure 6.
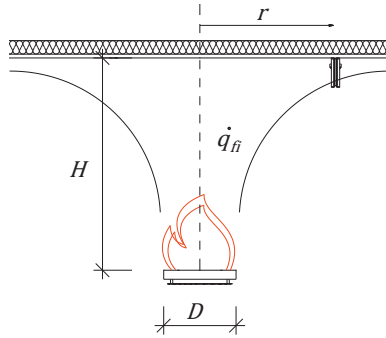
Figure 6 Parameters used for calculation of the fire exposure from the localized fire to elements at ceiling height.

3.3   Steel temperature– and resistance calculations

The element numbers of the steel truss are presented in Figure 7, and their properties are presented in Table 2.
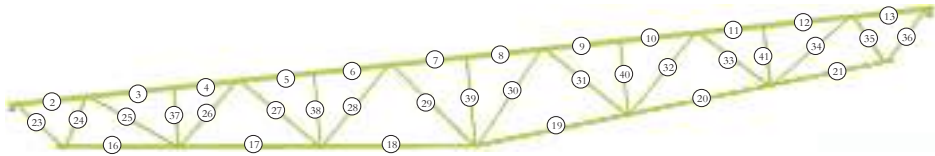
Figure 7 Steel truss layout and element numbers, from Sandström (2019).

Table 2 Steel properties of the elements of the steel truss, from Sandström (2019).

	Steel Quality, $f_{y,k}$	Dimensions	A_m/V	k_{sh}[i]
Upper chord	S420J	L 100x10	203 m^{-1}	0.63
Lower chord	S355J	L 100x10	203 m^{-1}	0.87
Diagonals	S355J	UNP 100	320 m^{-1}	0.78

[i] correction factor for the shadow effect.

The mean value of the steel is calculated from the characteristic value assuming a lognormal distribution and a coefficient of variation (COV) 0.07 as suggested by JCSS (2001). For each simulation, all elements are assigned yield strength independently and to include for uncertainties regarding geometrical imperfections, a coefficient of variation of 0.1 is assumed. The assumption of individual realization of yield strength was compared to fully correlated yield strengths for the entire steel truss and

was found to be on the safe side and was therefore used in this case study. The difference in results between the assumptions of statistical independence and full correlation was also small.

The critical steel temperature for each element in deterministic design, $T_{s,crit}$ is shown in Figure 8.
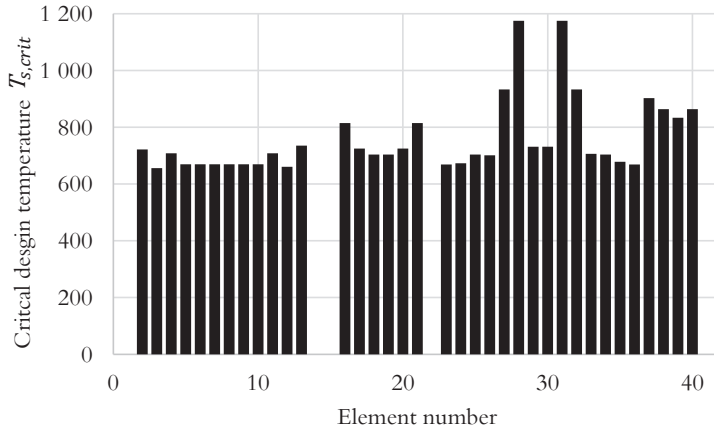
Figure 8 Critical design temperature for each element, $T_{s,crit}$.

For $T_{s,crit}$ is adjusted to a real critical temperature for every element, $T_{s,crit,real}$, calculated from the stochastic values realized for each simulation.

3.4 Load calculations

Data on the self-weight, G, is presented by the steel entrepreneur who provided the steel frame to the project. For this project it was assumed normally distributed with a mean value of 0.77 kN/m² and with a coefficient of variation of 0.05 according to JCSS handbook (JCSS, 2001).

The snow load was calculated based on historical data between 1961-2017 from the Swedish Meteorological and Hydrological Institute, regarding snow depth in Skövde, Sweden ("SMHI Open data | Meteorological Observations", n.d.). Using the conversion equations presented in JCSS handbook (JCSS, 2001), the snow load at an arbitrary point in time, Q, was found to be gamma distributed with a shape factor, $\alpha = 0.78$, and a scale factor, $\beta = 0.41$, see Figure 9.

According to the same statistics database, the probability of snow load, p_{snow}, for an arbitrary day was found to be 0.15. In each simulation, a uniformly distributed variable, ξ_i $(0 \leq \xi_i \leq 1)$, was realized and the load acting on the truss, E_i, was calculated as

$$E_i = \begin{cases} G_i + Q_i & for\ \xi_i \leq p_{snow} \\ G_i & for\ \xi_i > p_{snow} \end{cases} \tag{16}$$
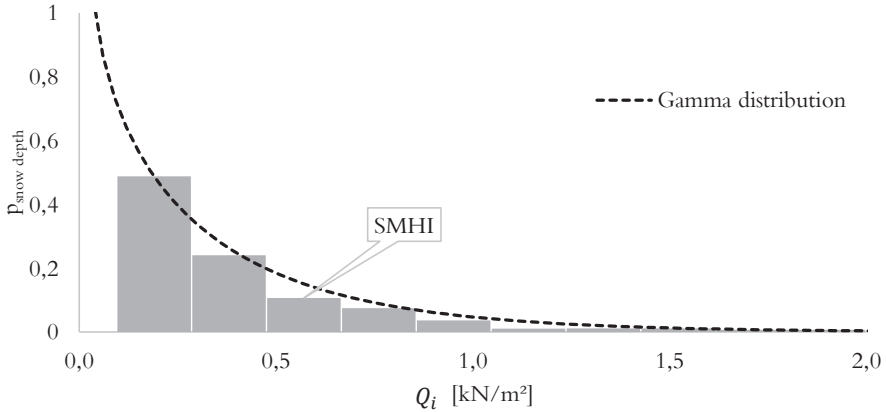
Figure 9 Gamma distribution for the snow load for an arbitrary point in time in Skövde, Sweden.

3.5 Probability of fire occurrence

The probability of one ignition, $P_{ignition}$, over a reference time interval of 50 years is calculated according to the Poisson distribution presented by Lie (1974) as

$$P_{ignition} = 50A_f\lambda_p e^{-50A_f\lambda_p} \tag{17}$$

where A_f is the building area, e.g. 3 654 m² and λ_p is the probability of ignition assumed to be $4 \cdot 10^{-7}$ per year and m² as recommended by Holický et al. (2005). Consideration is taken to the probability of occupants' and firefighter intervention, $P_{occupant} = 0.6$ and $P_{firefighter} = 0.9$ respectively as suggested for public spaces by Holický et al. (2005) and supported by Fontana et al. (1999). Sprinklers are not accounted for in this paper. The resulting probability of one severe fire occurrence, $P(sf)$, was calculated as

$$\begin{aligned} P(sf) = P_{ignition} \cdot \left(1 - P_{occupant}\right) \cdot \left(1 - P_{firefighter}\right) = \\ = 6.79 \cdot 10^{-2} \cdot (1 - 0.6) \cdot (1 - 0.9) = 2.72 \cdot 10^{-3} \end{aligned} \tag{18}$$

3.6 Calculation procedure

Figure 10 is an adaptation of the flowchart presented for the deterministic design case in Sandström (2019) and presents an overview of how the Monte Carlo method is applied in this case study. Blue boxes in Figure 10 represent the realization of stochastic values while black boxes represent deterministic calculations based on these values. If the statement in the final box, $t_{str} < t_{crit} + t_{margin}$, is true, a structural fire damage can lead to an unsafe outcome. t_{crit} is the time when the hot gas layer

produces thermal radiation to the floor level at all locations in the fire compartment equal to, or higher than 30 kW/m² and $t_{margin} = 150$ s, see section 2.2.
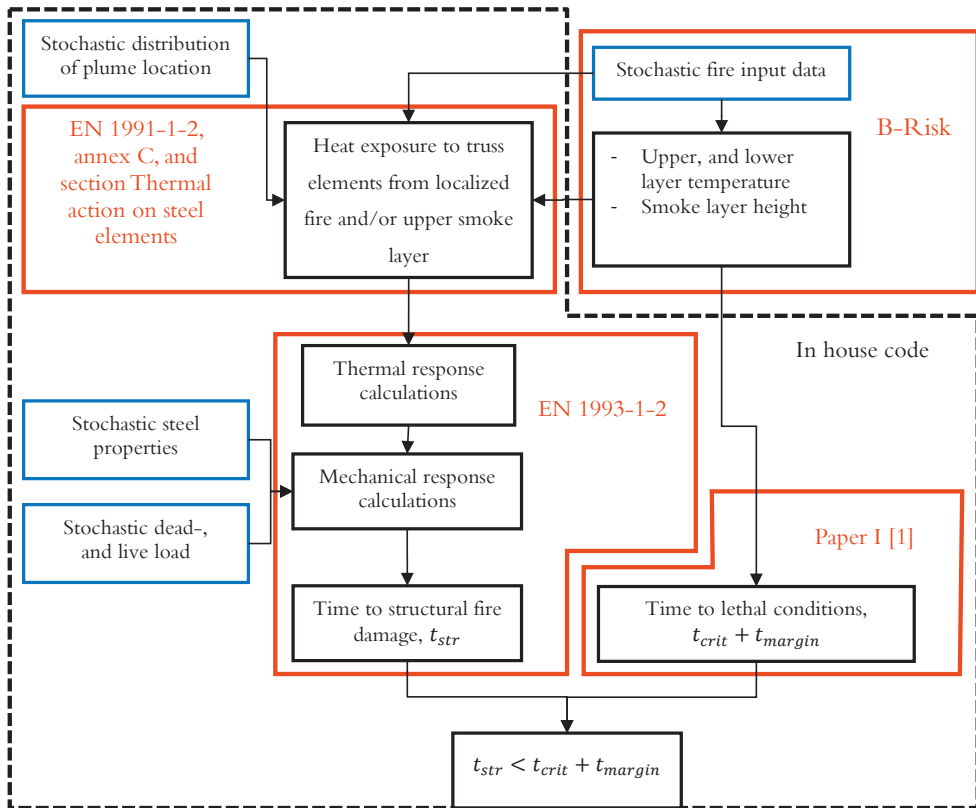
Figure 10 Flow chart describing the calculation process for each simulation when using the Monte Carlo method. An in-house code was written in the Java programming language with the purpose of automating the calculations according to the described methods and for realization of stochastic values for each simulation.

4 Results

The time at which occupants or firefighters are subjected to the lethal fire conditions is assumed deterministically and conservatively, see Sandström (2019). Using the Monte Carlo method aims at investigating the risk of lethality due to structural fire damage rather than death in a fire exposed building regardless of reason. The probability of structural fire damage before lethal fire conditions is therefore referred to as the probability of an unsafe outcome, $P(uo)$.

Of the 1000 simulations, structural fire damage (sfd) occurred 909 times, i.e. $P(sfd)$ is estimated to 0,909. In combination with the probability of one severe fire occurrence, $P(sf)$, (section 3.5) this yields a total probability of structural fire damage over the reference period of 50 years to

$$P(sf) \cdot P(sfd) = 2.72 \cdot 10^{-3} \cdot 0.909 = 2.47 \cdot 10^{-3} \tag{19}$$

The probability of structural fire damage is higher than the stipulated target probability, $7.23 \cdot 10^{-5}$, for the ultimate limit state with a reference period of 50 years and reliability class RC2 given in (*EN 1990. Basis of Structural Design*, 2002), thus leading to the conclusion that the structural configuration is unsafe. However, by adding consideration to the fire conditions in the compartment, it is observed in the calculations that $P(uo)$ is substantially lower, only 7 out of 1000 simulations, i.e. $P(uo)$ is estimated to $7 \cdot 10^{-3}$. Thus

$$P(sf) \cdot P(uo) = 2.72 \cdot 10^{-3} \cdot 7 \cdot 10^{-3} = 1.90 \cdot 10^{-5} \tag{20}$$

The probability for unsafe outcome is well below the target reliability for structures in the ultimate limit state. The conclusion is therefore that the probability of harm or death from structural fire damage is sufficiently low to accept the building design as safe.

The 7 out of 1000 simulations shows that the elements in the lower chord, being closest to the fire origin are the most sensitive to structural fire failure before the time to lethal fire conditions as seen in Figure 11.
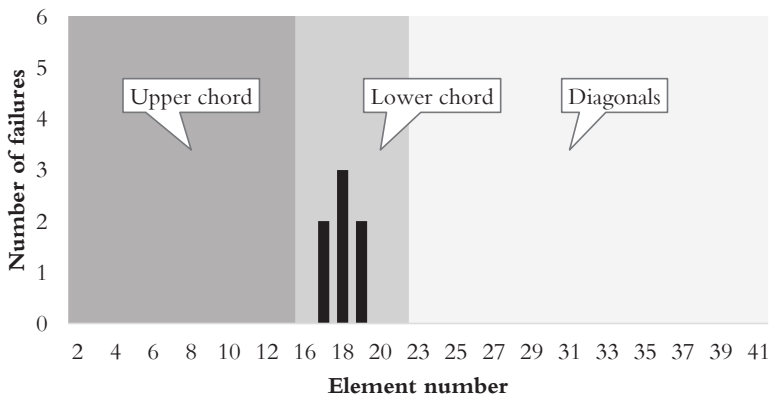
Figure 11 Number of structural fire damages with unsafe outcome out of the 1000 simulations for each truss member.

To understand what creates situations prone to induce risks for unsafe outcome, the thermal radiation at the time t_{str} was compared to different input parameters. Some interesting findings were observed, such that structural fire damage with unsafe outcome occurs early in a fire, see Figure 12.
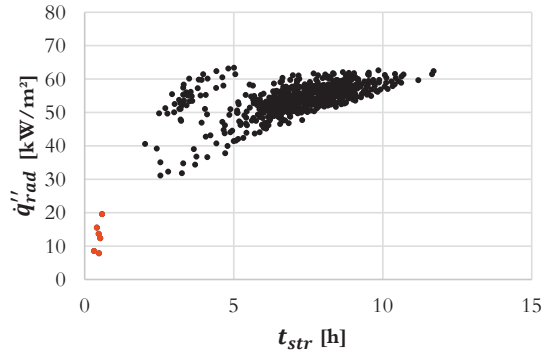
Figure 12 Time of structural damage t_{str} in relation to thermal radiation from the hot smoke layer $\dot{q}''_{rad}$. Red data points represent simulations with an unsafe outcome.

As shown in Figure 12, the time to structural fire damage is not a good predictor for unsafe outcome. It is, however, possible to conclude that structural fire damage with unsafe outcome tends to occur before accumulation of hot gases in the upper layer, i.e. when the thermal exposure is largely from the localized fire. It is therefore a much stronger correlation between the probability of unsafe outcome and the heat release rate per unit area, $\dot{q}''_{fi}$, at time $t_{str} - t_{margin}$, see Figure 13.
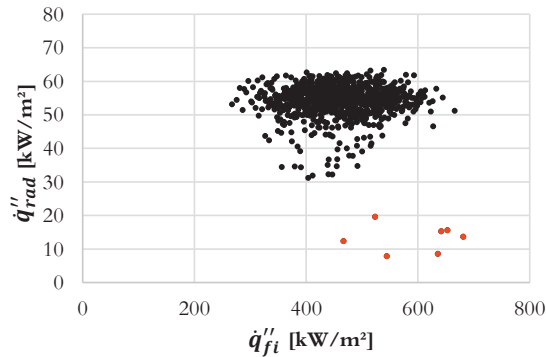
Figure 13 Heat release rate per unit area, $\dot{q}''_{fi}$, in relation to thermal radiation from hot smoke layer, $\dot{q}''_{rad}$ at time $t_{str} - t_{margin}$. Red data points represent simulations with an unsafe outcome.

A high value of $\dot{q}''_{fi}$ alone is not sufficient to induce a high probability of unsafe conditions. The maximum heat release rate of the localized fire, $\dot{q}_{fi,max}$, needs to be large enough and the horizontal distance from the plume central axis small enough to the lower chord where structural fire damage is most prone to induce unsafe conditions, i.e. element 17, 18 and 19. For $\dot{q}''_{fi} > 600$ kW/m², it is possible to observe that $\dot{q}_{fi,max} > 50$ MW in combination with a small horizontal distance, $r_{LC} < 2$ m from the plume central axis to the closest of element 17, 18 and 19 produce a high probability of structural fire damage with unsafe outcome, see Figure 14.
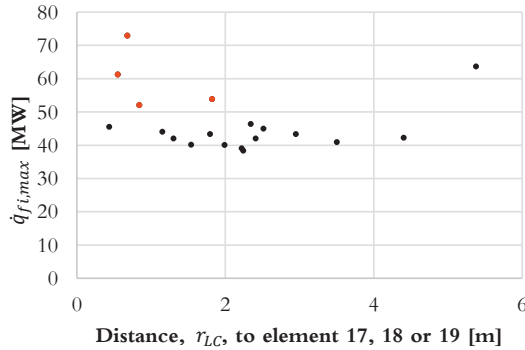
Figure 14 For simulations with $\dot{q}''_{fi} > 600$ kW/m², the combination of horizontal distance, r_{LC}, to element 17, 18 and 19 and $\dot{q}_{fi,max}$ at time $t_{str} - t_{margin}$ creates situations prone to induce a high probability of unsafe outcome. Structural fire damage is for most simulations unrelated to the real critical temperature, $T_{s,crit,real}$. Figure 15 shows the simulations yielding unsafe outcome in relation to the real critical temperature of the steel, $T_{s,crit,real}$, calculated from the stochastic values realized for each simulation. The general trend in Figure 15 with a line of black dots corresponds to structural fire damage in the upper chord and diagonals. The eight dots (seven red and one black) outside this general trend corresponds to structural fire damage in the lower chord due to direct exposure from the localized fire, see Figure 15.
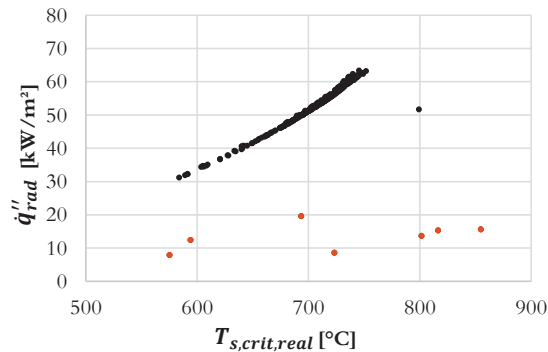
Figure 15 The real critical temperature, $T_{s,crit,real}$, in relation to thermal radiation from hot smoke layer, $\dot{q}''_{rad}$ at time $t_{str} - t_{margin}$. Red data points represent simulations with an unsafe outcome.

For the simulations where structural fire damage occurs in elements with low real critical temperatures, i.e. $T_{s,crit,real} < 600$ °C, $\dot{q}''_{fi}$ aid in explaining unsafe outcome, see Figure 16. The leftmost red data point in Figure 16 is from a simulation with almost perfect alignment of the plume central axis below element 18 where structural fire damage occurred.
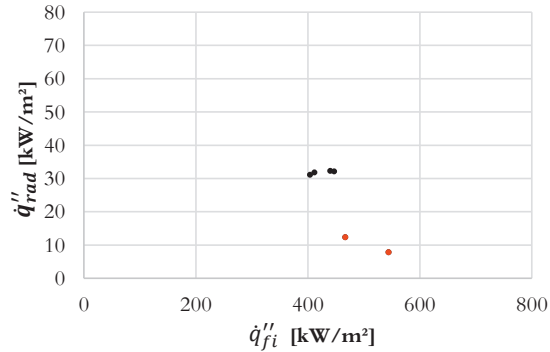
Figure 16 For simulations with $T_{s,crit,real}$ < 600 °C, the $\dot{q}''_{fi}$ > 450 kW/m² creates situations prone to induce a high probability of unsafe outcome.

For the seventh simulation with unsafe outcome, $\dot{q}''_{fi}$ is high, e.g. equal to 69 MW. Even though a high value of $\dot{q}''_{fi}$ alone is not sufficient to explain structural failure with unsafe outcome, the combination with all other parameters creates a situation with a resulting unsafe outcome.

5   Discussion

The studied building of shoe-box type with no interior walls is well suited for demonstration of the approach in this paper. Addressing situations with interior walls, partial collapse of the building envelope, and/or more complex structural configurations would require further elaboration of the approach without adding to the conceptual understanding.

Firefighting systems are not included in the studied case although it is possible to include it in the analysis, either as sprinkler or as roof vents. Consideration to sprinkler should be included in the calculation of the probability of a severe fire, $P(sf)$, while consideration to roof vents should be included in the fire model itself.

6   Conclusion

For buildings with the design objective of having *no failure during a limited duration of a fire*, the approach presented in this paper allows for the life safety objective to be evaluated in a much more nuanced way than previously possible. However, the approach does not replace deemed-to-satisfy solutions as presented in building codes, rather it constitutes a complement to these when determining the safety in more complex buildings where the objective is *no failure during an entire fire*.

The building investigated in this paper should be considered safe with regard to life safety. The probability for unsafe outcomes at the time of structural fire damage is small in comparison to other

accidental load designs. This correlates to the findings in the case study by Sandström (2019) where the same approach was used but with deterministic design values.

The analysis of data showed that combinations of some of the parameters tend to increase the probability of unsafe outcome. These parameters include:

- The maximum heat release rate, $\dot{q}_{fi,max}$,
- The heat release rate per unit area, $\dot{q}''_{fi}$,
- The real critical steel temperature, $T_{s,crit,real}$, and
- The distance from the plume centerline to the most sensitive elements in the lower chord, r_{LC},

However, no single parameter can alone induce unsafe conditions.

The approach in this paper presents a feasible complement for the design of buildings where life safety is the only objective. It also addresses structural fire safety design as an alternative to probabilistic approaches with a sole focus on structural fire failure during an entire fire. Still, there is much left to be explored with regards to the life safety objective in structural fire safety design and much data is needed on stochastic distributions and design values to enable the approach to its fullest. However, it is the authors strong conviction that this approach is a possible road forward and that it can lead to new and more informed/efficient structural fire safety designs.

7 Acknowledgments

8 References

van Antwerpen, H.J. and Greyvenstein, G.P. (2008), "Evaluation of a detailed radiation heat transfer model in a high temperature reactor systems simulation model", *Nuclear Engineering and Design*, No. 238, pp. 2985–2994.

Beyreis, James R., Monsen, H.W. and Abbasi, A.F. (1971), "Properties of Wood Crib Flames", *Fire Technology*, Vol. 7, pp. 145–155.

Brockmann, H. (1994), "Analytic angle factors for the radiant interchange among the surface elements of two concentric cylinders", *International Journal of Heat and Mass Transfer*, Vol. 37 No. 7, pp. 1095–1100.

Elms, D. and Brown, C.B. (2006), "Balancing Uncertainty in Structural Decisions", presented at the International Forum on Engineering Decision Making - Second IFED Forum, Lake Louise, Canada, p. 10.

EN 1990. Basis of Structural Design. (2002), , European Committee for Standardization, CEN, Brussels.

EN 1991-1-2. (2002), *Action on Structures - Part 1-2: General Actions - Actions on Structures Exposed to Fire*.

Fontana, M., Favre, J.P. and Fetz, C. (1999), "A survey of 40,000 building fires in Switzerland", *Fire Safety Journal*, Vol. 32 No. 2, pp. 137–158.

Frank, K., Spearpoint, M., Fleischmann, C.M. and Wade, C.A. (2011), "A Comparison of Sources of Uncertainty for Calculating Sprinkler Activation", *Fire Safety Science*, Vol. 10, pp. 1101–1114.

Guowei, Z., Guoqing, Z., Guanglin, Y. and Yong, W. (2016), "Quantitative risk assessment methods of evacuation safety for collapse of large steel structure gymnasium caused by localized fire", *Safety Science*, Vol. 87, pp. 234–242.

Hägglund, Bengt and Persson, L.-E. (1976), *The Heat Radiation from Petroleum Fires, FOA Report C20126 D6 (A3)*, Försvarets Forskningsanstalt.

Heskestad, G. (2008), "Fire Plumes, Flame Height, and Air Entrainment", in DiNenno, P.J. (Ed.), *SFPE Handbook of Fire Protection Engineering, 4th Edition*, National Fire Protection Associationr, Quincy, MA.

Holický, M., Materna, A., Sedlacek, G., Schleich, J.-B., Arteaga, A., Sanpolesi, L., Vrouwenvelder, T., et al. (2005), *Implementation of Eurocodes - Handbook 5 - Design of Buildings for the Fire Situation*, Leonardo da Vinci Pilot Project CZ/02/B/F/PP-134007, Luxembourg.

JCSS. (2001), *Probabilistic Model Code*, The Joint Committee on Structural Safety.

Lie, T.T. (1974), *Probabilistic Aspects of Fire in Buildings*, Technical Paper No. 422, National Research Council Canada, p. 48.

Metropolis, N. and Ulam, S. (1949), "The Monte Carlo Method", *Journal of the American Statistical Association*, Vol. 44 No. 247, pp. 335–341.

Mudan, K.S. and Croce, P.A. (1988), "Fire Hazard Calculations for Large open Hydrocarbon Fires", in DiNenno, P.J. (Ed.), *SFPE Handbook of Fire Protection Engineering, 2nd Edition*, National Fire Protection Association, pp. 2–45 – 2–87.

Parry, R., Wade, C.A. and Spearpoint, M. (2003), "Implementing a Glass Fracture Module in the BRANZFIRE Zone Model", *Journal of Fire Protection Engineering*, Vol. 13 No. 3, pp. 157–183.

PD 7974-1. (2003), *Application of Fire Safety Engineering Principles to the Design of Buildings - Part 1: Initiation and Development of Fire within the Enclosure of Origin (Sub-System 1)*, p. 76.

Sandström, J. (2019), "Life safety in single-story steel frame buildings, Part I – deterministic design", *Journal of Fire Protection Engineering (Accepted)*.

Sandström, J., Wickström, U., Thelandersson, S. and Lagerqvist, O. (2017), "The life safety objective in performance-based design for structural fire safety", *Proceedings of the 2nd International Conference on Structural Safety Under Fire and Blast Loading, CONFAB 2017*, Brunel University London, pp. 411–417.

Shi, K., Guo, Q. and Jeffers, A. (2013), "Stochastic Analysis of Structures in Fire by Monte Carlo Simulation", *Journal of Structural Fire Engineering*, Vol. 4 No. 1, pp. 37–46.

"SMHI Open data | Meteorological Observations". (n.d.). *SMHI*, available at: https://opendata-download-metobs.smhi.se/explore/?parameter=6# (accessed 7 November 2018).

Tien, C.-L., Lee, K.Y. and Stretton, A.J. (2008), "Radiation Heat Transfer", in DiNenno, P.J. (Ed.), *SFPE Handbook of Fire Protection Engineering, 4th Edition*, National Fire Protection Association, Quincy, Massachusetts, pp. 1-74-1–90.

Van Coile, R., Annerel, E., Caspeele, R. and Taerwe, L. (2013), "Full-Probabilistic Analysis of Concrete Beams During Fire", *Journal of Structural Fire Engineering*, Vol. 4 No. 3, available at:https://doi.org/10.1260/2040-2317.4.3.165.

Wade, C., Baker, G., Frank, K., Harrison, R. and Spearpoint, M. (2016), *B-RISK 2016 User Guide and Technical Manual*, BRANZ Ltd., Judgeford, New Zealand.

Wickström, U., Hunt, S., Lattimer, B., Barnett, J. and Beyler, C. (2018), "Technical comment—Ten fundamental principles on defining and expressing thermal exposure as boundary conditions in fire safety engineering", *Fire and Materials*, Vol. 42 No. 8, pp. 985–988.

PAPER D

Steel truss exposed to localized fires

Sandström, J., Wickström, U., Sjöström, J., Veljkovic, M., Iqbal, N. and Sundelin, J.

Brandforsk project no 312-131. Luleå (2015)

1   INTRODUCTION

1.1   Background

A series of experiments with focus on heat transfer to structures from localized fires have been conducted in collaboration between SP (Swedish Technical Research Institute) and LTU (Luleå University of Technology) [1] and [2]. Localized fires, in contrast to for example flash over, create a non-uniform environment with differentiated thermal exposure depending to a structural element depending on geometry and location of the fire. From this research, it has been noted that it is urgent to harmonize the methods for presenting thermal exposure to structures. Thermal exposure from localized fires to ceilings have been explored by Hasemi *et al* [4] which led to the correlation now included in the Eurocode EC1, [5]. The thermal exposure to the ceiling is, in this study, represented by heat flux from a localized fire to a cold surface. The simple design models from these tests, as well as more sophisticated combined models of fluid dynamics and finite element analysis of solid state temperature are, however, in need of validation such as performed by Kumar *et al* [6]. This is especially important as most experimental work has been conducted in small scale, hardly exceeding a ceiling height of 1 m. In addition, also with the exception of small scale experiments [7], no tests have, to the best of our knowledge, been reported for other common construction types like steel roof truss systems.

The main focus of these experiments, fire exposure from localized fires to a steel truss, has been to evaluate the plume centerline temperature distributions of free burning localized fires as well as the thermal exposure to the steel truss and ceiling in a typical light-weight industrial building supported by steel columns and trusses. The data is to be used for development of both simple and advanced models investigating the response of this type of construction to thermal exposure from localized fires.

This report outlines the full experimental setup and results. In addition, some key-features of thermal and mechanical response of the structure are highlighted.

1.2   Objectives and research questions

The aim of this series of experiments with fire exposure from localized fires to a steel truss has been to map the temperature distribution in a light steel frame building consisting of an insulated

roof sheet, a truss and a column subjected to localized fires. The aim was also to gain better understanding of the response and thermal exposure from localized fires to the structural steel elements. The data are presented to be used for development of both advanced and simple methods to evaluate the response of light-weight steel constructions exposed to localized fires.

1.3 Acknowledgements

2   EXPERIMENTAL SETUP

2.1   Steel frame

2.1.1   General

The setup used in the experiment was constructed to resemble an ordinary single story light-weight steel frame building. This is a common construction type in Sweden due to cost effectiveness and flexibility. The steel frame used in this experiment was manufactured by Maku steel in Borås, Sweden and assembled on site in Trondheim, Norway.

In the first and second experiments, with the fire located at the mid-span of the central truss, no wall was present. In the third experiment, however, a wall was mounted on the steel frame to evaluate difference in temperatures from a fire close to a wall.
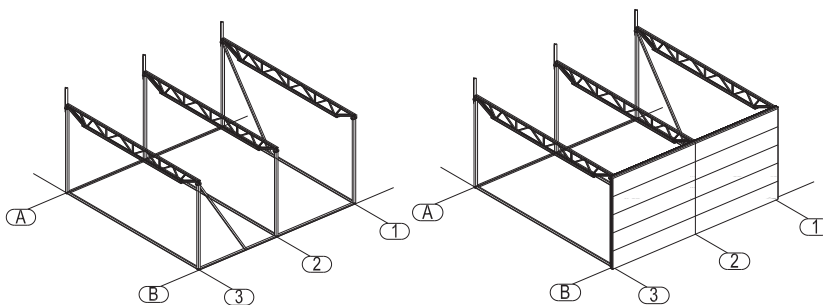
Figure 1. Set up of the steel frame with default grid lines from the manufacturer. The wall in the right hand figure was used in experiment 3. Profiled steel sheet was used on top of the frame for stabilization and for to transfer load to the trusses.

The three trusses supporting the roof were labelled F1, F2 and F3[1], as indicated in Figure 1. The side where the wall was mounted is labelled B and the opposite side A. The columns were, subsequently, labelled C1A, C1B etc. If not explicitly stated otherwise, any distance given along

---

[1] The label "F" is for "Fackverk", the Swedish word for truss.

the truss or the ceiling refers to an origin in the center of truss F2. Positive directions are towards the B-side or towards F3.

The steel frame was 10 m x 10 m with a height of 5 m. The columns were cold formed square hollow columns with the dimension 120 mm x 120 mm x 8 mm except C1B and C3B, which were 120 mm x 120 mm x 6 mm.

The tests were conducted in the large burn hall of SP Fire Research AS, in Trondheim, Norway, with floor area of 590 m² and a maximum ceiling height of 36 m. All ventilation to and from the hall was closed during the tests to avoid any external draft. All sides of the set-up were open with the side along truss F1 closest to a wall with a distance of 0.5 m from the outer wall of the hall. Thus smoke spread out along the ceiling with negligible accumulation of hot gases.

2.1.2 Steel truss

The steel truss consisted of an upper and lower chord separated by braces consisting of verticals and diagonals, see Figure 2.
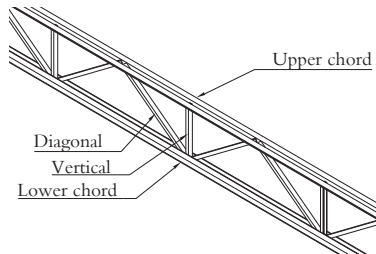
Figure 2. View of structural elements in the truss.

The lower and upper chord consists of angled profiles with dimensions 70 mm x 70 mm x 7 mm and the bracing consists of U-shaped profiles with dimensions 50 mm x 38 mm x 5 mm. The quality of the steel was S355.
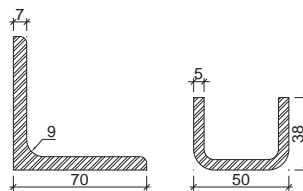
*Figure 3. Sections in the truss. Angled profiles in the lower and upper cord
and U-shaped profiles in the bracing.*

2.1.3 Truss to column connection

The connection between the truss and the column consists of a square hollow profile welded to the upper cord and to a steel U-shaped profile that is bolted to the top plate of the column. The

bolt is of quality 8.8 with the dimension M24. The thickness of the top plate is 15 mm and the bottom flange of the U-shaped profile is 5 mm thick.
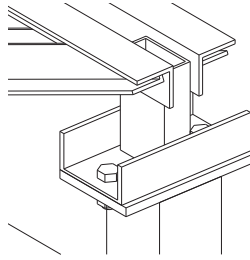
Figure 4. Detail of truss to column connection.

2.2 Roof

The roof consisted of corrugated steel sheet, LHP 130/65, manufactured by Lindab. The steel sheet was covered with 100 mm thick boards of rock wool with a density of 80 kg/m³, see Figure 5, and screwed to the upper chord in the trusses.
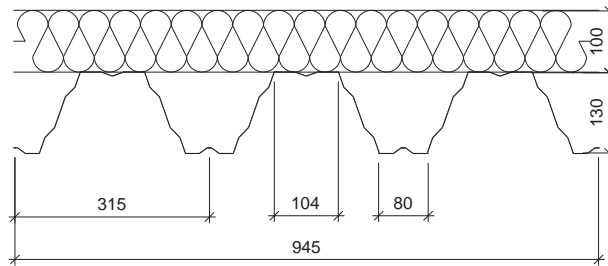
Figure 5. Dimensions of corrugated steel roof.

2.3 Wall

The wall at the B-side was used in one test alone. It was of sandwich panels with a 100 mm rock wool core covered by thin steel sheets. It was attached by screws drilled through the panels and into the columns. The vertical gap between the panels at column C2B was caulked with spare rock wool.

2.4 Fires

Three different heptane pool fires were used in the experiments. A 3 m² and a 2 m² fire at the center and a 2 m² fire close to column C2B, by the wall. The fire sizes are presented in Table 1, which also includes the heat release rate as calculated from mean value of tabulated fuel burning properties [8]. The distance from floor to fuel pan was 260 mm and the fuel pan had a 40 mm deep water layer in all tests.

Table 1. Fire size and position.

Experiment	Position	Size	Heat release rate estimated from [8]	Wall	Duration	Fuel mass
1	Center	2 m²	4,50 MW	No	17 min	87 kg
2	Center	3 m²	7,55 MW	No	10 min	97 kg
3	Wall	2 m²	4,50 MW	Yes	12 min	60 kg
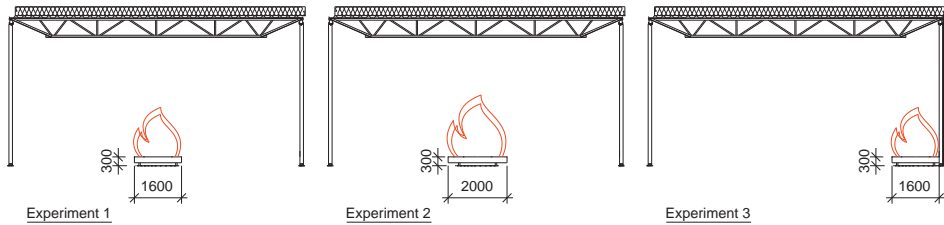
Figure 6. Positions of the heptane fires used in the experiment for the different experiments. The fuel pan was always located directly under truss F2. The wall included in the right hand figure was only present during experiment 3.

2.5 Instrumentation

Three different kinds of temperatures were measured; the steel temperature in the trusses, ceiling and column 2B; thermocouple temperatures in the fire plume and ceiling jets; and plate temperatures adjacent to the truss at specific locations. Other than that, the deflections of the truss in the z–direction and in y–direction at the column top were measured, as well as the mass loss from the fuel pan. The fuel pan was placed on an insulated balance to probe the mass loss rate during experiments. Full description of the measuring point locations are presented in Appendix A.

2.5.1 Gas phase thermocouple measurement

1 mm thick shielded thermocouples, type K, were used to monitor the ceiling jet and fire plume temperatures. These were mounted 100 mm below the upper chord of truss F2, from mid-span and every meter towards the B-side, see Figure 7.

Figure 7. Thermocouple mounted 100 mm below the upper chord of truss F2.

Additionally, a thermocouple tree was mounted centrally over the fuel pan in each test, see Figure 8.

Figure 8. Figure to the left shows the TC tree mounted centrally over the fuel pan just before test 1. In the same figure, parts of Truss F2 and F1 in the experimental setup can also be seen as well as the wall and column in the background which are not part of the test construction but a part of the burn hall itself. The figure to the right shows the TC tree mounted centrally over the fuel pan before test 3.

2.5.2   Steel temperature

Steel temperatures in the column were measured with shielded thermocouples, type K. The thermocouples were peened into 3 mm deep, drilled holes. The temperatures were probed at six different heights facing the fire and at two different heights on the unexposed side of the column, see Appendix A. In the ceiling and truss, non-shielded thermocouples were welded directly to the steel, see Figure 9.

Figure 9. TC welded to the lower chord of truss F2.

In the ceiling, thermocouples was welded to the upper side of the steel sheet and covered locally with stone wool to minimize local cooling by convection and to ensure comparison of temperatures measured at the top and lower parts of the ribs, see Figure 10.
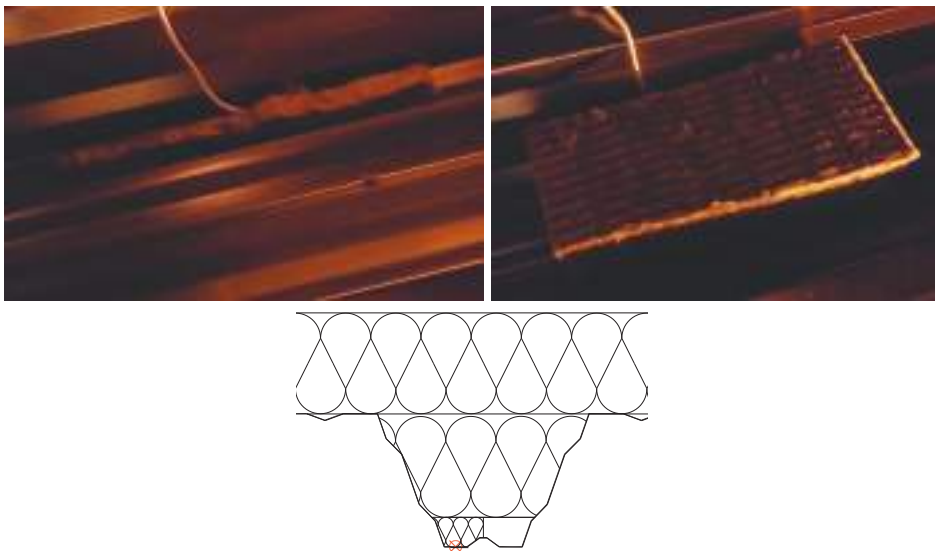
Figure 10. TC mounted on the steel ceiling upper surface and the local insulation added. Before the tests, an additional, completely covering layer of rock wool (100 mm) was added to the ceiling. Illustration of the location is added for clarity.

2.5.3 Plate thermometers

Standard plate thermometers (PT), as detailed in EN 1636-1, were mounted in all directions around the vertical section and the upper and lower chord close to the central position of truss F2, see Figure 11. In addition, PT facing the floor was mounted under the lower chord at several positions between the center and the C2B column, see Figure 12 and Appendix A for details.

Figure 11. Location of plate thermometers adjacent to the vertical directly above the fire (left), the upper chord (middle) and the lower chord (right).

The PTs were added to measure thermal exposure to the steel in the form of adiabatic surface temperatures [10] [11]. This has proven to be a valid method for transferring thermal exposure from experiments to numerical calculations as shown in [1] and [2].

Figure 12. Plate thermometer placed adjacent to the lower chord facing the floor.

2.5.4 Displacement measurements

Linear position transducers were positioned on floor level with strings connected to the lower chord ±2 m from the central position of the truss, measuring the vertical displacement of the lower chord. In addition, horizontal displacements of the top of the central columns (CA2 and CB2) were measured using the same technique, see Figure 13 and Appendix A.

Figure 13. Displacement meters attached to the beam parallel to and directly under F2 for vertical measures (left) and to the wall of the burn hall for horizontal measures (right).

3 RESULTS

The full set of results from the experiments is presented in Annex B. Below, a general description of each test and of the visual damages on the steel structure is presented. Thereafter, temperature and deflection measurements are given. Videos of the tests can be found on the internet, [12].

3.1 General behavior

First test

In the first test, the fuel burned with a constant plume. The plume reached the lower chord during the main part of the test but no flames affecting the ceiling. Four representative photos are given in Figure 14.

The plume hit the ceiling centrally above the fuel pan. After 8.5 minutes, the ventilation in the burn hall was turned on creating a draught that tilted the plume slightly (0.5-1 m) towards truss F1, see Figure 17. After the turning on the ventilation, temperatures about one meter along the truss increased on behalf of the temperatures just above the fuel pan. There were no visible damage to the steel frame apart from significant soot deposition and a white region on the section of the truss subjected to the most severe thermal impact.

Second test

In the second test, ventilation was turned off during the entire test. Nevertheless, the plume tilted in the same direction as the plume did in test 1 at the later stage of the test. During this test, flames impinged the ceiling creating a white region on the steel sheet with the most severe thermal impact.

Third test

In the third test, the wall on side B was erected and the fuel pan relocated adjacent to column C2B. As expected, the flame tilted towards the wall during the test due to the asymmetric entrainment of air. Flames reached the lower truss but most of the time, not the entire way up to the ceiling. The burn pattern on the wall and a white region in the ceiling, visible after the test, suggested a more severe impact towards truss 1, see Figure 16.
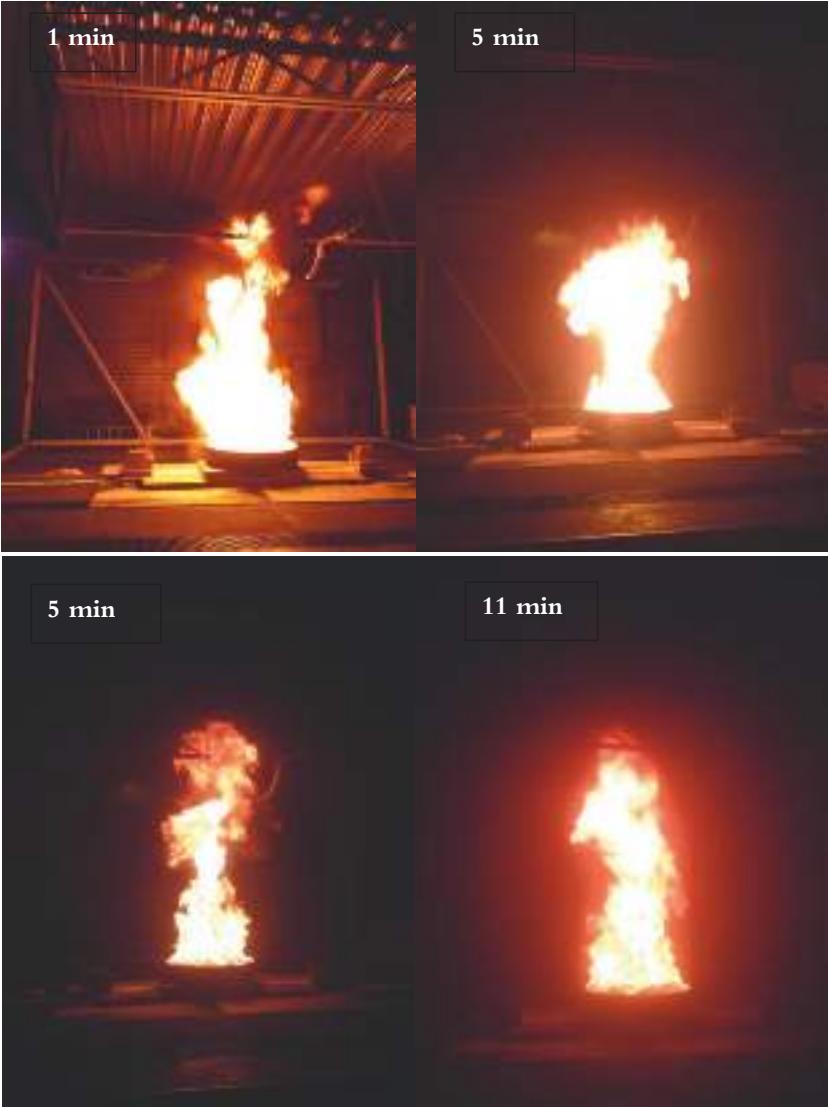
Figure 14. Photos from Test 1 at four different times. Note the decrease in visibility over time.
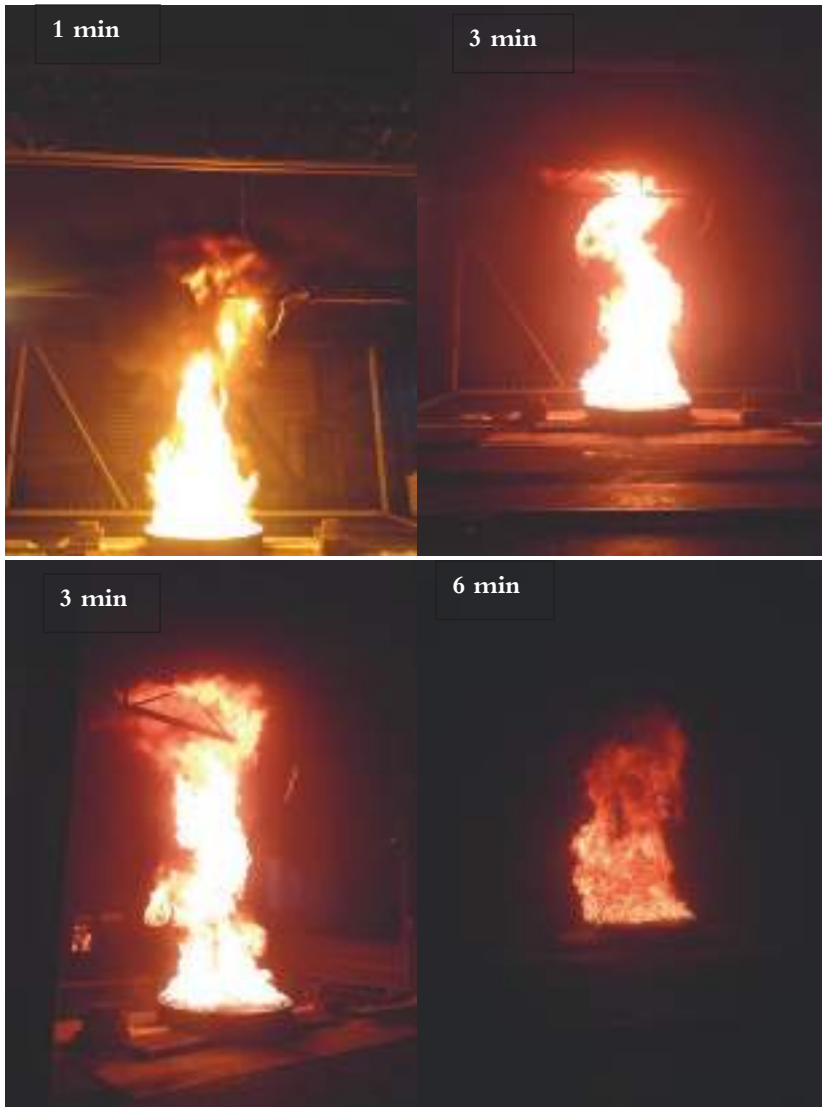
Figure 15. Photos from test 2 at four different times.
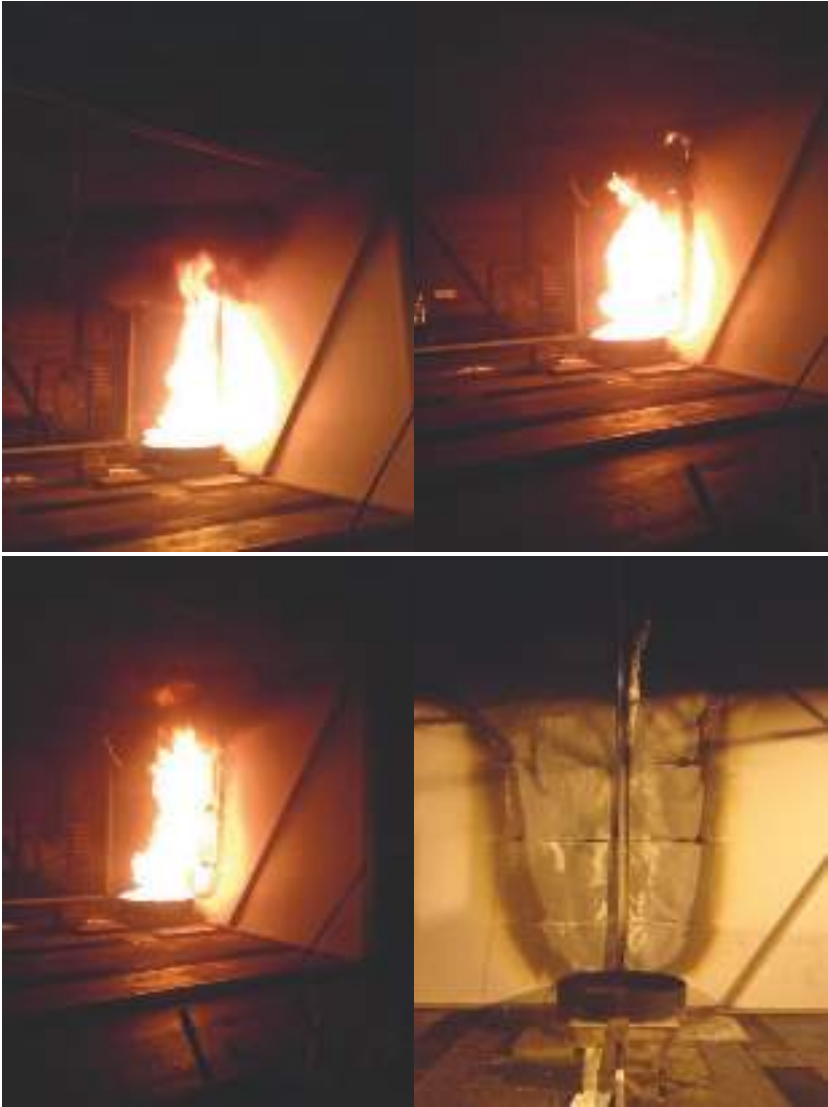
Figure 16. Photos of test 3 at three different times and also the burn pattern on the wall after the test.

Figure 17 presents an illustration of where the plume hit the ceiling in the different tests.
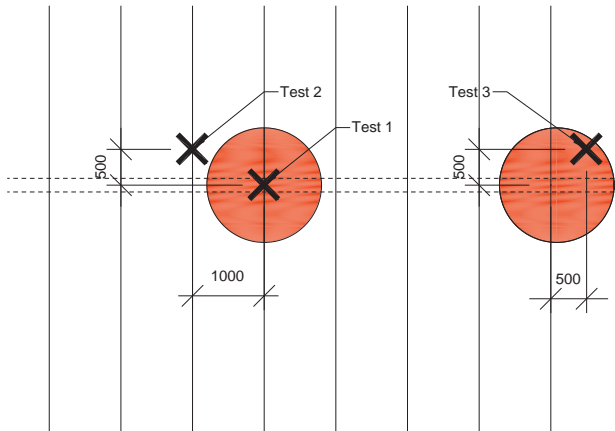
Figure 17. Locations of where the plume hit the ceiling.

The balance under the fuel pan malfunctioned during most part of test 3. However, enough data was recovered to calculate the mean mass loss rate during experiment. The data and the fitted mean data can be found in Appendix B, Mass loss. The mass loss rate is used to calculate the chemical heat release rate (HRR) during the test, which is the heat release rate if complete combustion would take place, see Figure 18.
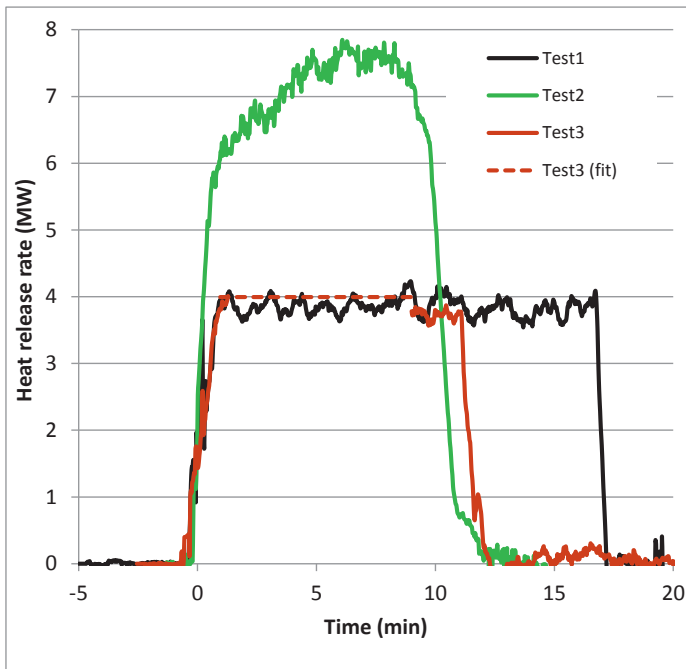
Figure 18. Chemical HRR during the tests.

3.2 Gas phase TC temperature

Apart from the normal fluctuations of TC temperatures within the plume during the tests, even the temperatures far from the plume centerline had significant fluctuations. This was due to the inclination of the plumes especially in the later parts of test 1 and 2. The average TC temperatures in the early stage of the tests are shown in Figure 19.
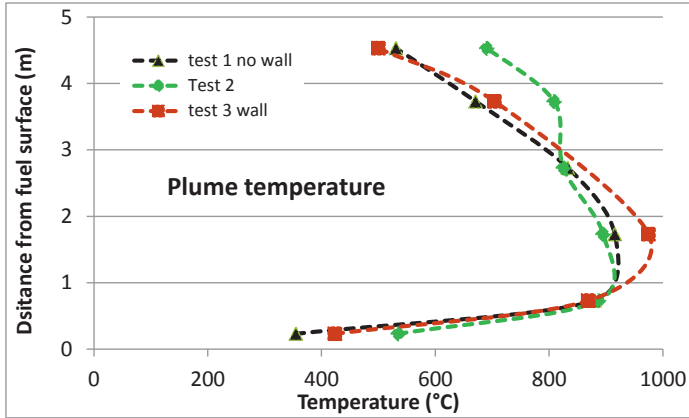
Figure 19. Average temperatures of the TC tree in the early parts of the tests.

The TC temperatures in the gas phase close to the ceiling were measured 100 mm below the upper chord of truss F2, see Figure 7. In the first part of each test, these temperatures increased steadily due to cooling of the hot gas by the colder structure. The temperatures stabilized completely in the later part of each test and Figure 20 shows the average temperatures during the last three minutes of each test. As expected, the larger fire of test 2 resulted in higher temperatures along the truss compared to test 1. Additionally, test 3, with the wall preventing gas flow in one direction, resulted in higher temperatures compared to the larger fire of test 2 for distances ≥2 m from the plume center line.
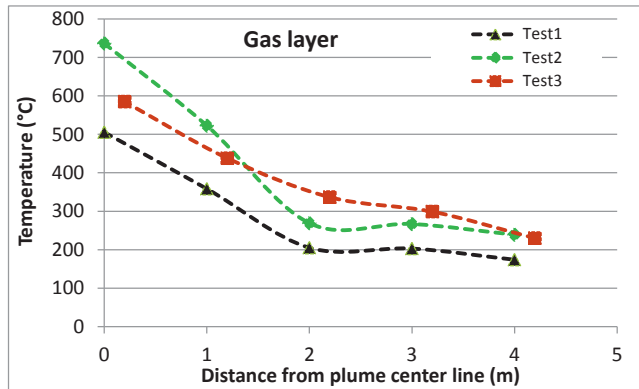
Figure 20. TC temperatures in the hot gas layer along the truss. The distance is from straight above the center of the fuel pan 100 mm below the upper chord.

3.3 Truss temperature

Figure 21 shows the temperature evolution of the upper and lower chord at the centerline and two meters down the truss during test 1. In the near field, i.e. close to the plume centerline, the steel reached close to steady state temperatures before the end of the tests which was not the case in the far field, i.e. away from the plume, The change in inclination of the plume, however, yielded a slight decrease in temperature in the near field at the end of the test. Directly above the plume, the upper chord was cooler than the lower chord by 60-130 °C due to decline in plume centerline temperature and radiative intensity from the flame with increasing height. 3 m away from the plume centerline, the upper chord is heated primarily by hot gases travelling along the ceiling and therefore the upper chord is hotter than the lower one.
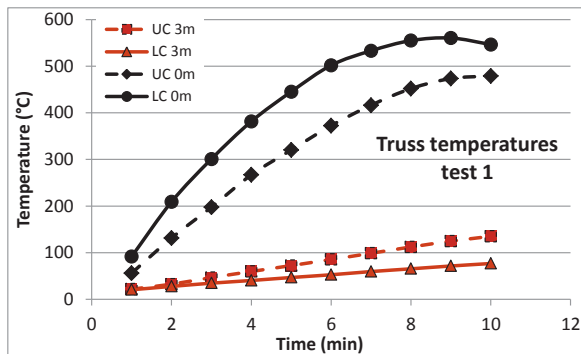
Figure 21. Truss temperatures in the upper (dashed lines) and lower (solid lines) chord in test 1. The temperatures are evaluated above the plume center line and 3 m along truss.

The temperature distribution along the truss is fairly symmetric in test 1 and 2 (bearing in mind the inclination of the plume). The temperatures decrease rapidly with the distance from the plume center line. For test 2, the upper chord is hotter than the lower one at all distances measured including directly above the fuel pan.
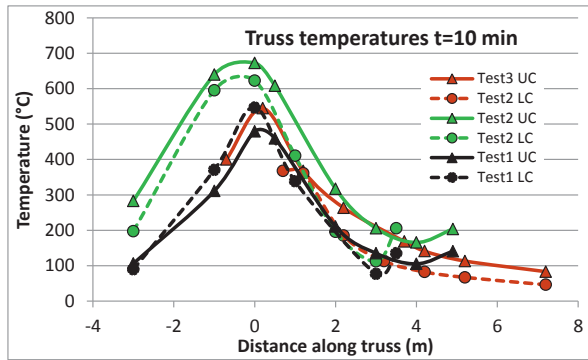
Figure 22. Temperature distribution in the truss after 10 minutes of each test.

The trusses running parallel five meters from F2 have, as expected, significantly lower temperatures than the central one, see Figure 23.
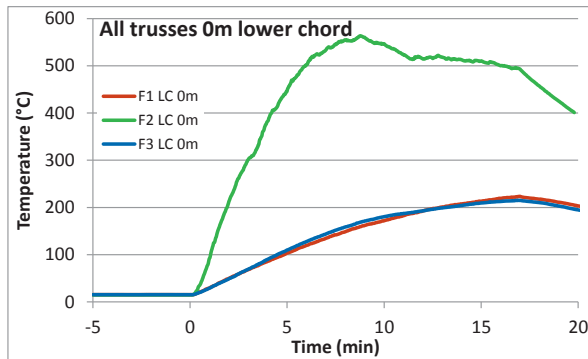
Figure 23. Temperature development at mid-span of the lower chord of all three trusses in test 1.

Two steel L-sections form the upper and lower chords. The possible difference in heating of the two parts of the L-section as well as in the verticals/diagonals is investigated at different locations. The vertical U-section at mid-span shows the same temperature for the two measuring points, one facing the B-side and one facing truss 3. The lower chord at mid-span (0 m) shows a faster and more severe heat impact in the horizontally oriented part of the L-section compared to the vertically oriented. This could be partially due to an increased radiant heat flux for the part facing the fire but since the same phenomenon is noticed in the cooling phase (faster cooling of the horizontally oriented part) the most significant reason is probably the fact that the vertically oriented part is connected to the vertical U-section and thereby exhibits more mass per exposed surface area compared to the horizontally oriented part. This is also supported by the result from the diagonal at 4.25 m and the upper chord at 0.5 m. In both these cases, the heating is very similar in both parts of the L-section. In neither of these measurement points is any part of the L-section connected to any other steel section. Figure 24 shows some of the temperatures from test 1 but the same behavior is noticed also for tests 2 and 3.
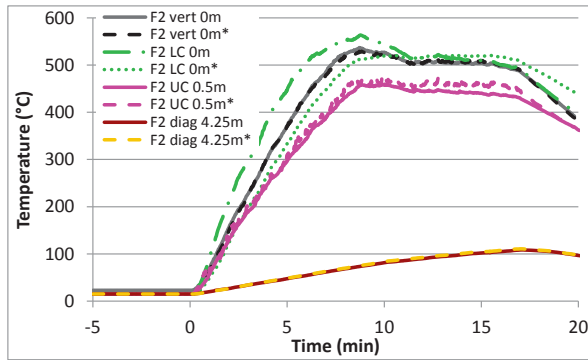
Figure 24. Temperature evolution of horizontal (⋆) and vertical parts of the L-section at different locations.

The ceiling is always hotter than the truss during the heating period due to the lower surface to mass ratio in the steel sheet compared to the truss elements this difference vanishes once reaching steady state. This could be seen close to the fire plume but at 2 m distance or more from the plume center line, steady state is never reached and the ceiling is therefore hotter than any part of the truss during the entire test.

3.4 Ceiling temperature

The ceiling heats up much faster than the truss due to the higher surface to mass ratio (A_m/V) of the steel sheet in combination with the insulation on top. Figure 26 to Figure 28 shows the temperature distribution in the ceiling in all three tests. For test 1, the temperatures are taken 8 minutes into the test, just before the plume started tilting due to the ventilation. For test 2 and 3, the temperatures are taken 10 minutes into the test, after reaching stable values.

The distribution is to be considered axi-symmetric around the plume center line. The decrease in temperature with distance is marginally more significant in the direction parallel to the truss compared to orthogonal to the trusses. This might be due to the profile of the steel sheet which makes it easier for the gas to flow in the direction of the ribs (orthogonal to the trusses). This effect is small but can be seen in all three tests.
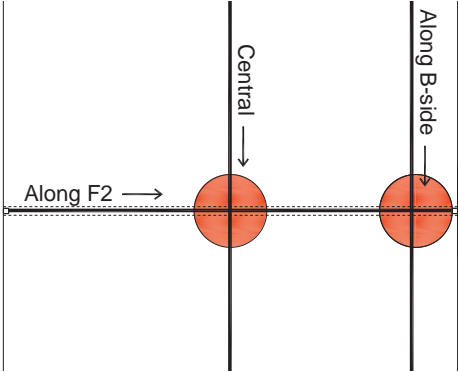
Figure 25. Illustration of lines is Figure 26 to Figure 28.
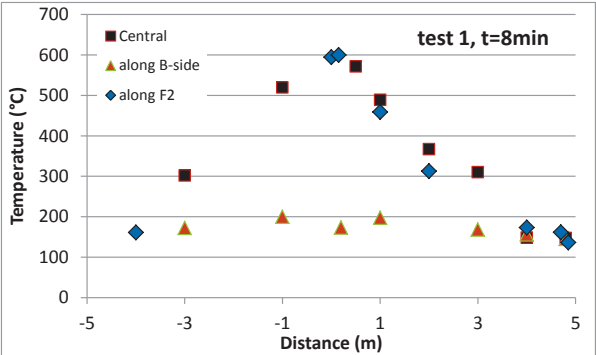
Figure 26. Ceiling temperatures at t=8 min of test 1.
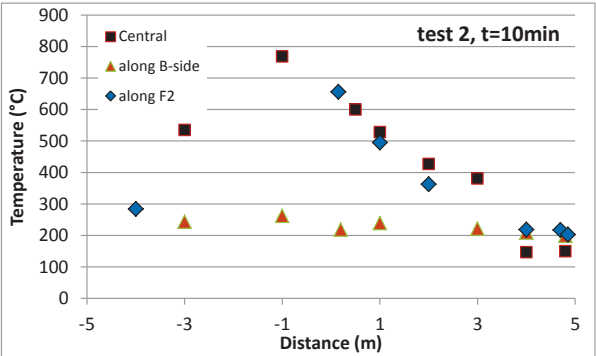
Figure 27. Temperatures in the ceiling in test 2.
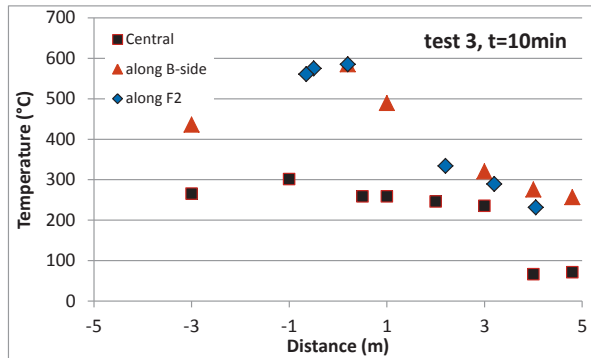
Figure 28. Temperatures in the ceiling in test 3. The distance along F2 is given as the distance from the plume central line close to column C2B.

3.5 Column temperature

The temperatures in C2B reached over 600 °C in test 3 where the fuel pan was located adjacent to the column. In test 1 and 2, however, the maximum temperatures in C2B were well below 100 °C during the entire tests. For test 3, with the fire adjacent to the column, the temperatures along the height of column C2B in test 3 are shown in Figure 29 with the maximum temperature registered about 1 m above the fuel height. The temperature difference between the exposed and unexposed side is after five minutes well over 300 °C. This difference, however, decreases with time. At the exposed surface, the temperature increases very little between 10 and 11 minutes after ignition whereas the temperature on the unexposed side increases significantly during this minute. This was due to substantial heat transfer from the exposed to the unexposed side of the 120 mm x 120 mm x 8 mm hollow square column. The mode of heat transfer has previously been shown to be primarily to a large extent by internal radiation and convection rather than conduction in the steel [2].
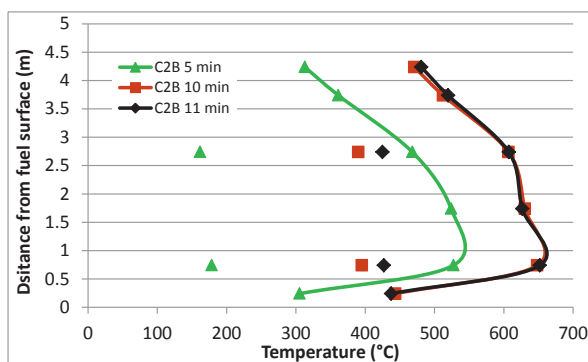
Figure 29. Steel temperatures in column C2B (adjacent to fire) in test 3 after 5, 10 and 11 minutes. The data points connected by a line are measured on the exposed side of the square section and the unconnected data points are on the opposite side, adjacent to the wall.

3.6 Temperatures in the truss to beam connection.

In the six measurement points in the connection the temperatures vary less than 100 °C during the entire test 3, see Figure 30. The hottest temperatures are found in the upper chord next to the insulated ceiling. The square hollow section in the support is somewhat colder whereas the top plate of column C2B is the coldest. The reason for this is a lower surface to mass ratio, (A_m/V), which imposes a long time constant for heating.
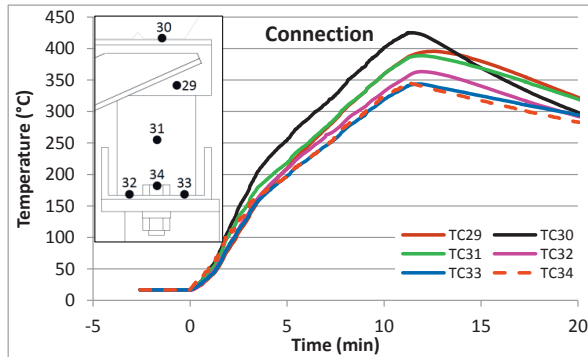

Figure 30. Temperatures in the connection during test 3.

The temperatures in the connection are substantially lower compared to the vertical element closest to the connection. An overview of the temperatures in the truss close to the connection at 10 minutes after ignition in test 3 can be found in Figure 31. The steel temperatures in the truss in the near field, i.e. close to the fire, are close to steady state. The steel temperatures in the far field, however, still increases after ten minutes. This is due to a difference in the time constant with different fire exposure and convective properties.

For the tests 1 and 2, where the fire was situated at the mid-span of the truss, the temperatures in the connection were much lower. The upper chord above column C2B reached only 150 °C after 15 minutes of fire and the rest of the connection reached temperatures between 65 and 100 °C.
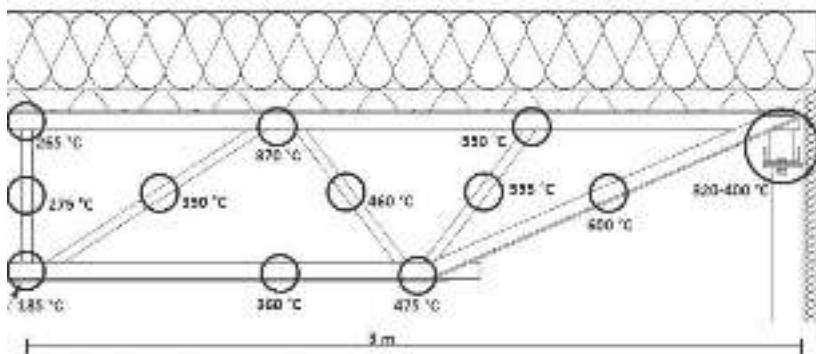
Figure 31. Steel temperatures close to the truss to beam connection after ten minutes of test 3.

3.7 Deflections

In test 1, the deflections were symmetric around the mid-span as shown in Figure 32. In the early stage, the lower chord is locally hotter than the upper chord creating a downwards deflection due to the asymmetric thermal expansion. In the later stage of heating, ceiling jets heats the upper chord while the lower chord remains colder further away from the plume centerline. As the overall temperature is higher in the upper chord, deflection upwards starts to dominate. During the whole test the truss pushes the columns further and further apart at the height of the supports.
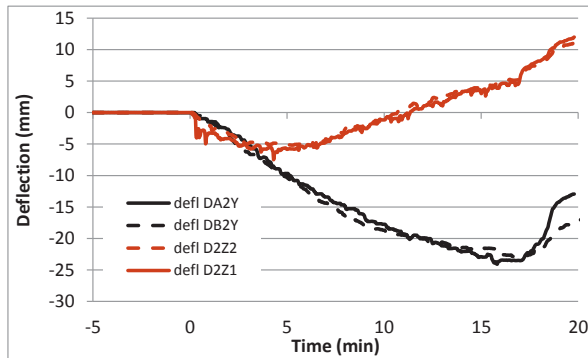
Figure 32. Vertical deflections in the lower chord at ±2 m from the mid-span as well as horizontal deflections at both supports during test 1. See Appendix A.

The same phenomenon was observed in test 2 but with larger deflections. Higher effect results in hotter gases at the upper chord even further away from the plume centerline, as can be seen in Figure 20. This results in a larger upwards deflection due to thermal bowing than could be observed in test 1.

During the asymmetric heating of test 3, the thermal bowing downwards was very short lived and only noticed within the first minute of heating close to the fire. Thereafter the deflection was upwards as the majority of the truss was hotter on the upper chord compared to the lower chord. Deflections were larger close to the fire where the temperature gradient was larger. Column C2A, at the cold end of truss F2, was pulled towards the fire by the truss during half of test 3, see Figure 33. This was most likely due to the thermal bowing of column 2B. Since the lower support of the column was fixed (and colder than the rest) the bowing of the column made it pull the truss inwards. The initial negative deflection at the top of column 2B was not a consequence of the truss pushing but the thermal bowing of the column. Later in the test, the deflection at the top of column 2A was negative (away from the center of the truss). As the overall temperature became higher in the truss and the thermal gradient in column C2B decreased, the horizontal forces due to thermal expansion started to dominate and both columns were pushed outwards.
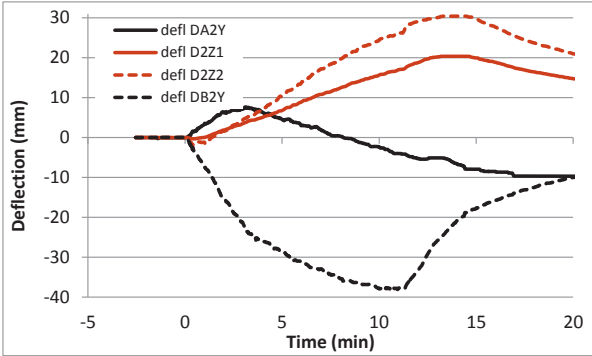
*Figure 33. Deflections during test 3.*

4 REFERENCES

[1] U. Wickström, R. Jansson och H. Touvinen, "Experiments and theory on heat transfer and temperature analysis of fire exposed steel beams," SP Report 2009:19, Borås, 2009.

[2] A. Byström, J. Sjöström, U. Wickström, D. Lange och M. Veljkovic, "Large Scale Test on a Steel Column Exposed to Localized Fire," *Journal of Structural Fire Engineering,* vol. 5, pp. 147-160, 2014.

[3] C. Gutiérrez-Montes, E. Sanmiguel-Rojas, A. Viedma och G. Rein, "Experimental data and numerical modeling of 1.3 and 2.3 MW fires in a 20 m cubic atrium," *Building and Environment,* vol. 44, pp. 1824-1839, 2009.

[4] Y. Hasemi, Y. Yokobayashi, T. Wakamatsu och A. V. Ptchelintsev, "Modeling of heating mechanism and thermal response of structural components exposed to localized fires: a new application of diffusion flame modeling to fire safety engineering. NIST internal report 6030," National Institute of Standards and Technology, Gaithersburg, Maryland, 1997.

[5] "Eurocode 1: actions on structures — part 1-2: general actions — actions on structures," 2002.

[6] S. Kumar, S. Miles, S. Welch, O. Vassart, B. Zhao, A. D. Lemaire, L. M. Noordijk, J. H. H. Fellinger och J.-M. Franssen, "FIRESTRUC - integrating advanced three-dimensional modelling mehodologies for predicting thermo-mechanical behaviour of steel and composite structures subjected to natural fires, RFS-CR-03030," European Commission, 2006.

[7] C.-k. Chen och W. Zhang, "Structural behaviors of steel roof truss exposed to pool fire," *Journal of Central South University,* vol. 19, pp. 2054-2060, 2012.

[8] A. Tewarson, "Generation of Heat and Gaseous, Liquid and Solid Products in Fires," i *SFPE Handbook of Fire Protection Engineering, 4th edition*, Quincy, MA, Natl Fire Protection Assn, 2008.

[9] "EN 1363-1 Fire Resistance tests. General requirements," 2012.

[10] U. Wickström, "Adiabatic Surface Temperature and the Plate Thermometer for Calculating Heat Transfer and Controlling Fire Resistance Furnaces," i *Fire Safety Science 9*, Karlsruhe, 2008.

[11] U. Wickström, "The plate thermometer - a simple instrument for reaching harmonized fire resistance tests," *Fire Technology,* vol. 30, pp. 195-208, May 1994.

[12] [Online]. Available: www.later.com.

[13] U. Wickström, "The Adiabatic Surface Temperature and the Plate Thermometer," i *Fire safety science - Proceedings of the thenth international symposium*, Collage Park, MD, 2011.

[14] U. Wickström, D. Duthinh och K. McGrattan, "Adiabatic Surface Temperature for Calculating Heat Transfer to Fire Exposed Structures," i *Proceedings of the 11th International Conference on Fire Science and Engineering - Interflam*, London, 2007.

APPENDIX A

Steel temperature positions
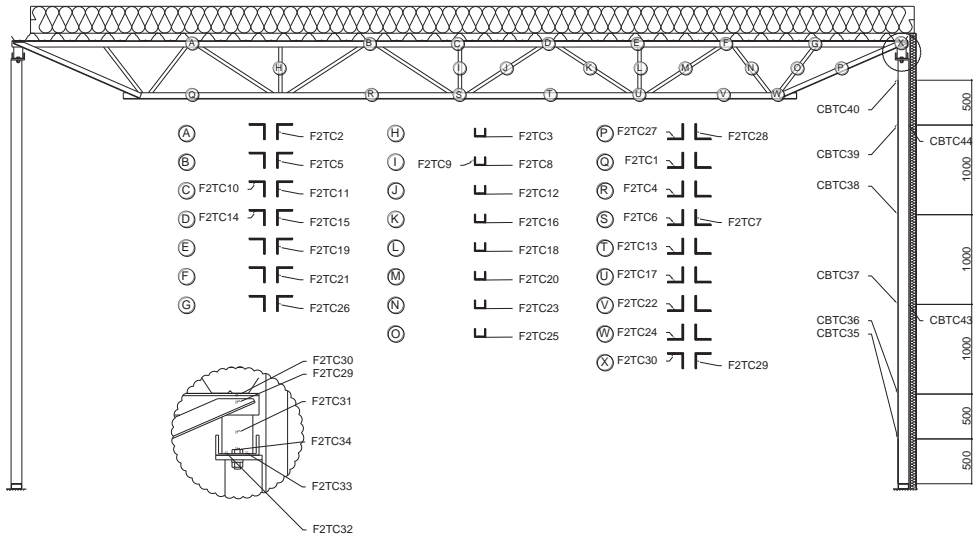
Gas temperature positions
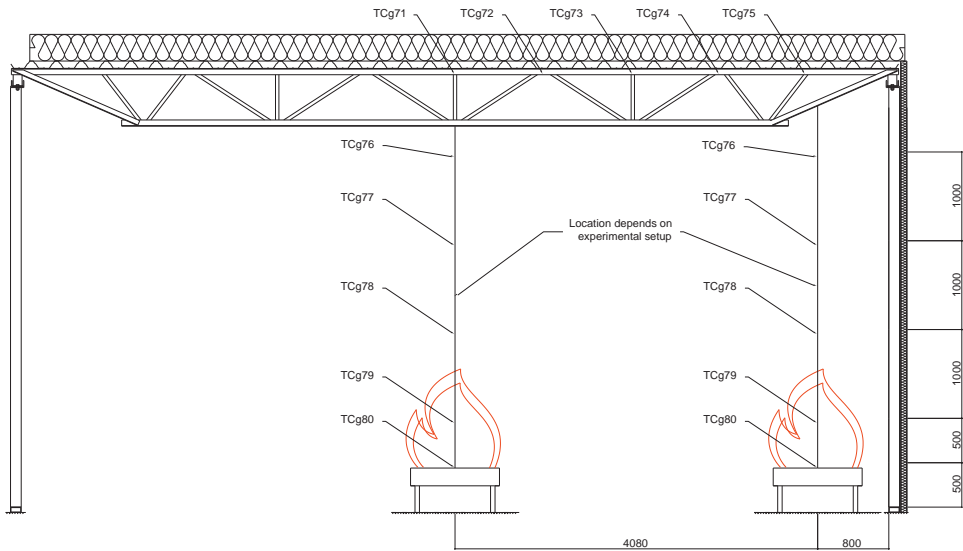
Plate thermometer positions

Truss beam
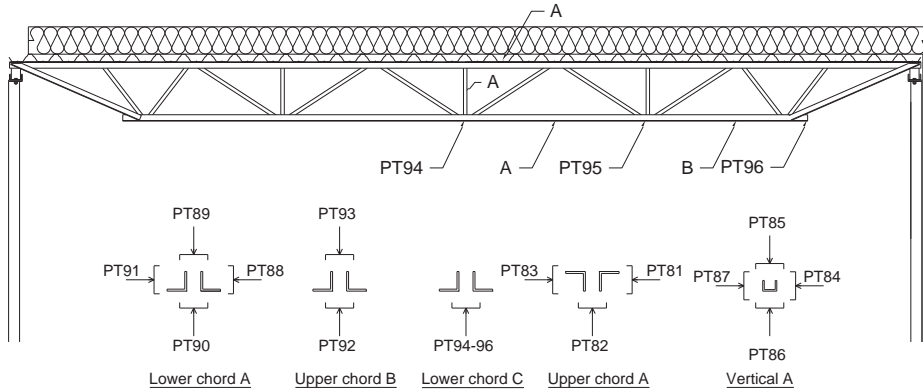
Roof
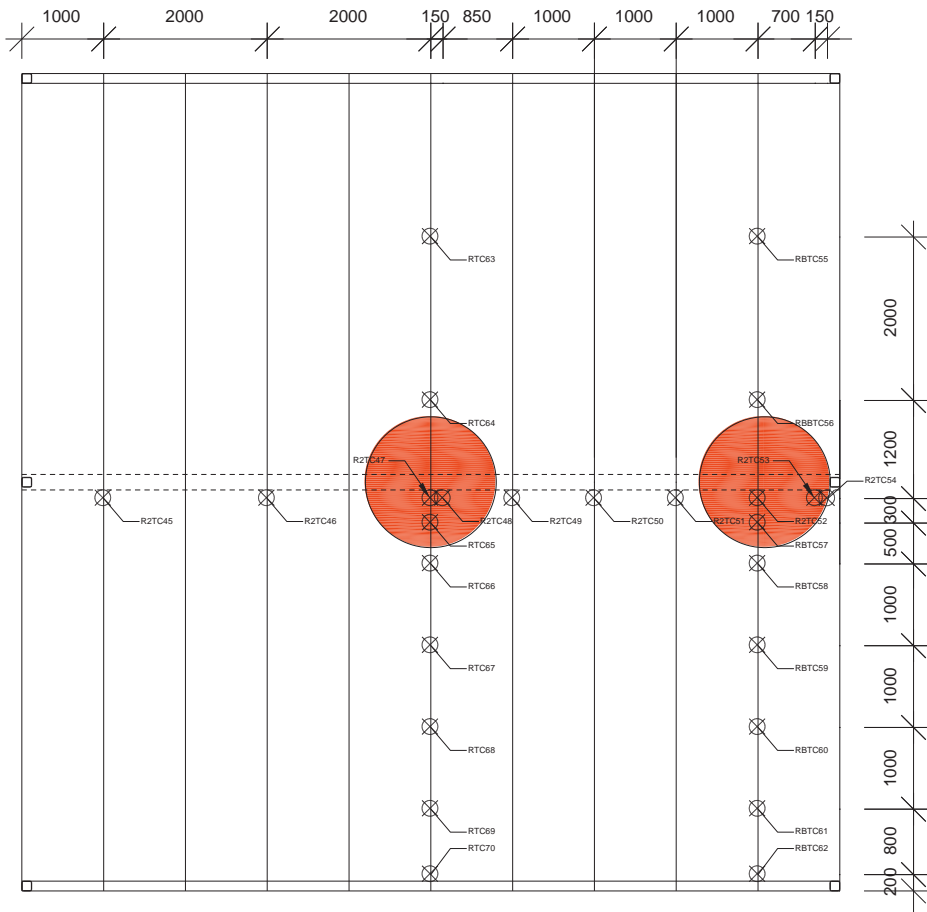
Deflection meter positions
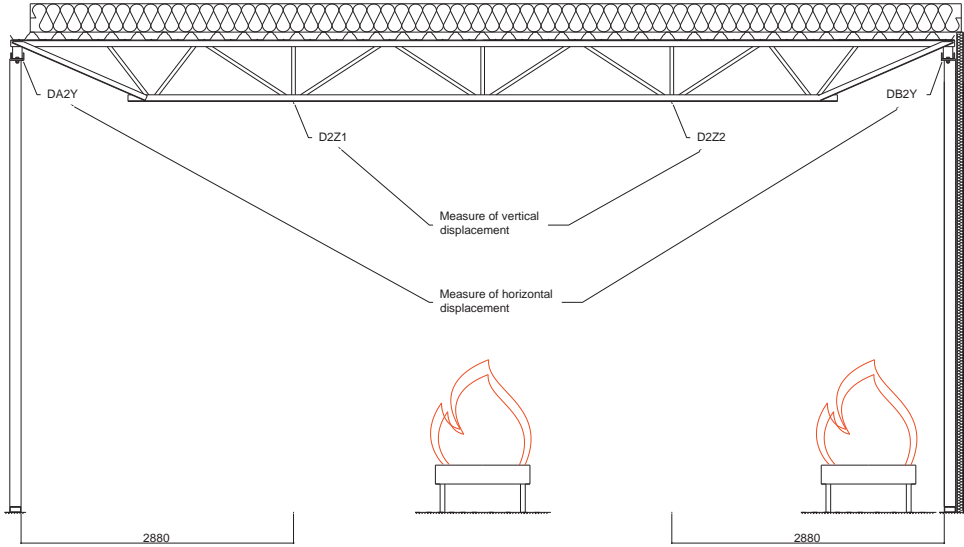
APPENDIX B

TC temperature in the gas phase along the plume centerline and ceiling
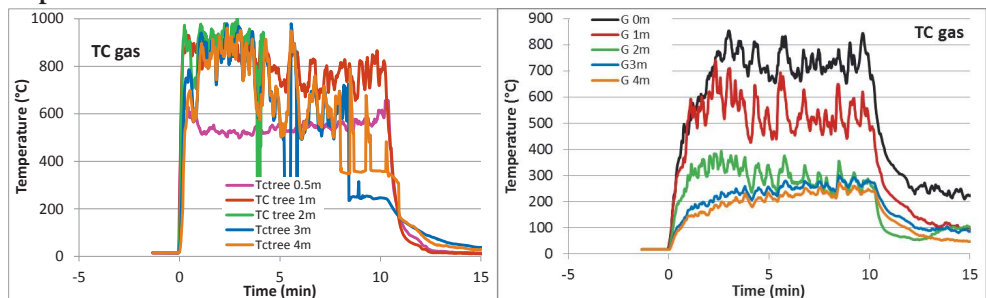
4.1.1.1   Nomenclature

G – TC in gas phase. Distance is given in meters from the central position of truss F2 towards side B.

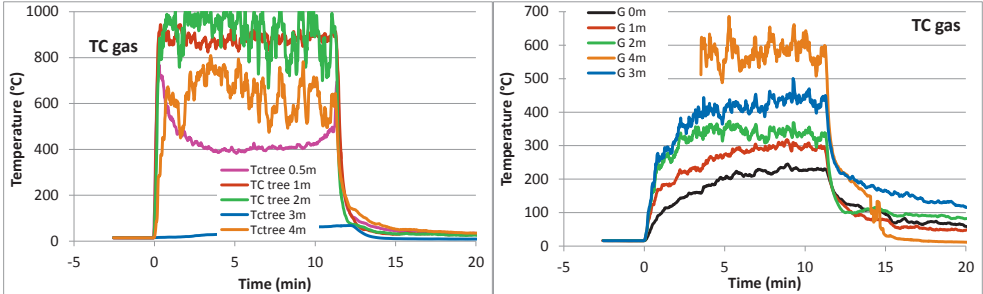TC tree - TC in the fire plume. Distance is given with reference to the floor level.

Experiment 1
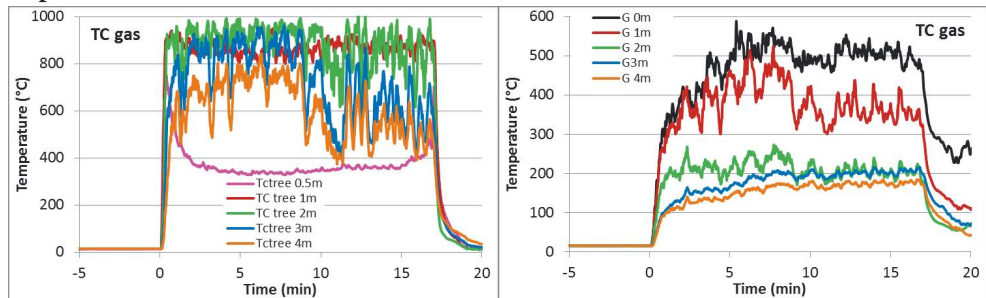
Experiment 2

Experiment 3

Ceiling temperatures

4.1.1.2 Nomenclature

R2 – Roof positions along truss F2 (shifted 200 mm towards side 3). Distance relative central position.

RB – Roof positions along a line one meter from side B. Distance relative the position of truss F2.

RC – Roof position along the central line crossing the central truss, F2. Distance relative F2.
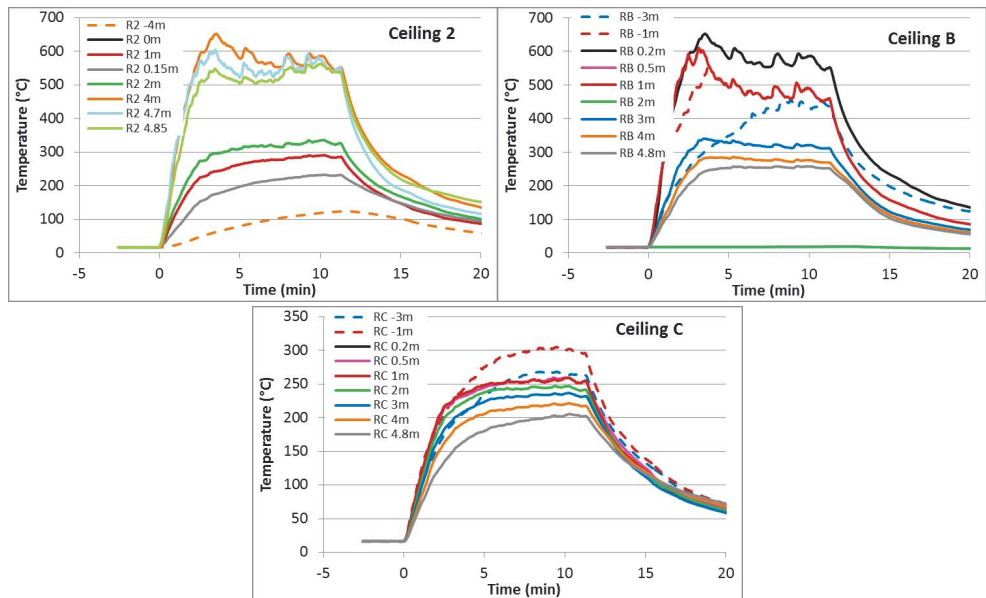
Experiment 1
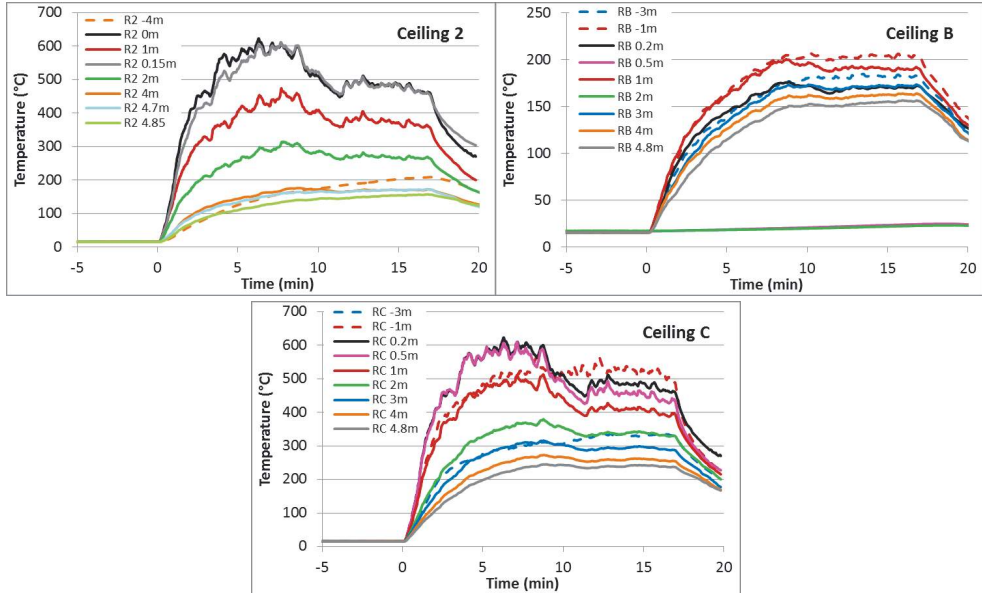
Experiment 2
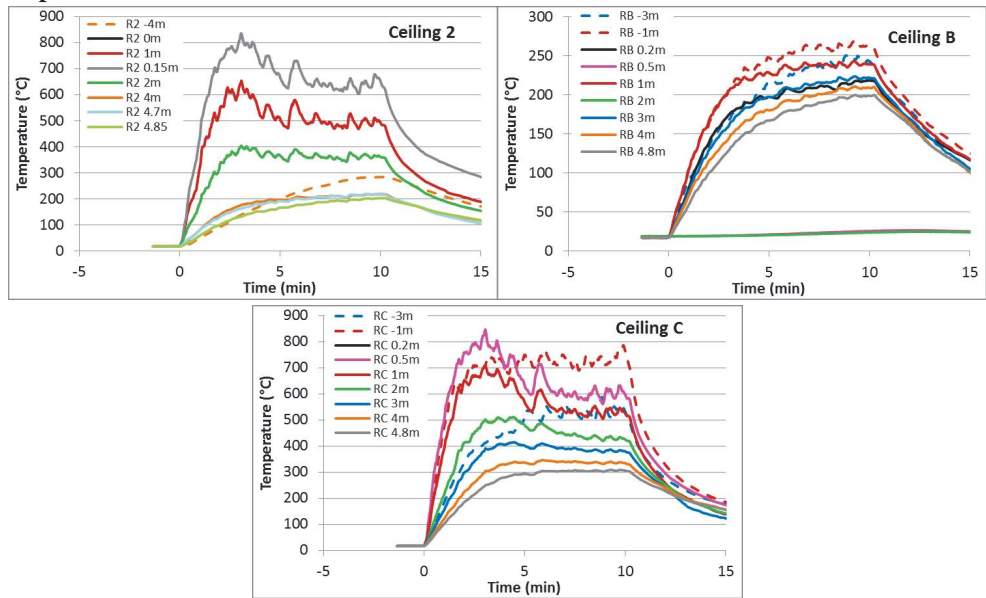
Experiment 3

Ceiling 2 distances still refer to the position relative the mid–span
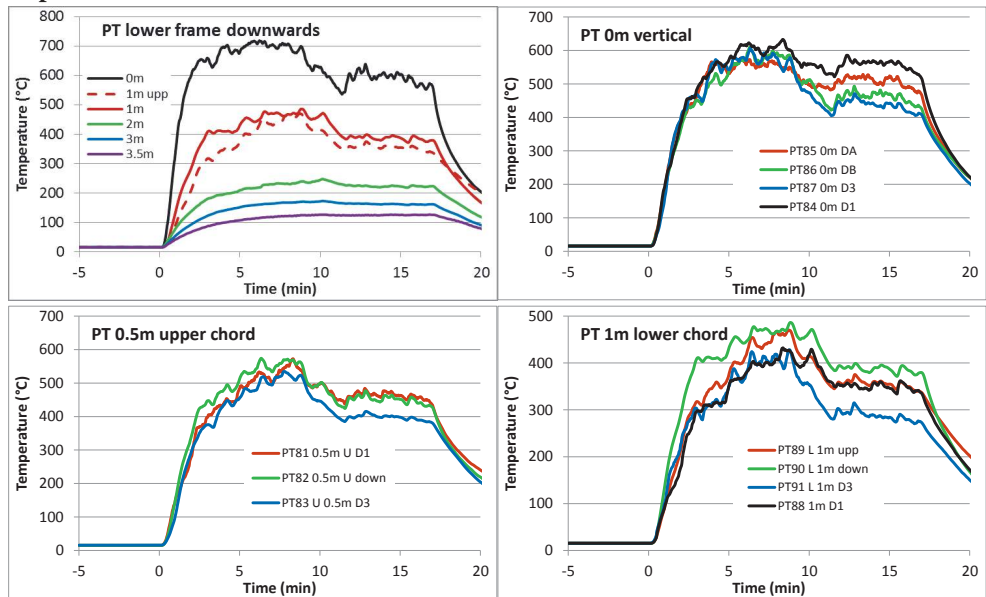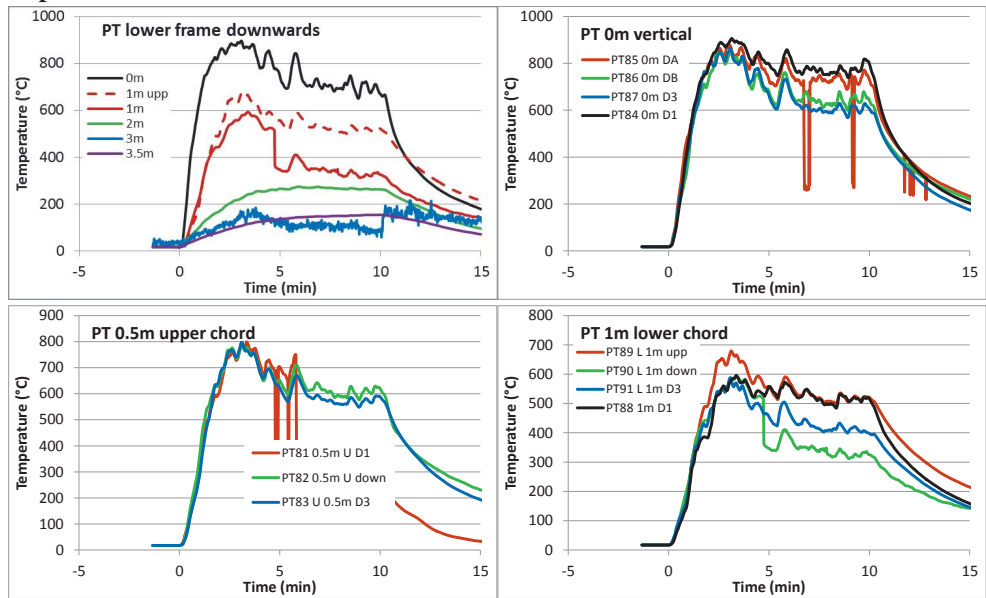
FIRE EXPOSURE TO THE TRUSS BEAM

4.1.1.3   Nomenclature

DA, DB, D1 and D3 – PT exposed surface direction against side A, B, 1 and 3, respectively.
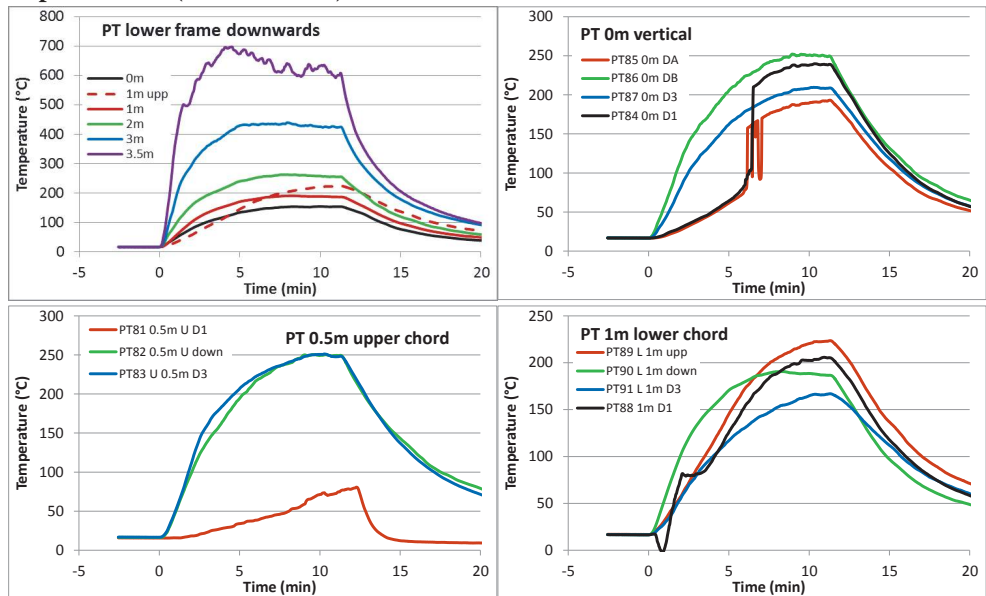Upp, down – direction of the exposed surface of the PT.

Experiment 1
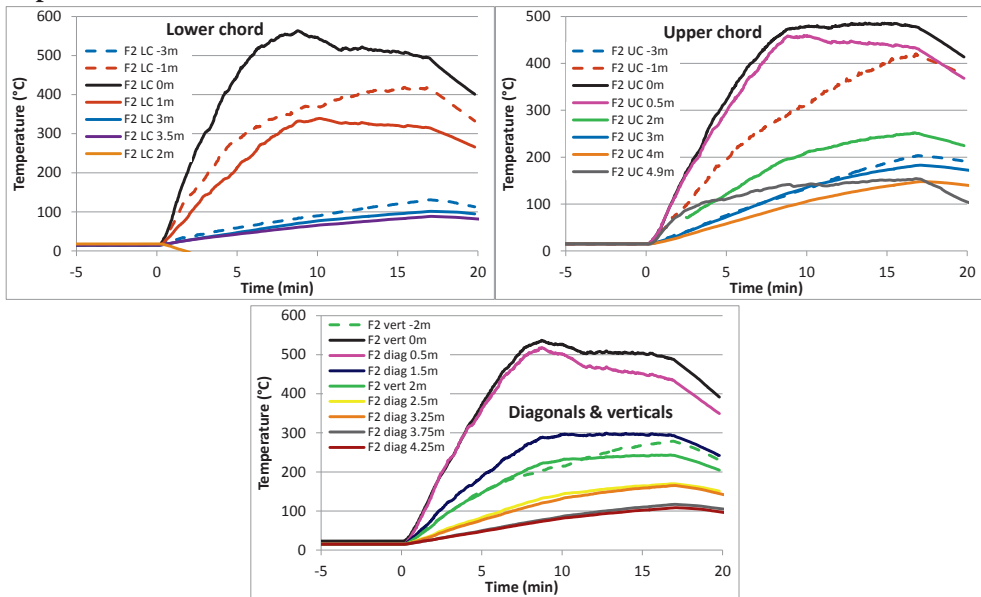
Experiment 2

Experiment 3 (reverse order)

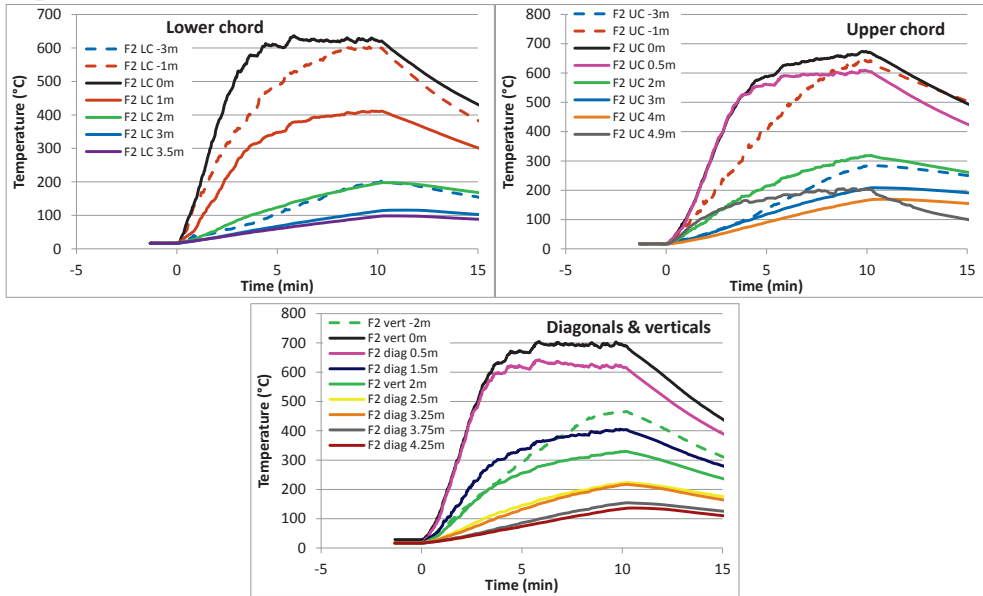# STEEL TEMPERATURE IN THE TRUSS BEAM

4.1.1.4   Nomenclature

F2 – central truss, distance relative the midspan.

LC, UC – Lower and upper chord, respectively.

Experiment 1
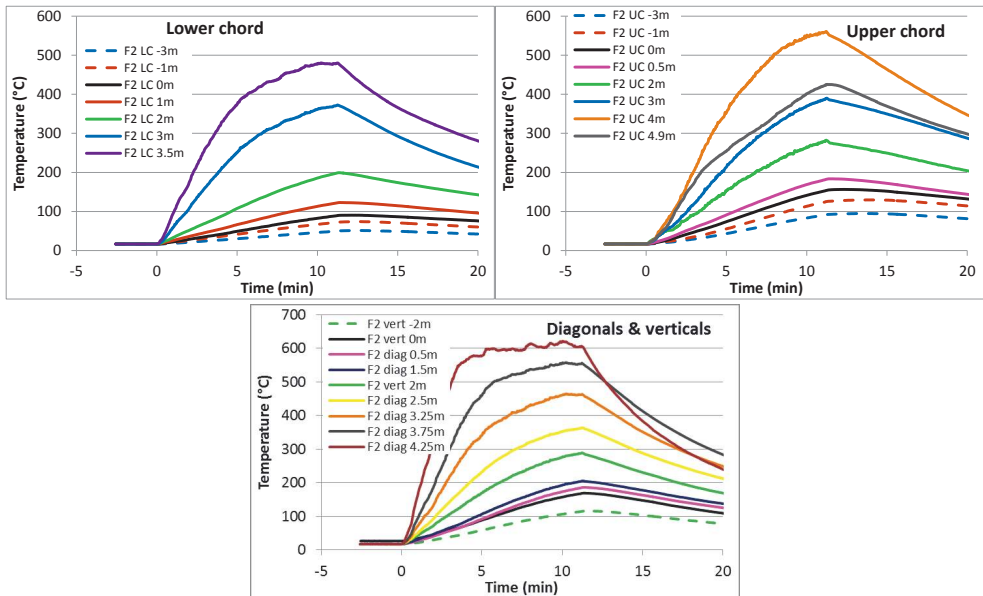
Experiment 2

Experiment 3

Position is relative the midspan. Thus, the fire plume central line is at the distance 4.08 m from the midspan.

Steel temperature column and connection

4.1.1.5 Nomenclature

Back – TC in the non–exposed side of column CB2.

Experiment 1
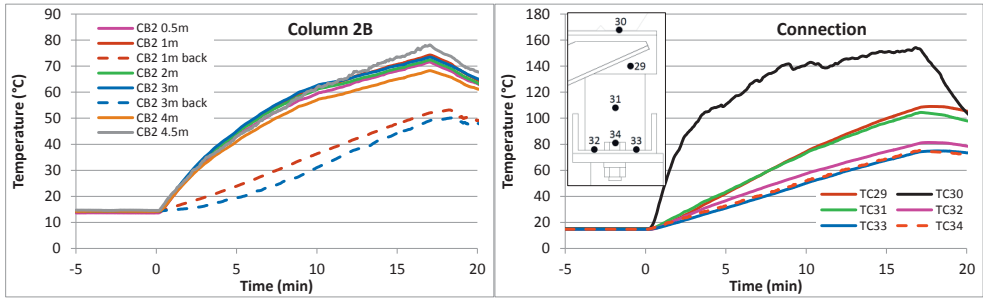
Experiment 2
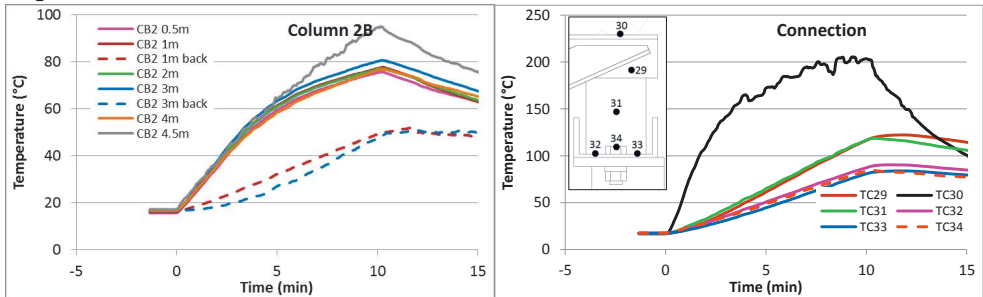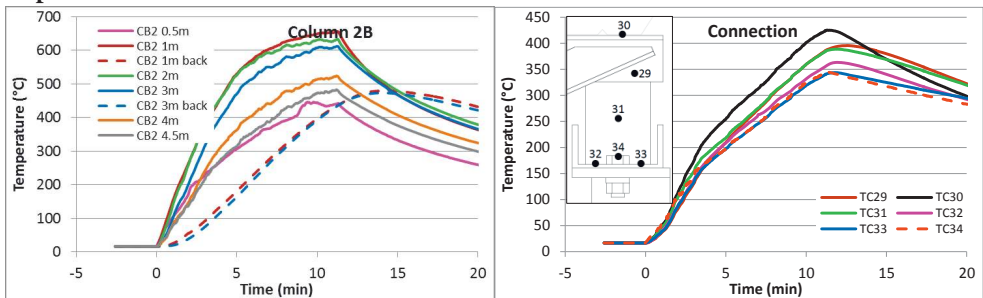
Experiment 3

Deflection

Experiment 1

Experiment 2

Experiment 3

Mass loss

Experiment 1

Experiment 2
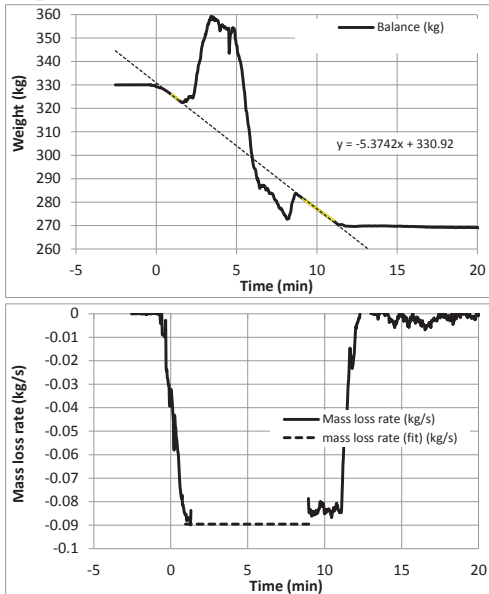
Experiment 3

$y = -5.3742x + 330.92$

PAPER E

*Thermal exposure from localized fires
to horizontal surfaces below the hot gas layer*

Sandström, J., Sjöström, J. and Wickström, U.

Brandforsk project no 312-131. Luleå (2019)

ABSTRACT

The temperature in the lower chord of steel trusses subjected to localized fires is difficult to estimate as most thermal exposure correlation formulas presented in the literature focus on heating along the ceiling where the temperature is very different from that of t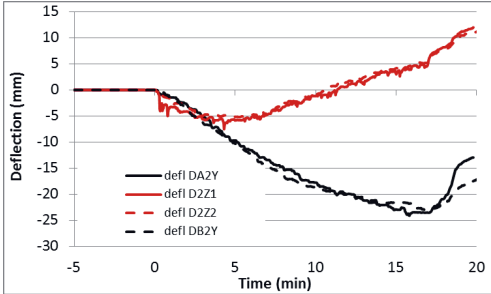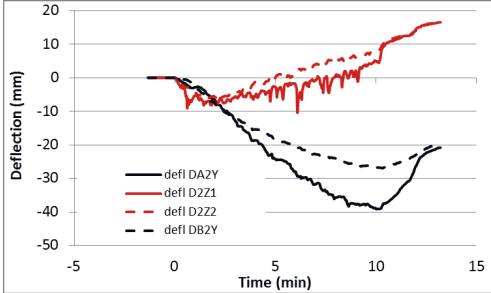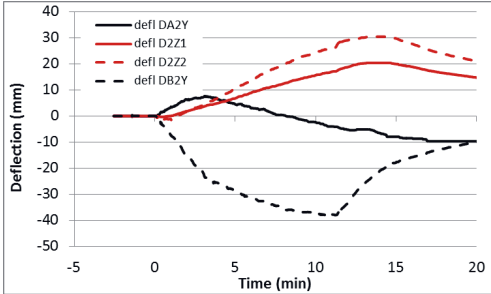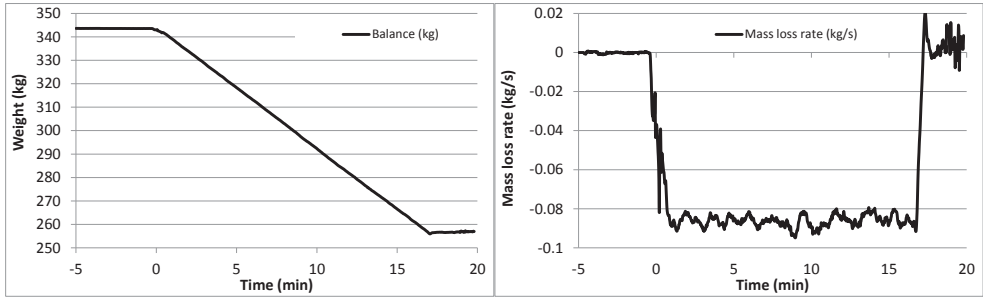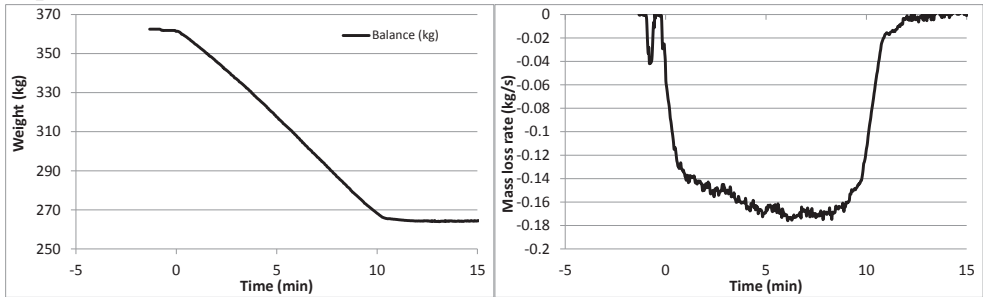he lower chord [1], [2]. At the same time as the upper chord is engulfed in a ceiling jet from a localized fire, the lower chord may be surrounded by air at ambient temperature.

Two existing methods by Zhang and Usmani [3] and Guowei et al. [4], [5] along with one new approach for calculating the thermal exposure of the lower chord are presented in this paper and compared to the results from experiments conducted in Trondheim 2015 [6].

A new approach presented in this paper is evaluated based on two separate assumptions of the thermal exposure. Outside the plume, the radiative contribution is assumed originating from the plume in the form of a cylinder and inside the plume, the temperature is assumed decreasing according to a Gaussian shape from the central axis temperature to the temperature down to the temperature from the first part of the model at the transition between inside and outside the plume.

All models provide good correlation to the experimental data outside the plume perimeter. Inside the plume perimeter, the thermal impact depends to a high degree to the relation between the flame height and the height of the horizontal surface of interest.

KEYWORDS: Performance based design, heat transfer, CFD, localized fires

NOMENCLATURE

Latin lower case

h	Heat transfer coefficient	$[W/m^2K]$
q	Heat	$[J]$
r	Radius	$[m]$
t	Time	$[s]$
z	Distance along central plume axis	$[m]$

Latin upper case

A	Area	$[m^2]$
H	Vertical distance from fuel surface	$[m]$
L	Length	$[m]$
Q	Heat	$[J \ or \ Ws]$
T	Temperature	$[K]$
V	Volume	$[m^3]$

Greek lower case

ε	Emissivity	$[-]$
σ	Stefan–Boltzmann constant	$[W/(m^2K^4)]$
κ	Extinction coefficient for the plume	$[m^{-1}]$

Greek upper case

Φ	View factor	$[-]$

Subscript

tot	Total (heat flux)	$[-]$
rad	Radiation (heat flux)	$[-]$
con	Convection (heat flux)	$[-]$
inc	Incident radiation (heat flux)	$[-]$
in	Incoming heat (heat flux)	$[-]$
b	Beam (length)	$[-]$
c	Convective	$[-]$
fl	Flame	$[-]$
g	Gas (temperature)	$[K]$
r	Radiation (temperature)	$[K]$
s	Surface	$[-]$
AST	Adiabatic Surface Temperature	$[-]$
0	Virtual origin	$[-]$
∞	Ambient conditions (temperature)	$[K]$

Superscript

$''$	Per unit area	$[m^{-2}]$
$\cdot$	Per unit time	$[s^{-1}]$

1 INTRODUCTION

When designing steel trusses exposed to localized fires in large open spaces, there is a lack of analytical methods for calculating the thermal exposure to the lower chord. The thermal exposure is often over-estimated by assuming standard fire temperature according to ISO 834 or EN 1363-1 or the ceiling temperature according to EN 1991-1-2 Annex C. To present a complete design tool for thermal exposure calculation to trusses, a complimentary method needs to be established.

This paper evaluates two previous methods along with a new method. The latter includes radiation from a fire plume to the lower chord. the plume is modelled assuming a Gaussian temperature distribution according to Heskestad [7].

The previous methods apply different approaches. Zhang and Usmani [3] calculate radiation from segments of the flame facing upwards, while Guowei et al. (2014), refined (2016), calculate radiation to the truss assuming it originates from the flame in the form of a point source [4], [5].

The methods are compared with experiments performed in Trondheim 2015 [6] as described below.

2   TRONDHEIM EXPERIMENTS

In 2015, experiments were conducted at SP Fire Research AS in Trondheim, Norway, burning Heptane fuel below a steel truss. They were documented in an experimental report [6] and therefore only briefly commentated on here.

The experiments were performed in a steel frame skeleton with dimensions 10 m by 10 m and 5 m high with no walls. A fuel pan was placed at the mid span of the steel truss at a center position, see Fig. 1. The roof was of corrugated steel sheets with insulation on top as is common in Swedish single-story steel frame buildings.
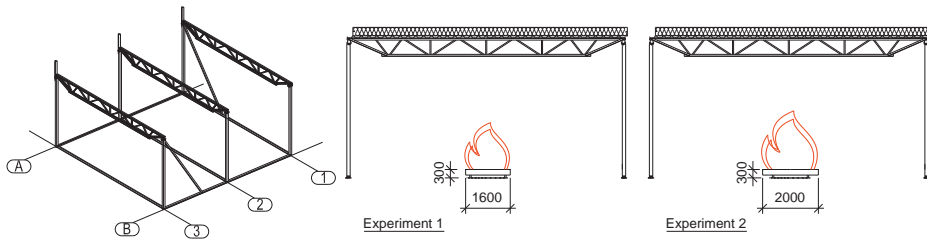
Fig. 1 Set up in the Trondheim experiments [6]. Ceiling height was 5.0 m

Both the thermal action on the lower chord of the central truss and its thermal response was measured. The thermal action was measured with plate thermometers, PT, mounted below the lower chord with a spacing of one meter, see Fig. 2. The lower chord was located at a height of 4.06 m from the fuel surface.
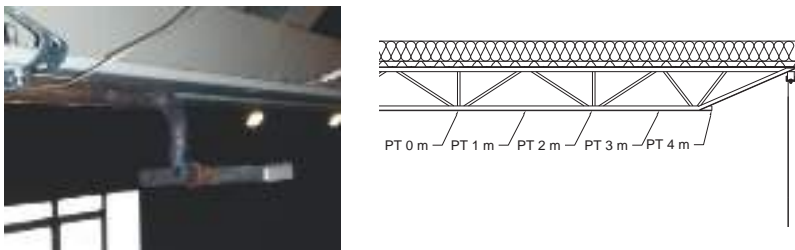
Fig. 2 Plate thermometers located 100 mm below the lower chord of the steel truss with a 1 m spacing from the plume central axis [6].

The PTs reached steady state temperatures during the experiments indicating a heat flux to the surface close to zero. Zero heat flux occurs when the surface temperature is equal to the adiabatic surface temperature, T_{AST}, see section 1. The loss of heat through conduction to the back of the plate thermometer is neglected.

Two different setups were used from the experiment, both of which used Heptane as fuel, see Table 1.

Table 1. Fuel pan diameter and heat release rate from Sandström et al. [6].

Experiment	Pan diameter	Heat release rate	Duration
1	0.8 m	4.50 MW	17 min
2	1 m	7.55 MW	10 min

3 HEAT TRANSFER

The heat flux $\dot{q}''_{tot}$ from a fire to a surface is the sum of the radiative $\dot{q}''_{rad}$ and convective $\dot{q}''_{con}$ contributions [8], see equation (1). These can be either positive or negative depending on the exposure and the surface temperature.

$$\dot{q}''_{tot} = \dot{q}''_{rad} + \dot{q}''_{con} \tag{1}$$

The radiative exposure level can be expressed in terms of incident radiation or as the radiation temperature T_r as defined in equation (2).

$$T_r \equiv \sqrt[4]{\frac{\dot{q}''_{inc}}{\sigma}} \tag{2}$$

The convective exposure level is the gas temperature T_g. Thus, the total heat flux can be expressed as in equation (3)

$$\dot{q}''_{tot} = \varepsilon_s \sigma \left[T_r{}^4 - T_s{}^4 \right] + h_c \left(T_g - T_s \right) \tag{3}$$

where h_c = 4 W/m²K, is the convective heat transfer coefficient for surfaces with natural convection according to EN 1991-1-2 and ε_s = 0.7 as suggested by EN 1993-1-2 for steel surfaces.

For practical purposes, thermal exposure can in many cases be presented as an adiabatic surface temperature, T_{AST}, see e.g. [8]. T_{AST} is a fictitious surface temperature between T_r and T_g defined by equation (4).

$$\dot{q}''_{tot} = \varepsilon_s \sigma \left[T_r{}^4 - T_{AST}{}^4 \right] + h_c \left(T_g - T_{AST} \right) = 0 \tag{4}$$

As no heat flux is present at the adiabatic surface in equation (4), it can be subtracted from equation (3) making it possible to replace T_r and T_g with T_{AST} by solving equation (4) for instance by using the method presented by Malendowski [9]. This largely simplifies calculations of the heat flux to a surface which now can written

$$\dot{q}''_{tot} = \varepsilon_s \sigma \left[T_{AST}{}^4 - T_s{}^4 \right] + h_c \left(T_{AST} - T_s \right) \tag{5}$$

This facilitates comparisons between calculations and test results as the plate thermometer measurements approximately yields AST.

4 PLUME CENTRAL AXIS TEMPERATURE

There are several methods for calculation of the plume central axis temperature [10]–[12]. None of these presents a comprehensive method for temperatures outside the central axis even though rough estimations are made. Zukoski [10] assumes a uniform temperature over the cross section and Heskestad [11] a Gaussian distribution of the temperature reaching half the temperature of the central axis at the edge of the plume width. In this paper the Heskestad approach is assumed for the calculation of plume central axis, see Fig. 3.
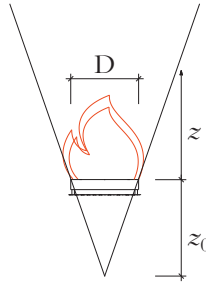
Fig. 3 Key concepts in the Heskestad plume correlation used in this paper.

The calculation according to Heskestad is presented in a simplified form in Eurocode reprinted here in equation (6).

$$T(z) = 20 + 0.25 Q_c^{2/3} (z - z_0)^{-5/3} \leq 900^\circ \ C \qquad (6)$$

The fictitious base height, z_0, of the plume is calculated as

$$z_0 = -1.02D + 0.00524 Q^{2/5} \qquad (7)$$

The temperatures calculated according to (6) are used in all calculations throughout this paper for assessing the plume temperatures at different heights, z. The convective part, Q_c/Q, of the total heat release rate is assumed to be 0.8 as stipulated as a generic design value in the Eurocodes [2].

5 ANALYTICAL CALCULATIONS OF THERMAL EXPOSURE TO THE LOWER CHORD

In this section, three different methods, A, B and C, for calculation of thermal action to horizontal surfaces above the fire plume are presented. Each method is presented to work by its own. The Gaussian assumption for thermal action inside the plume perimeter for method A can however be used in combination with temperatures outside the plume using methods B and C.

The proposed model assumes mixed boundary conditions when expressing the thermal impact on the exposed steel elements. In the experiments, no accumulation of hot gases was observed and the gas/air temperatures outside the plume perimeter in this paper is therefore assumed to be ambient, T_∞. This assumption implies cooling of the member by convection.

The following sections will describe different methods for calculating the radiation temperature, T_r, and/or T_{AST} directly.

5.1 Method A – Gauss and cylindrical perimeter assumption

This method is presented as a combination of two methods as each of the methods are insufficient in describing the thermal action for the entire horizontal plane in- and outside the fire plume radius.

5.1.1 Thermal exposure to horizontal surfaces outside the plume radius

By assuming the fire plume in the form of a cylinder, view factors to an annual ring, Φ, can be calculated as proposed by Brockmann [13] and Siegel and Howell [14] with adjustments by Antwerpen and Greyvenstein [15]. To compensate for different flame temperatures along the height, the fire plume cylinder is divided into segments, each of which radiates to concentric rings at the height of the lower chord, see Fig. 4. Each segment radiates as a surface with a uniform temperature equal to the plume central axis temperature at the corresponding height.
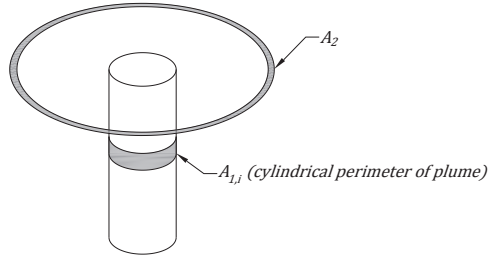
Fig. 4 Radiation from cylindrical surface of a segment of the fire plume to a concentric ring at the height of a presumed lower chord surface.

The view factor to the annual ring, Φ_i, radiating area, $A_{1,i}$, and flame temperature, $T_{fl,i}$ are calculated for each flame segments along the plume height. The incident radiation is then adjusted to the receiving area, A_2, and translated to T_r according to equation (8).

$$T_r = \sqrt[4]{\frac{1}{A_2} \sum_{i=1} A_{1,i} \Phi_i \varepsilon_{fl} T_{fl,i}^4} \tag{8}$$

The flame emissivity, ε_{fl} is calculated with equation (9) [8], [16], [17] and assumed equal over the entire flame height.

$$\varepsilon_{fl} = 1 - e^{-\kappa L_b} \tag{9}$$

κ is assumed 0.45 m^{-1}. As no data was found for n–heptane which was used in the Trondheim experiment, the κ-value is an approximation for heavy hydrocarbons based on Yuen and Tien [18], Rew [19] and Drysdale [20]. L_b is the *mean beam length* of the fire cylinder as proposed in equation (10) by Tien et al. [17] for an arbitrary grey gas volume, V, with surface area, A

$$L_b = 3.6 \frac{V}{A} \tag{10}$$

5.1.2 Thermal exposure to horizontal surfaces inside the plume radius

The definition of plume radius, $b_{\Delta T}$, by Heskestad is that $b_{\Delta T}$ is equal to the horizontal distance from the plume central axis to a position where the temperature is equal to $(T(z) + T_\infty)/2$. Inside the plume radius, thermal exposure is derived using a Gaussian distribution from the plume central axis temperature to the temperature at $b_{\Delta T}$. The temperature at $b_{\Delta T}$ is adjusted to the temperature calculated according to section 5.1.1 for a smooth transition between models, see Fig. 5.
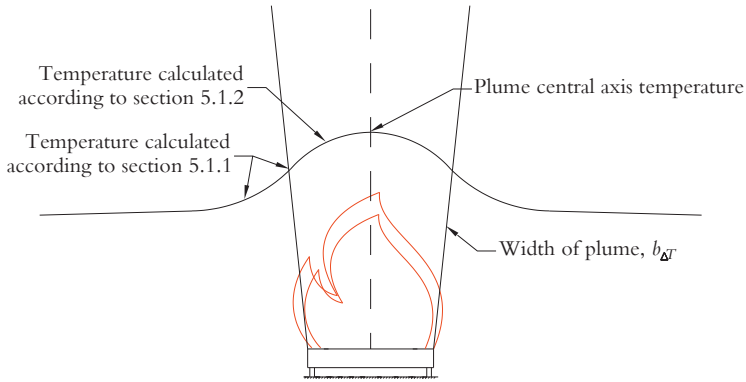
Fig. 5 Key concepts in method A.

5.2 Method B – radiating segments assumption

In the paper by Zhang and Usmani [3], a method for calculation of thermal exposure is presented using radiation from segments of the plume with varying temperatures, see Fig. 6. Each segment radiates as a surface with a uniform temperature equal to the plume central axis temperature at the corresponding height. The view factors to the receiving surface is calculated as annual rings and the results are converted to T_r using equation (2), see Fig. 4.
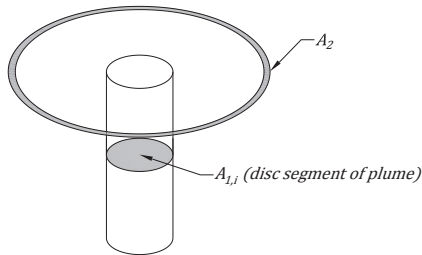
Fig. 6 Radiating segments as presented by Zhang and Usmani [3].

This model is assumed both inside and outside the plume perimeter.

5.3 Method C – point-source assumption

As presented in the paper by Beyler [21] and refined for practical applications by Guowei et al. [4], the radiation from a plume can be calculated as radiation originating from a point source at half the flame height, see Fig. 7.
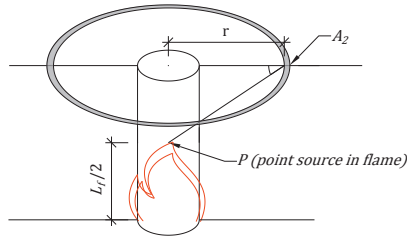
Fig. 7 Radiation from the flame originating from a point source [5], [21].

This model is applied both inside and outside the plume perimeter.

5.4 Summary of methods

The different methods for calculation of the thermal exposure to horizontal surfaces in localized fires are described in Table 2.

Table 2 Description of input from the different methods for calculation of T_{AST}.

	Inside plume perimeter		Outside plume perimeter	
	T_r	T_g	$T_r / \dot{q}''_{inc}$	T_g
Method A	Heskestad/Gauss			T_∞
Method B				T_∞
Method C				T_∞
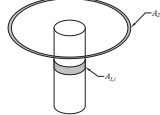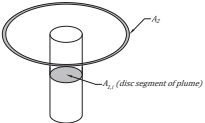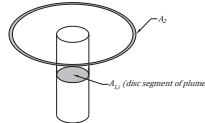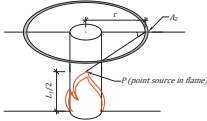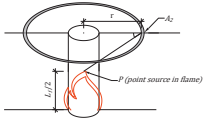
6   RESULTS

Calculated adiabatic surface temperatures according to Equation (*4*) are compared to the measured plate thermometer temperatures [6]. In the Trondheim experiment 1, a small pan yielding a total heat release rate, $\dot{q}$, of 4.50 MW was used, and in experiment 2 a larger pan yielding a heat release rate of 7.55 MW, see Table 1.

In the analytical calculations, except for the point source assumption, method C, all plume central axis temperatures were derived from Heskestad's plume correlation. Comparisons between calculated and the measured temperatures from the Trondheim experiment are shown in Fig. 8.
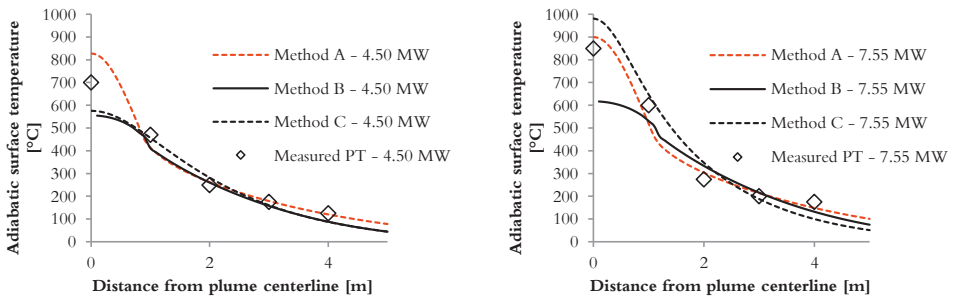
Fig. 8 Adiabatic surface temperatures derived from PT measurements at the lower chord compared to analytical solutions.

All calculations show accurate results outside the plume perimeter. However, method B, the radiating disc assumption, lack precision inside the plume perimeter. The point source, and the Heskestad/Gauss assumption show reasonable correlation to the experimental data. However, the Heskestad/Gauss assumption is more consistent inside the plume with regards to predicting temperatures on the safe/unsafe side.

6.1   Sensitivity analysis

To evaluate the importance of different parameters, two different comparisons are being made. The first, varies the heat transfer conditions at the surface, and the second varies the convective fraction of the total HRR. The surface properties are shown as the relation between h_c and ε_s as used by Wickström [8], see Table 3. For a surface with natural convection, as assumed for these calculations, h_c/ε_s is assumed equal to 5.71 (shown as 6 in the figures).

Table 3 h_c/ε_s for different values of the heat transfer coefficient parameters.

h_c/ε_s	h_c [W/m²K]	ε_s [-]
0	0	0.7
5.71	4	0.7
12.86	9	0.7
35.71	25	0.7
50	35	0.7

The second parameter is the convective fraction of the total HRR, $\chi_c = \dot{Q}_c/\dot{Q}$, in EN 1991-1-2 assumed $\chi_c = 0.8$ as a default value.

The effect of changing h_c/ε_s is shown in Fig. 9 for all methods.
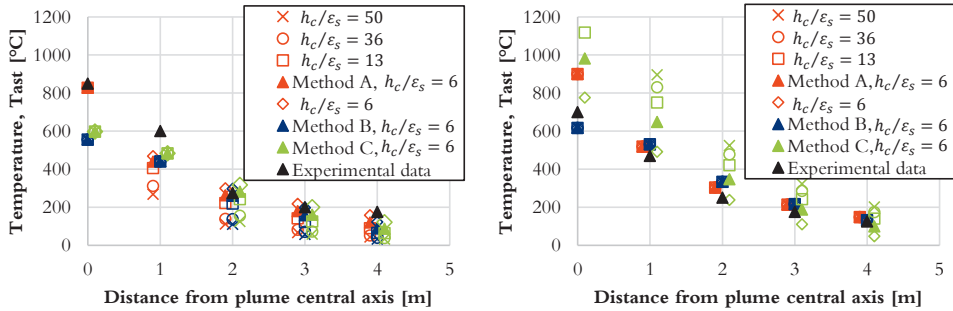
Fig. 9 Variation of calculated results for different assumptions regarding h_c/ε_s. Experiment with 4.50 MW to the left and 7.55 MW to the right.

The results show a variation of results with changing h_c/ε_s. This difference is bigger outside the plume radius as the difference between T_r and T_g is larger there.

Changing the convective part of the total heat released from the fire, $\chi_c = Q_c/Q$, have a larger impact on the results, see Fig. 10.
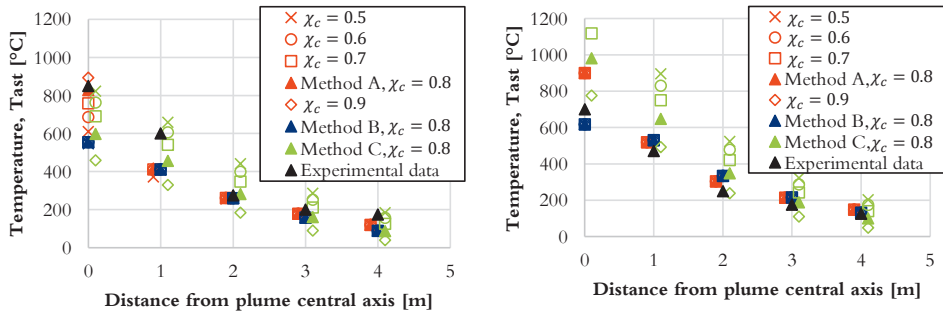
Fig. 10 Variation of calculated results for different assumptions regarding χ_c. Experiment with 4.50 MW to the left and 7.55 MW to the right.

Change in χ_c does not affect method B and at the plume central axis for method A. However, the impact on the results in method C is significant. Both methods A and B are independent of the flame height as the calculations are performed in discrete steps over the plume height with a plume temperature being consistent over the height between calculations.

7 DISCUSSION

All the three methods predict the thermal exposure outside the plume with reasonable accuracy. Inside the plume, however, the Heskestad/Gauss approach is recommended as it yields accurate predictions on the safe side, higher temperatures than measured making it more suitable for design purposes.

For calculation of thermal exposure of surfaces inside the fire plume, T_r and T_g are assumed equal. This was shown feasible by Sjöström et al. [7] and can be observed in the experimental data from the Trondheim experiments as well [6]. The use of a Gaussian temperature distribution appears, in this paper to be a good but rough estimation of temperature decrease with increasing distance from the plume central axis. This statement must, however, be examined further for other fuels and geometrical configurations.

Expressing thermal exposure in terms of T_{AST} is convenient and facilitates subsequent calculations of thermal response in the structural elements. T_{AST} has also the benefit of being measurable to an acceptable accuracy in fire tests with plate thermometers as well as assessed numerically in design calculations. This provides means for easy comparison between experimental and calculated data of the thermal exposure.

8 CONCLUSION

The proposed method A for calculating thermal exposure of lower chords yield good agreements with measured values both inside, and outside the plume perimeter. The proposed method B presents good agreement outside the plume perimeter but not inside the plume where it under–predicts the thermal exposures. Method C yields good results outside the plume, but it has difficulties inside the plume perimeter.

More investigations are needed with other geometries and fuel configurations than investigated here to further develop models of thermal exposures from localized fires for design purposes. This study represents a way forward for the development of a rational simple design method for steel trusses.

9   ACKNOWLEDGEMENTS

10 REFERENCES

[1] Y. Hasemi, Y. Yokobayashi, T. Wakamatsu, and A. Pchelintsev, "Fire Safety of Building Components Exposed to a Localized Fire - Scope and Experiments on Ceiling/Beam System Exposed to a Localized Fire," in *ASIAFLAM's 95 Hong Kong*, 1995.

[2] *EN 1991-1-2*. 2002.

[3] C. Zhang and A. Usmani, "Heat transfer principles in thermal calculation of structures in fire," *Fire safety Journal*, 2015.

[4] Z. Guowei, Z. Guoqing, and H. Lili, "Temperature development in steel members exposed to localized fire in large enclosure," *Safety Science*, 2014.

[5] Z. Guowei, Z. Guoqing, Y. Guanglin, and W. Yong, "Quantitative risk assessment methods of evacuation safety for collapse of large steel structure gymnasium caused by localized fire," *Safety Science*, vol. 87, pp. 234–242, Aug. 2016.

[6] J. Sandström, U. Wickström, J. Sjöström, M. Veljkovic, N. Iqbal, and J. Sundelin, "Steel truss exposed to localized fires, Brandforsk project no 312-131," Brandforsk, Luleå, 2015.

[7] J. Sjöström, A. Byström, and U. Wickström, "Large scale test on thermal exposure to steel column exposed to pool fires," SP Report 2012:04, Borås, 2012.

[8] U. Wickström, *Temperature Calculation in Fire Safety Engineering*. Springer-Verlag, 2016.

[9] M. Malendowski, "Analytical Solution for Adiabatic Surface Temperature (AST)," *Fire Technology*, vol. 53, no. 1, pp. 413–420, Jan. 2017.

[10] E. E. Zukoski, T. Kubota, and B. Cetegen, "Entrainment in Fire Plumes," *Fire Safety Journal*, 1980.

[11] G. Heskestad, "Fire Plumes, Flame Height, and Air Entrainment," in *SFPE Handbook of Fire Protection Engineering, 4th Edition*, P. J. DiNenno, Ed. Quincy, MA: National Fire Protection Associationr, 2008.

[12] B. J. McCaffrey, "Purely Buoyant Diffusion Flames: Some Experimental Results (NBSIR 791910)," 1979.

[13] H. Brockmann, "Analytic angle factors for the radiant interchange among the surface elements of two concentric cylinders," *International Journal of Heat and Mass Transfer*, vol. 37, no. 7, pp. 1095–1100, May 1994.

[14] J. R. Howell and R. Siegel, *Thermal Radiation Heat Transfer, 5th ed*. Boca Raton: CRC Press Inc, 2010.

[15] H. J. van Antwerpen and G. P. Greyvenstein, "Evaluation of a detailed radiation heat transfer model in a high temperature reactor systems simulation model," *Nuclear Engineering and Design*, no. 238, pp. 2985–2994, 2008.

[16] K. S. Mudan and P. A. Croce, "Fire Hazard Calculations for Large open Hydrocarbon Fires," in *SFPE Handbook of Fire Protection Engineering, 2nd Edition*, P. J. DiNenno, Ed. National Fire Protection Association, 1988, pp. 2–45 − 2–87.

[17] C.-L. Tien, K. Y. Lee, and A. J. Stretton, "Radiation Heat Transfer," in *SFPE Handbook of Fire Protection Engineering, 4th Edition*, P. J. DiNenno, Ed. Quincy, Massachusetts: National Fire Protection Association, 2008, pp. 1-74-1–90.

[18] W. W. Yuen and C.-L. Tien, "A simple calculation scheme for the luminous–flame emissivity," *Symposium (International) on Combustion*, vol. 16, no. 1, pp. 1481–1487, 1977.

[19] P. J. Rew, W. G. Hulbert, and D. M. Deaves, "Modelling of Thermal Radiation From External Hydrocarbon Pool Fires," *Process Safety and Environmental Protection*, 1997.

[20] D. Drysdale, *An Introduction to Fire Dynamics, Second Edition*. Chichester: John Wiley & Sons, 1998.

[21] C. L. Beyler, "Fire Hazard Calculations for Large open Hydrocarbon Fires," in *SFPE Handbook of Fire Protection Engineering, 3nd Edition*, P. J. DiNenno, Ed. National Fire Protection Association, 2002, pp. 2–45 – 2–87.

PAPER F

Comparing performance-based fire safety design using stochastic modelling to Eurocode partial coefficient method

Sandström, J. and Thelandersson, S.

Book of Abstract Nordic Fire & Safety Days (accepted 2018)

Comparing performance-based fire safety design using stochastic modelling to Eurocode partial coefficient method

Joakim Sandström[a]
Sven Thelandersson[b]

[a]Luleå University of Technology/Brandskyddslaget AB
[b]Lund University

Abstract

In performance based structural fire safety design using the parametric fire curve, Eurocode has adopted a partial coefficient applied only on the fuel load density for calibrating the code to the desired safety level. Probabilistic analyses are presented in this paper to investigate the impact on the reliability due to variation of opening factor, and thermal inertia as well as the ratio between variable and permanent static load. It is shown that the partial coefficient method in Eurocode, with fire exposure expressed via parametric fire curves gives adequate reliability levels with certain margins on the safe side. This margin is particularly high for load combinations with dominating variable load.

Keywords: *Performance Based Design, Fire resistance, Reliability analysis, Monte Carlo simulation*

Introduction

Background and purpose

Probabilistic design in structural fire safety design dates back to the seventies [1], but has increased in interest during recent years. Due to the inherent non-linearity of probabilistic fire safety design of structures, Eurocode is calibrated using a method by Schleich where the fuel load density is adjusted to achieve the desired safety [2, 3]. However, this approach has a one-sided focus on the fuel load density, ignoring the impact from assuming the live load as arbitrary-point-in-time and the impact from choice of parameter such as the opening factor and/or thermal inertia.

Previous papers have shown the use of Monte Carlo modelling of fire exposed load-bearing elements assessing the safety index of a limited number of structural configurations [4, 5]. In this paper the effect from these parameters on the reliability of a steel structure is investigated using Monte Carlo simulations in comparison to the partial coefficient method presented in the Eurocode [6].

Limitations

The structural case used in the paper is simplified with regards to

- Steel in pure bending,
- Linear thermal properties for insulation material,
- The investigated parameters are limited to
  - The opening factor,
  - The thermal inertia of the compartment lining, and

        o   The load combination.
- The compartment size and fire risk area are fixed to 100 m², and 1000 m² respectively,
- Only the parametric fire curve assumption is used as it is presented in the Eurocode [6].

Structural fire safety design

Steel resistance at elevated temperatures

As the primary objective of this paper is to investigate the importance of different parameters in the Eurocode parametric fire curve, the simplifications described below are deemed to be reasonable. The calculated steel temperature, and subsequently reduced structural resistance, should be regarded a measure of fire severity, not as a representation of reality.

Prior to the simulations, the design values regarding resistance and load were initiated. For this study, the design resistance was determined from the assumptions presented here

1. The critical design temperature is determined to θ_{crit} = 540°C, to correspond to the simplified max utilization for steel, η_{fi} = 0.65 presented in EN 1993-1-2,

2. The beam used in the study is a simply supported HEA180 with a length of 4 meters, a section modulus, $W_y = 294 \cdot 10^3 \, mm^3$, and a section factor for the steel of $A_m/V = 115 \, m^{-1}$, and

3. The characteristic yield strength of the beam is $f_y = 355 \, MPa$.

The maximum design resistance in case of fire was then calculated as

$$R_{fi,d} = f_y k_{y,540} W_y \approx 67.8 \, kNm \tag{1}$$

The steel temperature was calculated using the lumped heat assumption according to EN 1993-1-2 for insulated members [7]. From this calculation, the steel temperature, $\theta_{a,t}$, is converted to a reduction in yield strength, $k_{y,\theta}$, according to EN 1993-1-2 [7].

Thermal load from the Eurocode parametric fire curve

The concept of temperature development in compartments exposed to natural fires were explored by Kawagoe and Sekine [8] as well as Ödeen [9]. This concept was later developed by Magnusson and Thelandersson [10] creating an opportunity to translate geometry and fuel to a thermal action.

Their work was later adapted by Wickström [11] to an analytical solution which eventually was incorporated in the Eurocode system as the parametric fire [6]. The expression for the heating phase used in the Eurocodes is for clarity shown here in equation (2).

$$\theta_{g,t} = 20 + 1325(1 - 0.324e^{-0.2t\Gamma} - 0.204e^{-1.7t\Gamma} - 0.472e^{-19t\Gamma}) \tag{2}$$

The Γ-factor adjusts the time scale of the heating and a high value of Γ results in a rapid heating and cooling whereas a low value of Γ results in slow heating and cooling. The Γ-factor is calculated from the opening factor, O, e.g. the ventilation conditions, and the thermal inertia of the surrounding structure, b, see equation (3).

$$\Gamma = \frac{\left(O/0.04\right)^2}{\left(b/1160\right)^2} \qquad (3)$$

The application of the parametric fire curve is limited to values of the opening factor between 0.02 and 0.2 in Eurocode [6]. A typical office building in Sweden should have at least 10 % window openings in relation to floor area [12] yielding an approximate lower bound for most compartments of $O = 0.03$.

The opening factor is, however, the parameter along with the total amount of fuel load in the compartment, Q_d, used for deciding the time, t_{max}, to the maximum temperature in the fire compartment, see equation (4).

$$t_{max} = \frac{0.2 \cdot 10^{-3} Q_d}{O} \qquad (4)$$

For a typical fire compartment of normal concrete for all surfaces, b is approximately 1920 $Ws^{\frac{1}{2}}/m^2K$. For a lightweight construction of gypsum and rockwool, however, b is closer to 400 $Ws^{\frac{1}{2}}/m^2K$. Both values are well within the limitation of $100 \leq b \leq 2200$ for the parametric fire curve in Eurocode [6].

For very short fires, Eurocode uses a lower limit for the duration of a fire. In this paper, a medium fire growth rate is assumed yielding $t_{lim} = 20$ minutes.

Fuel load density

Fuel load can be divided into two different categories, permanent and variable [6]. The permanent fuel load, q_p, consists of construction material such as wooden boards, studs etc. The variable fuel load, q_v, on the other hand, consists of movable things such as furniture, books, paintings etc. As not all fuel is consumed, the theoretical fuel load is multiplied with a combustion efficiency, $m = 0.8$.

Fuel load density, q_f

With regards to permanent fuel load, there is to the authors knowledge no statistical data found in the literature. Hence, the mean value of the permanent fuel load, $q_{p,mean}$, is approximated based on typical Swedish structural light-weight configuration [13], i.e. $q_{p,mean} = 50$ MJ/m² surrounding area or approximately 162 MJ/m² floor area.

The permanent fuel load is further divided in protected and unprotected fuel loads. According to Eurocode, a minimum of 10 % of the permanent fuel load should be unprotected while 90 % is protected to some extent, a relation used in this paper. The protection is assessed by using the factor Ψ with a value between 0 and 1 as

$$q_p = q_{p,unprotected} + q_{p,protected} = (0.1 + 0.9\Psi)q_{p,mean} \qquad (5)$$

In this paper, $\Psi_{mean} = 0.5$ and a coefficient of variation, $V_\Psi = 0.1$ is assumed for the stochastic calculation. $q_{p,mean}$ is distributed according to the normal distribution with a coefficient of variation $V_{q_p} = 0.3$.

The mean value of the variable fuel load, $q_{v,mean}$, is assumed for each calculation. The coefficient of variation, $V_{q_v} = 0.3$, the same value as adopted by the Eurocode. However, the Eurocode assumes a Gumbel distribution, while in this paper a normal distribution is used as it presents a better fit to earlier investigations of fuel load densities by Magnusson et al. [14], and Thomas [15].

The total fuel load density, q_f, used in each simulation is calculated as

$$q_f = m(q_v + q_p) \tag{6}$$

Eurocode design fuel load, $q_{f,d}$

The permanent fuel load density is calculated according to equation (5) assuming $\Psi = \Psi_{mean}$.

The Eurocode characteristic value for the variable fuel load density, $q_{v,k}$, is adapted for the 80th, the 90th or the 95th percentile from a statistically relevant sample assuming a Gumbel distribution [6, 16, 17]. The choice of percentile is made on a national level depending on the desired safety level.

To compensate for the increased probability of a fire with unacceptable consequences, Eurocode uses a coefficient, δ_{q1} to account for the size of the fire risk area. For 1 000 m², $\delta_{q1} = 1.74$. The design calculation of the fuel load density can therefore be written as

$$q_{f,d} = m\delta_{q1}(q_{v,k} + q_p) \tag{7}$$

Load in case of fire

The live-, and dead load acting on the steel was calculated assuming maximum utilization in structural fire design, i.e. the design load was assumed to equal the design resistance, $E_{fi,d} = R_{fi,d}$. The characteristic live load, Q_k, and dead load, G_k, was derived using equations (8) and (9) based on the load ratio $\alpha = Q_k/(Q_k + G_k)$.

$$Q_k = \frac{E_{fi,d}}{\left(\frac{1}{\alpha} - 1 + \psi_2\right)} \tag{8}$$

$$G_k = Q_k \left(\frac{1}{\alpha} - 1\right) \tag{9}$$

The mean value of G is assumed equal to G_k, while the mean value, $Q_{2,mean}$, for the arbitrary point in time distribution, Q_2, is approximated as

$$Q_{2,mean} = \psi_2 Q_{mean} = \psi_2 \frac{Q_k}{1 - V_Q \frac{\sqrt{6}}{\pi}\left(0.577 + ln(-ln(0.98))\right)} \tag{10}$$

where Q_{mean} is the mean value of the annual maximum load Q and V_Q is the coefficient of variation of Q assumed as 0.3. It is also assumed that Q is described by a Gumbel distribution. The coefficient of variation, V_{Q_2}, for Q_2, however, is estimated from live load survey data

presented in [25] see table 1. Q_2 is also assumed to follow a Gamma distribution, see reference [18, 19] .

This assumption of $Q_{2,mean}$ shall be regarded as an approximation as the analytical solution is non-trivial. Using ψ_2=0.3 for offices according to Eurocode in equation (10) correlates roughly to the arbitrary-point-in-time sustained load presented in [18], and the assumption presented in [16] and [20].

Probability of failure

The probability of failure P_f in case of fire was calculated from equation (11).

$$P_f = P(E) \cdot P(F|E) \tag{11}$$

with each of the parameters as defined below.

$P(E) = P(I) \cdot \left(1 - P(IN)\right)$ represents the probability of a fully developed fire with the capability of leading to collapse if not prevented. In this paper, the following aspects were considered for calculation of $P(E)$:

1. The probability for ignition, $P(I)$ and

2. The probability $P(IN)$ of intervention, i.e. the fire is stopped by occupants or by the fire rescue services.

The values for office buildings were used, see Table 1.

$P(I)$ is, in this paper, calculated based on a fire risk area of 1 000 m².

No active fire protection systems were considered in the simulations but can be accounted for by modification of equation 11 based on the probability that the active systems fail, $P(\bar{A})$.

$P(IN)$, or the probability of intervention by occupants or the fire rescue services are assumed from the study referred in [16] for office buildings.

$P(F|E)$ represents the probability of failure given that a fully developed fire occurs.

The target probability, p_{target}, for this study was assumed for a reference period of 50 years as suggested by the EN 1990 for risk class 2, RC2 [21] with a safety index, $\beta = 3.8$.

Limit state function

The limit state function used in this study was defined as the collapse of the fire exposed steel beam.

$$g(R, S) = R - S \tag{12}$$

where R and S is defined as

$$R = f_y W_y k_{y,\theta} \tag{13}$$

$$S = G + Q_2 \tag{14}$$

For each calculation, G and Q_2 are random values at an arbitrary point in time.

Random variables

The statistical distributions and parameter values used in the simulation are presented in table 1. These values are based on a combination of estimations and sources [3, 22–24]. Steel properties are temperature dependent according to Eurocode [7] while the mean values of the insulation properties are independent of temperature as suggested in ECCS [25].

Table 1 Stochastic variables for Monte Carlo simulation.

No	Category of variables	Basic variable	Symbol	Dim.	Dist[i]	Mean	CoV	Ref
1.	Actions	Permanent	G	kN/m²	N	[ii]	0.1	[26]
2.		Arbitrary-point-in-time load	Q_2	kN/m²	GA	[ii]	0.54	[18, 19]
3.		Quasi permanent value factor	ψ_2	–	D	0.3	–	[27]
4.	Steel	Yield strength	f_y	MPa	LN	400	0.1[iii]	[23]
5.		Bending resistance	W_y	m³	D	$2.94 \cdot 10^{-3}$	–	–
6.		Section Factor	A_m/V	m⁻¹	D	115	–	–
7.		Density	ρ_a	kg/m³	D	7850	–	[7]
8.		Conductivity	λ_a	W/mK	D	[iv]	–	[7]
9.		Specific heat	c_a	J/kgK	D	[iv]	–	[7]
10.	Insulation	Thickness	d_i	m	N	[v]	0.1	Est.
11.		Density	ρ_i	Kg/m³	N	170	0.1	[25] Est.
12.		Conductivity	λ_i	W/mK	N	0.2	0.1	[25] Est.
13.		Specific heat	c_i	J/kgK	N	1030	0.1	[25] Est.
14.	Fire	Permanent fuel load	q_p	MJ/m²	N	50	0.3	[6]
15.		Variable fuel load	q_v	MJ/m²	N	[vi]	0.3	[22]
16.		Fuel load percentile	%	–	D	[vii]	–	[6]
17.		Combustion efficiency	m	–	N	0.8	–	[6]
18.		Shielding of fuel load	Ψ_i	–	N	0.5	0.1	Est.
19.		Size coefficient	δ_{q1}		D	1.74	–	[6]
20.		Prob. of ignition	$P(I)$	m⁻²year⁻¹	D	$1.0 \cdot 10^{-5}$	–	[16]
21.		Prob. of intervention	$P(IN)$	–	D	0.94[viii]	–	[16]
22.	Geometry	Opening factor	O	m½	D	[vi]	–	–
23.		Thermal inertia	b	J/m²s½K	D	[vi]	–	–
24.	Numerical	Number of calculations	-	–	–	10 000	–	–

---

[i] D stands for deterministic value; N for Normal–, LN for Lognormal–, and GA for Gamma distribution.
[ii] See section "Load in case of fire".
[iii] Slightly higher than in the reference to include for geometrical imperfections of the cross section.
[iv] Varying with temperature according to EN1993-1-2 [8]
[v] Calculated to obtain the desired safety index.
[vi] Varied with calculations.
[vii] Varied with calculations
[viii] Calculated as a combination of the probability of intervention by occupants and fire rescue services for offices according to [22].

Calculation of insulation thickness

Probabilistic modelling

The required insulation thickness to obtain $\beta = 3.8$ was found via an iterative process. In the Monte Carlo simulation, the insulation thickness was tested with 10 000 calculations in each iteration to evaluate the reliability of the beam in fire. This process was repeated for each combination of parameters.

Eurocode design

For the comparative design calculation using the partial coefficient method in Eurocode, all stochastic variables were set to the corresponding design value. To evaluate the safety levels in the Eurocode, iterations to find the insulation thickness for the steel beam was performed for the 80th, the 90th or the 95th percentile of fuel load, assuming a parametric fire and a fire risk area of 1 000 m² [6].

Results

The results are presented as insulation thickness d_i on the y-axis for a steel element with a section factor of $A_m/V = 115\ m^{-1}$. The insulation thickness and section factor are proportional and by changing one, the other will subsequently change.

For cases with very low fuel load densities, no applied fire protection is required to obtain a safe building. These results are omitted, and the results are only shown for the fuel load density span where there is a need for applied fire protection.

Comparison with Eurocode partial coefficient method

Design according to Eurocode in this section is based on the assumption that the characteristic value of the variable fuel load is defined as the 80th percentile.

The difference in safety when comparing the Monte Carlo results to the Eurocode calculation is shown for the 80th percentile in Figure 1 to Figure 3. The effect of the opening factor on d_i is shown in Figure 1 for a load combination factor, $\alpha = Q_k/(Q_k + G_k) = 0.5$, and a thermal inertia, $b =$1160 J/m²s$^{\frac{1}{2}}$K.
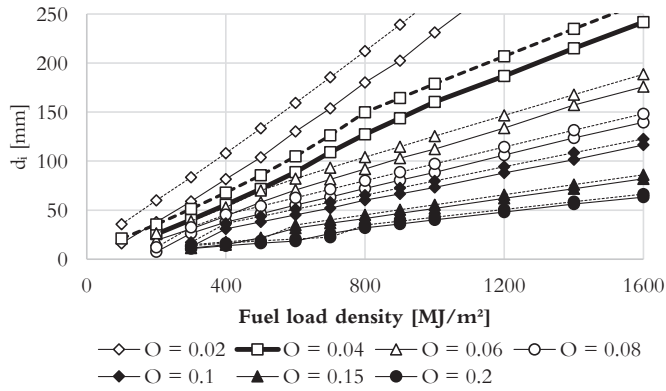
Figure 1 d_i required for obtaining p_{target} for different opening factors in relation to the mean value of the variable fuel load density. Solid lines represents the Monte Carlo simulation and the dashed lines, the Eurocode calculations.

The Eurocode partial coefficient method combined with parametric design fire exposure provides design with slightly larger value of d_i for the same scenario. This effect is smaller for larger opening factors, O.

The effect of thermal inertia is shown in Figure 2 for a load combination factor, $\alpha = Q_k/(Q_k + G_k) = 0.5$, and an opening factor, $O = 0.04$ m$^{\frac{1}{2}}$.
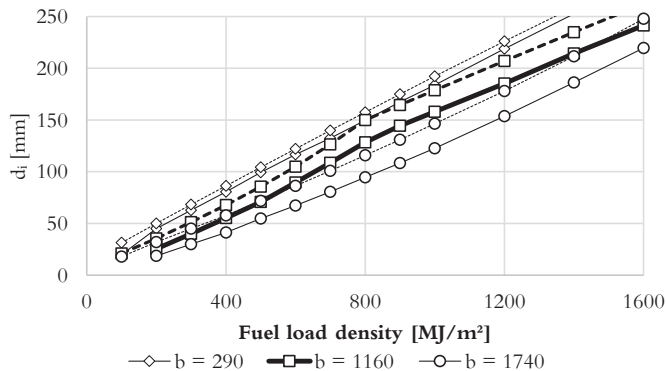

Figure 2 d_i required for obtaining p_{target} for different thermal inertia in relation to the mean value of the variable fuel load density. Solid line represents the Monte Carlo simulation and the dashed line, the Eurocode calculations.

The Eurocode partial coefficient method generally provides a design with slightly larger value of d_i for scenario with low values of thermal inertia, b. The difference in d_i is increased with higher values of thermal inertia, b.

The effect of load ratio is shown in Figure 3 for opening factor, $O = 0.04$ m$^{\frac{1}{2}}$, and thermal inertia, $b = 1160$ J/m²s$^{\frac{1}{2}}$K.
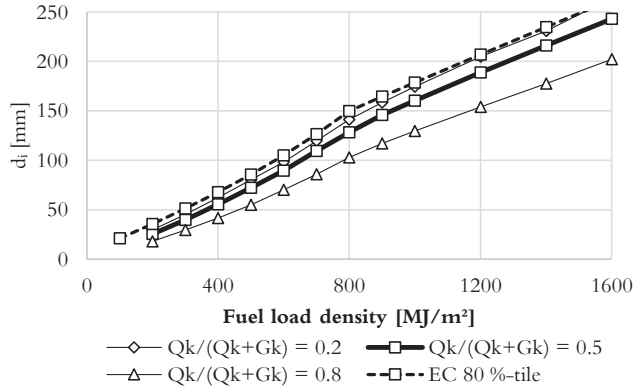
Figure 3 d_i required for obtaining p_{target} for different load combinations in relation to the mean value of the variable fuel load density. Solid line represents the Monte Carlo simulation and the dashed line, the Eurocode calculations.

The Eurocode partial coefficient method seems to overestimate the need for insulation for load combinations where variable load is dominating (i.e. for light-weight structures). The difference is of the order 25 %.

Effect of definition of characteristic fuel load

With a load combination factor, $\alpha = Q_k/(Q_k + G_k) = 0.5$, an opening factor, $O = 0.04$ m^{½}, and a thermal inertia, $b = 1160$ J/m²s^{½}K. d_i required to obtain p_{target} for different percentiles of the fuel load density, $q_{f,k}$, is shown in Figure 4.
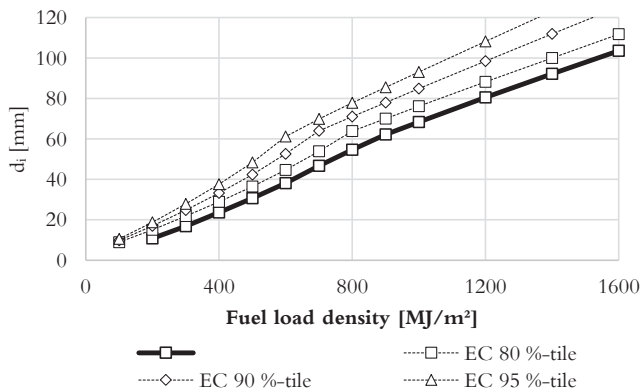

Figure 4 d_i required for obtaining p_{target} for different fuel load density percentiles in relation to the mean value of the variable fuel load density.

In all cases the Eurocode is conservative compared to the results from the probabilistic analysis.

Discussion

Generally, a structural fire resistance design based on parametric fire exposure according to Eurocode seems to give a rather adequate reliability although slightly conservative compared to the probabilistic investigation presented in this paper. Fire, however, is slightly different from single element design in consequence it poses a threat to all structural members in a compartment during the event of a fire.

The safety margin increases for low values of Γ, i.e. small opening factors and/or large thermal inertia. This is assumed to be an effect of the slower heating with a more consistent rate of change in steel temperature over a longer time when exposed to fire. This also explains the relatively large difference in required fire protection for small fuel load densities independent of Γ, the rate of change in steel temperature is high when cooling starts. The safety margin is also higher for structures with large ratio between variable and permanent load, i.e. light-weight structures.

When performing stochastic modelling of natural fires, there are difficulties in finding proper parameters for the statistical distributions. The fuel load density is, for example, more fitting to a standard deviation as in [14] than to a Gumbel deviation as stated in [16]. The coefficient of variation in the first source is closer to 0.15-0.2 or lower while the second source states 0.3 to include for uncertainties. This, along with the uncertainties in material property variations among other parameters, needs to be addressed in some way.

The choice of target probability proves difficult for fire as the probability of occurrence is small and strongly dependent on the building size, or the fire risk area. For an office building with a sufficiently small fire risk area, the probability of fire ignition could be smaller than the target probability itself. This effect could lead to some small buildings left without any protection, a situation that could lead to very large consequences even for very small fires in these buildings. Due to this, it could be argued that a higher safety index should be assumed in case of fire or that a special set of safety indexes are assumed for fire safety design interpreted as conditional given a fully developed fire.

Another aspect of determining the probability of ignition in relation to area is the lack of connection to number of occupants or cooking facilities that has proven to be one of the largest sources of ignition [28]. A more relevant measure could be ignition per family or number of kitchens. This is difficult to find in the literature where only a crude measure of area is used.

Conclusion

For structural fire safety design, with the characteristic fuel load density represented by the 80th percentile seems to give the most reasonable results when compared to probabilistic modelling. Even with a conservative assumption regarding the arbitrary-point-in-time load, the 80th percentile is slightly conservative for most cases.

For structural fire safety design, there is a need for a special set of safety indexes due to the difficulty of addressing buildings with a small fire risk area in a proper way. This needs further work regarding the assessment of probability for fully developed fire to occur. Statistics allowing a more precise estimate of this probability is needed to better address the overall reliability of structures in fire.

There is a higher inherent safety margin for low values of Γ and cases with dominating variable load, Q. The effect of this should be acknowledged when setting up a stochastic model using

only one set of assumptions regarding the opening factor and thermal inertia as the effect depends largely on the choice of parameters.

Acknowledgments

References

1. Magnusson S-E (1974) Probabilistic analysis of fire exposed steel structures. Lund Institute of Technology, Division of structural mechanics and concrete construction

2. Schleich J-B (2009) Performance Based Design for the Fire situation, Theory and Practice. In: Proceedings of Nordic Steel Construction Conference 2009. pp 146–155

3. Schleich J-B (2005) Calibration of Reliability Parameters. Implementation of Eurocodes, Handbook 5 - Design of Buildings for the Fire Situation

4. Khorosani NE, Garlock M, Gardoni P (2016) Probabilistic performance-based evaluation of a tall steel moment resisting frame under post-earhquake fires. Journal of Structural Fire Engineering 7:193–216. doi: https://doi.org/10.1108/JSFE-09-2016-014

5. Coile R Van, Annerel E, Caspeele R, Taerwe L (2013) Full-Probabilistic Analysis of Concrete Beams During Fire. Journal of Structural Fire Engineering. doi: https://doi.org/10.1260/2040-2317.4.3.165

6. (2002) EN 1991-1-2. Action on structures - Part 1-2: General Actions - Actions on structures exposed to fire. European Committee for Standardization, CEN, Brussels

7. (2005) EN 1993-1-2. Design of steel structures - Part 1-2: General rules - structural fire design. European Committee for Standardization, CEN, Brussels

8. Kawagoe K, Sekine T (1963) Estimation of Fire Temperature-Time Curve in Rooms. Building Research institute, Tokyo

9. Ödeen K (1963) Theoretical Study of Fire Characteristics in Enclosed Spaces. Division of Building Construction, Royal Insitute of Technology, Stockholm

10. Magnusson S-E, Thelandersson S (1970) Time - Temperature Curves of Complete Process of Fire Development; Theoretical Study of Wood Fuel Fires in Enclosed Spaces. Acta Polytechnica Scandinavia, Civil Engineering and Building Construction Series No 65

11. Wickström U (1985) Application of the Standard Fire Curve for Expressing Natural Fires for Design Purposes. Fire Safety: Science and Engineering 145–159.

12. (2017) Boverkets byggregler, BFS 2011:6 med ändringar till BFS 2017:5. Boverket, Karlskrona

13. (2010) Gyproc Handbok, utgåva 8. Gyproc AB, Bålsta

14. Magnusson S-E, Pettersson O, Thor J (1974) Brandteknisk dimensionering av stålkonstruktioner, SBI Publikation 38. Stålbyggnadsinstitutet, Stockholm

15. Thomas PH (1986) Design Guide Structural Fire Safety, Workshop CIB W14. Fire Safety 10:77–137. doi: doi:10.1016/0379-7112(86)90041–X

16. Holicki M, Materna A, Selacek G, et al. (2005) Implementation of Eurocodes, Handbook 5 - Design of Buildings for the Fire Situation. Leonardo da Vinci Pilot Project CZ/02/B/F/PP-134007, Luxembourg

17. Zalok E (2011) Validation of Methodologies to Determine Fire Load for Use in Structural Fire Protection. The Fire Protection Research Foundation

18. Corotis RB, Sentler L (1989) Actions on structures, live loads in buildings, Publication 116. CIB W81

19. Iqbal S, Harichandran S Ronald (2010) Capacity Reduction and Fire Load Factors for Design of Steel Members Exposed to Fire. Journal of Structural Engineering 136:1554–1562. doi: 10.1061/(ASCE)ST.1943-541X.0000256

20. Iqbal S, Harichandran RS (2010) Reliability-Based Capacity Reduction and Fire Load Factors for Design of Steel Members Exposed to Fire. In: Structures in Fire: Proceedings of the Sixth International Conference. pp 75–82

21. (2002) EN 1990. Basis of structural design. European Committee for Standardization, CEN, Brussels

22. Cajot L-G, Pierre M (2001) Valorisation Project, Natural Fire Safety Concept. 82.

23. JCSS (2001) Probabilistic Model Code. The Joint Committee on Structural Safety

24. Sanctis G de, Faber MH, Fontana M (2014) Assessing the Level of Safety for Performance Based and Prescriptive Structural Fire Design of Steel Structures. Fire Safety Science – Proceedings of the Eleventh International Symposium

25. (1995) Fire Resistance of Steel Structures. ECCS Technical Note No. 89, Brussels, Belgium

26. Tichý M (1989) Actions on structures, Self-weigth load, Publication 115s. CIB W81

27. (2013) Boverkets föreskrifter och allmänna råd om tillämpning av europeiska konstruktionsstandarder (eurocoder), BFS 2013:10. Boverket, Karlskrona

28. Winberg D (2016) International Fire Death Rate Trends, SP Report 2016:32. SP Technical Research Institute of Sweden

Department of Civil, Environmental and Natural Resources Engineering
Division of Structural and Fire Engineering

LULEÅ
UNIVERSITY
OF TECHNOLOGY